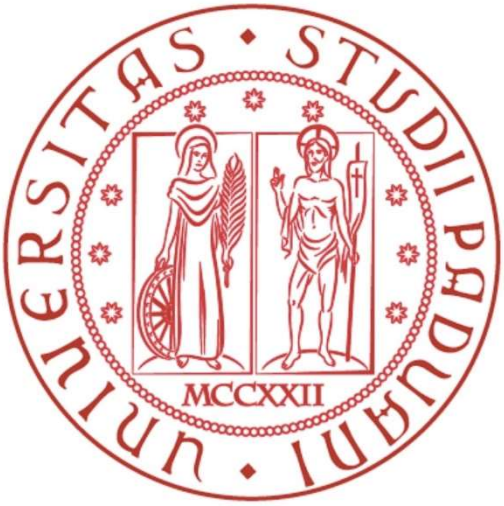

UNIVERSITÀ DEGLI STUDI DI PADOVA

DIPARTIMENTO DI INGEGNERIA INDUSTRIALE

Tesi di Laurea in Ingegneria dei Materiali

IN-SITU SYNTHESIS OF MOFs IN A POLYMER DURING EXTRUSION

Laureando: Alessandro Del Francia

Relatore: Dott.ssa Alessandra Lorenzetti

Correlatore: Prof. Tony McNally

ANNO ACCADEMICO 2018/19

ABSTRACT

This work is the product of five months spent at University of Warwick in the International Institute of Nanocomposites Manufacturing thanks to Erasmus Traineeship project. It consists on the mechanochemical synthesis of a metal-organic framework (MOF) and the production and characterization of a composite material, that has been filled with the metal-organic framework already synthetized or with the metal-organic framework synthetized in-situ. The aim of this work is to find new solution for making scalable and suitable to industrial quantities the production process of the composites filled with metal-organic frameworks.

The composite with a polymeric matrix and a metal-organic framework as a filler, that are usually termed as mixed matrix membranes, have received in the recent time a lot of interest thanks to their ability in adsorbing and separating gases. These abilities are due to the combination of properties, such as permeability and selectivity, of the polymeric material and the metal-organic framework. If this type of composite is produced in form of a membrane it can be used, for example, to separate or adsorb the flue gases of industry, thus reducing the emissions of the CO_2 in the atmosphere, or to separate the extracted methane by the impurities contained in it. The problem is that there are some difficulties in scaling up the process because the composites are mainly obtained by solution casting, indeed this this work explores a practically new field for the production techniques of this type of composites. The same problem there is even with the synthesis of MOF, that are mostly obtained with solvothermal synthesis, this can be partially resolved with mechanochemical synthesis that can lead to a considerably higher yield. Performing this synthesis in-situ and combining it with the extrusion process in an industrial scale can heavily enhance the production rates of this materials suitable for adsorbing or separating gases.

RIASSUNTO

Questo lavoro è il frutto di cinque mesi trascorsi all'Università di Warwick nell'International Institute of Nanocomposites Manufacturing grazie al progetto Erasmus Traineeship. Consiste nella sintesi meccanochimica di un metal-organic framework (MOF) e nella produzione e caratterizzazione di un materiale composito, il quale è stato caricato con il metal-organic framework già sintetizzato o con il metal-organic framework sintetizzato in-situ. Lo scopo di questo lavoro è di trovare nuove soluzioni per rendere scalabile e adatto alle quantità industriali il processo di produzione dei materiali compositi caricati con metal-organic frameworks.

La classe di compositi con una matrice polimerica e un metal-organic framework come filler, detti anche mixed-matrix membranes, hanno ricevuto negli ultimi tempi un grande interesse grazie alle loro capacità di adsorbimento e separazione dei gas. Questa abilità è dovuta alla combinazione di proprietà, come permeabilità e selettività, del materiale polimerico e del metal-organic framework stesso. Se questo tipo di composito viene prodotto sotto forma di membrana delle possibili applicazioni sarebbero, ad esempio, adsorbire o separare i gas di scarico dell'industria, e quindi ridurre le emissioni di CO2 nell'atmosfera, o separare il metano estratto dalle impurità in esso contenute. Il problema è che ci sono alcune difficoltà nello scalare il processo perché i compositi sono ottenuti principalmente per solution-casting, infatti questo lavoro esplora un campo praticamente nuovo per le tecniche di produzione di questo tipo di materiali compositi. Lo stesso problema esiste anche con la sintesi di metal-organic frameworks, che sono principalmente ottenuti tramite sintesi solvo-termale, questo fatto può essere parzialmente risolto con la sintesi meccanochimica che può portare a una produzione con una resa nettamente superiore. Eseguendo questa sintesi in-situ e combinandola con il processo di estrusione su scala industriale, sarebbe dunque possibile migliorare notevolmente i tassi di produzione di questi materiali atti all'adsorbimento o alla separazione dei gas.

Summary

1 INTRODUCTION

1.1 Background

1.1.1 Microporous materials

In the last decades porous materials have attracted a lot of attention in the research area due to their possible applications in drug delivery, catalysis, gas separation and storage of guest molecules [1]. Porous materials are classified by the size of their pores as microporous, mesoporous and macroporous. A material can be defined microporous if the pore diameter is less than 20 Å, mesoporous if the pore diameter is between 20 Å and 500 Å and macroporous if the pore diameter is above 500 Å [2]. The pore size directly affects the properties of the material and accordingly their suitability for different applications. For this reason, the more suitable type of porous materials in most of the applications mentioned before are the microporous ones.

Figure 1.1 – Pore diameter scale

Highly crystalline microporous materials include interconnected cavities or channels with a diameter that ranges from ~2.5 Å up to 20 Å, which is comparable to molecular dimensions. The layout of these interconnected channels determines if the pore system in the material has a framework that is mono-dimensional, bi-dimensional or three-dimensional. Since typically the pore size distribution of the micropores is very narrow and the pore size are comparable to molecular dimension these materials can adsorb or separate molecules based on their size and shape. This property is called shape selectivity and establishes which molecules can pass through or form in the material by controlling which reactant molecule can enter into the pores, which product can get out of the material or the geometry of the transition state that forms in the material. [3]

Furthermore, these materials have properties such as large internal surface areas and pore volumes that typically have values above 300 m^2g^{-1} and 0.1 cm^3g^{-1} respectively and when functional groups are added on the original chemical structure these materials became highly reactive, thanks to their high internal surface area, and this is useful for enhancing even more catalytic, adsorption and separation properties. These features render microporous materials interesting for useful in the fields of catalysis and separation (molecular sieving and adsorption) that are even the areas where these materials have their main commercial applications [3].

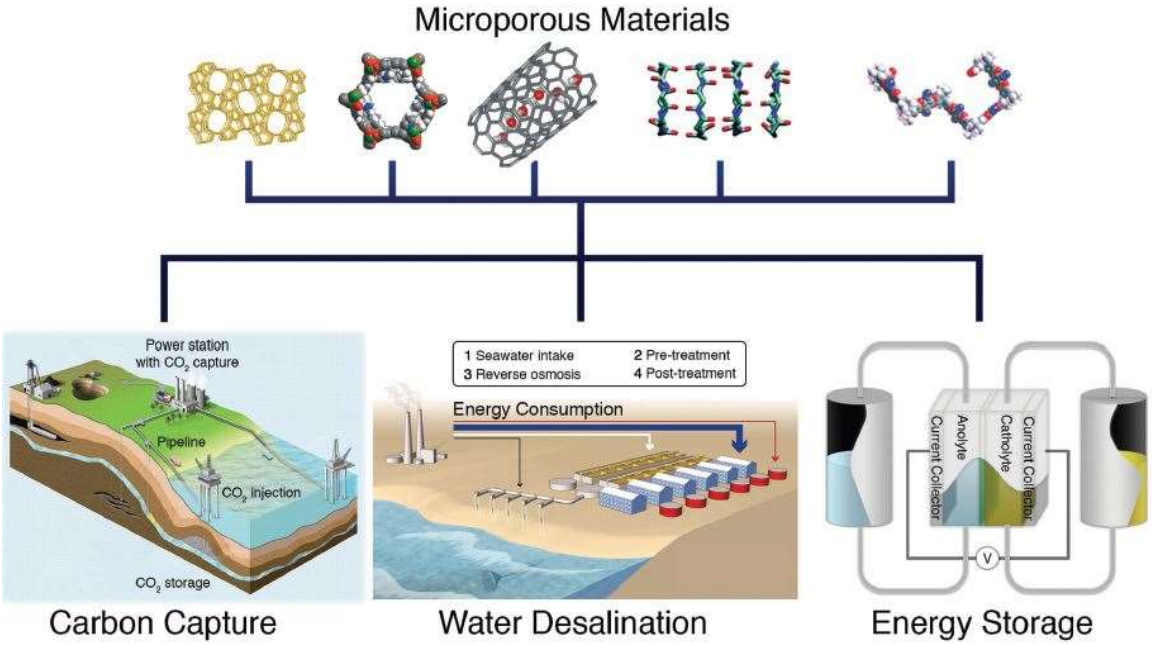

Figure 1.2 – Possible applications of porous materials [4]

The primary classes of microporous materials are; inorganics, made of ordered inorganic units (i.e. zeolites), hybrids, made by the ordered union of organic and inorganic units (i.e. metal-organic frameworks), carbons, ordered structures made by joining carbon atoms in various ways (i.e. carbon nanotubes and carbon molecular sieves) and organics, made of ordered organic units (i.e., microporous polymers and organic nanotubes) [4].

1.1.2 Metal-Organic Frameworks (MOFs)

Metal-organic frameworks are a class of materials that are made by joining metal-ion units with organic linkers which are alternatively linked through a strong bond to create highly ordered crystalline structures. The term metal-organic framework was first mentioned by Yaghi et al. in 1995 when they produced a copper-based metal-organic framework

through hydrothermal synthesis [5]. The way those metal-ions and organic likers are bonded can lead to mono-, bi- and tri-dimensional networks (Figure 1.2).

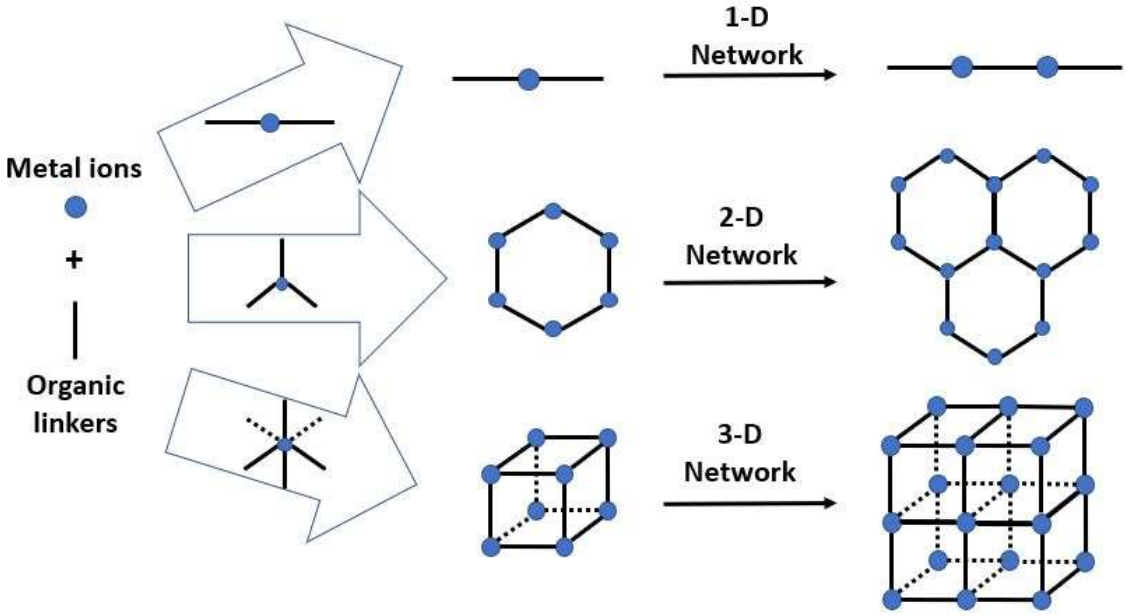

Figure 1.3 – Metal-organic frameworks different networks obtained starting from metal ions and organic linkers

Furthermore, the flexibility of this combination of both inorganic and organic units leads to a very high number of compounds and networks, the metal-organic frameworks already synthetized are nearly 70000 [6], but the growth is ongoing and every year the number of metal-organic framework structure reported increases (Figure 1.3).

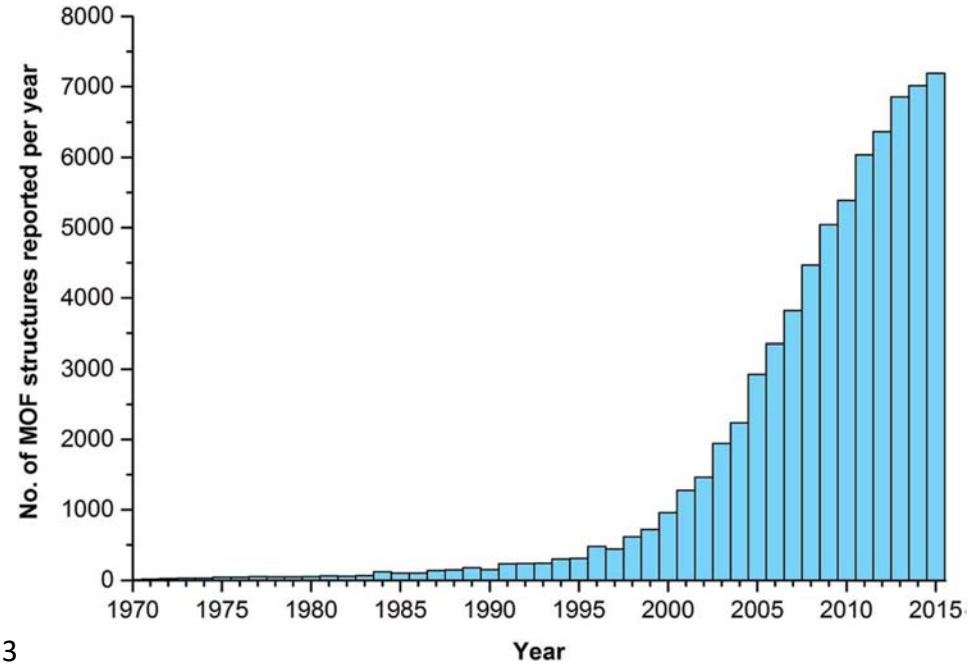

3

Figure 1.4 – Temporal growth of the metal-organic framework structures reported per year [7]

The precision commonly exercised in their chemical modification and the ability to expand their metrics without changing the underlain topology have not been already achieved with other solids. The fact that metal-organic frameworks can be synthetized from a high variety of organic and inorganic compounds leads them to have a broad range of properties that can be tuned varying both the organic or the inorganic part. These properties, such as diverse topology, very low density, high porosity, tuneable pore size of molecular dimensions and record-breaking surface areas (up to 7800 cm^2g^{-1}) [8], made metal-organic frameworks a very attractive class of materials. This is because traditional porous materials like zeolites, structured carbons, porous polymers, etc. usually have only some of these features, but only metal-organic frameworks can group them all. These properties make these materials of high interest for several applications including the classic uses of porous materials in catalysis and gas storage and separation, which are based on the pore shape and size and are becoming more important due to environmental concerns, but also applications in other fields like biomedical and sensors areas [9]. So, the uniqueness of metal-organic frameworks among porous material have made metal-organic frameworks to be studied deeply in the last years.

Depending on the choice of the metal ion and the organic linkers the shape of the particles, the pore size, the framework topology can be affected and then the overall chemical functionality of the structure. Furthermore, the possibility to design metal-organic framework structures at molecular level in a tailored way is interesting tool and gives the possibility to choose if the added functionality can be inserted directly into the structure with a functionalized component, either the metal ion with an exposed cation site or the organic linker functionalized with amine or polarizing groups for example, or can be added after the synthesis via post-synthetic modification [3, 10]. The first is applicable when the functional groups are stable at the synthesis condition and don't interfere with the formation of the frameworks, instead with post-synthetic modification the advantage is that the functional groups only need to be compatible with the final material and with the relative reaction conditions [11]. These ways to functionalize the material can enhance or give additional properties to metal-organic frameworks for many specific applications and furthermore this ease of functionalize is a great advantage over the other microporous materials.

Although metal-organic frameworks seem to be very promising for the applications mentioned before, they have even some drawbacks. Indeed, metal-organic frameworks have a relatively limited thermal and chemical stability, that depends on the relatively weak bonds that are formed between the metal ion and the inorganic linkers, compared to their inorganic counterparts; some of them are air and moisture sensitive after the evacuation of the pores and there is the need for careful handling under an inert atmosphere. [3, 12].

A property that hasn't been yet fully investigated, but that should be considered for CO_2 capture applications, is the mechanical stability of the metal-organic frameworks.

These materials should have a sufficient mechanical stability to allow a dense packing of the adsorbent surface without loss of the framework, slight perturbations to the structural or chemical features under a high mechanical pressure could have could change the properties of the structure and have an effect on the capture performances [12]. For example, it was demonstrated that the application of high pressures, on the order of GPa, can lower the lattice volume of a metal-organic framework, in this case the HKUST-1, up to the 10 % [13].

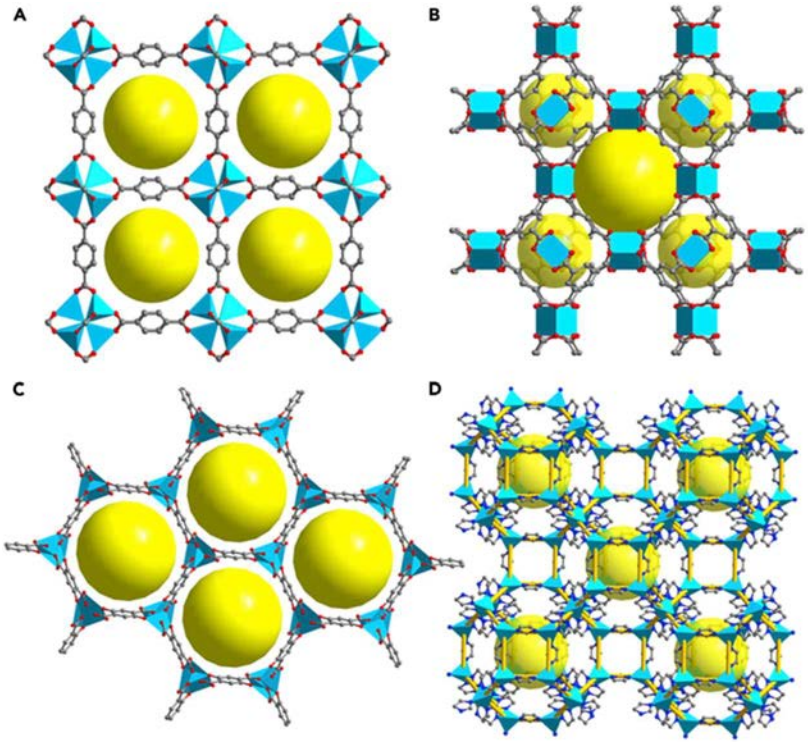

Figure 1.5 – (A) MOF-5, (B) HKUST-1, (C) Mg-MOF-74, (D) ZIF-8.

C is represented in grey, O in red and N in blue. The yellow balls represent the porosities. [14]

Even though is not already fully understood how this reduction of the volume of the lattice would affect the adsorption properties, for applications in the real world would be worthen a more specific investigation. Another problem is that they can be synthetized mainly at gram scale and with discontinuous processes, so they are not already suitable for quantitative or industrial production [15].
Some of the most representative and studied metal-organic frameworks nowadays are MOF-5, HKUST-1, Mg-MOF-74 and ZIF-8, their structure is shown in Figure 1.4.

1.1.3 Mechanochemical synthesis

Even though the apparent ease of synthetize metal-organic frameworks with a modular approach, a great challenge is to optimize the reaction condition for obtaining the wanted metal-organic framework with a high crystallinity and a high yield. Small changes in the reaction parameters such as the presence of a cosolvent, metal counter-anion, metal-to-linker ratio, the reactant concentration, solution pH, reaction time, and reaction temperature could lead to have a great impact in the products obtained [12]. Should be noted that there are many connectivity combinations even when just only a metal ion and an organic linker are combined and probably many of them have not even porous structures that are required when dealing with gas adsorption and separation application. Thus, the knowledge of best conditions that lead to the desired product can involve many trial and error stages in which the reaction parameters are systematically varied.
Nowadays the MOFs are synthetized mainly under solvothermal conditions. This type of synthesis consists in the dissolution of precursors in organic solvents in sealed reactors and heated to temperatures and pressures such as to cause the reaction to take place, then the excess solvent is evaporated, thereby causing the reaction products to remain in solid state [15]. These reactions allow to obtain MOF with good purity and excellent crystallinity, but also present several problems. The main problems are that they have a very low yield, since they typically require a lot of time to react, and the process is non-scalable, it is therefore difficult to obtain a massive production [15]. Furthermore, there are also environmental problems because very often organic solvents can't be recovered and therefore large quantities must be disposed of to produce significant amounts of

MOF. Many alternative methods have been evaluated to shorten the synthesis times and increase the quantities produced and make the process scalable, such as microwave-assisted solvothermal synthesis to reduce reaction times, sonochemical synthesis where ultrasounds are used to increase the crystal growth rate, electrochemical synthesis that makes the reaction more efficient and finally the mechanochemical synthesis which is a method of synthesizing through the grinding of the reagents without using any solvents or using small amounts of them [16, 17, 18, 19, 20, 21].

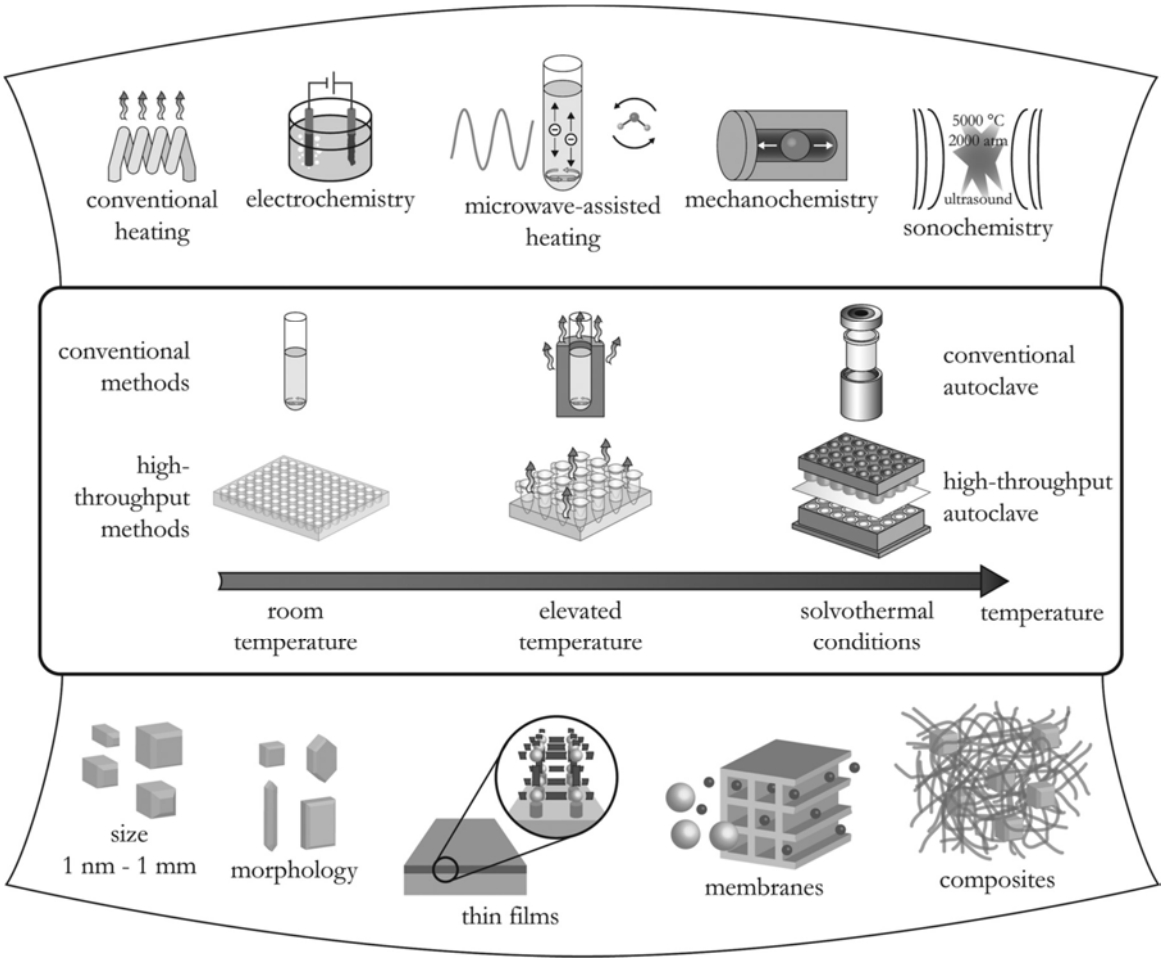

Figure 1.6 - Overview of synthesis methods, reaction temperatures and final products in MOF synthesis. [21]

The latter technique is one of the most interesting, since it can solve some of the problems seen previously for solvothermal synthesis.

Mechanochemical synthesis is a technique that comes from metallurgy and mineral processing but within in the last few decades it has developed rapidly into many areas of chemistry such as inorganic chemistry, catalysis and pharmaceutical synthesis [15]. This type of synthesis is based on performing chemical reactions exploiting the shear stress

applied by milling or grinding processes on the solid reagents without any or with only small quantity of solvents and can be done either at room temperature or tailoring the temperature depending on the need [15]. With this approach the traditional solvothermal MOF reactors are replaced by a mortar and pestle or automated ball mills [15]. In addition to the solvent-free conditions, this type of synthesis provides a route to a faster and more efficient synthesis of MOFs obtaining higher yields and allows the use MOF precursors with low solubility such as oxides, hydroxides and carbonates [15]. However, the big limitation is the up-scaling of mechanochemical synthesis, it is essentially a batch processing technique with a relatively low rate of production. Furthermore, it should be noted that despite a solvent-free synthesis, in the purification or activation step may still be required the use of a solvent, or a catalytic amount of solvent could be needed so that the reaction can take place [22]. Anyway, this synthesis approach can be considered the most environmentally friendly technique to produce metal-organic frameworks if compared with the other methods and could also reduce the production cost [23].

There are three types of mechano-chemical synthesis. The former is called solvent-free grinding (SFG) and consists of grinding totally avoiding the use solvent, then there are liquid-assisted grinding (LAG) and ion-liquid assisted grinding (IALG) that both uses catalytic amounts of liquid for increasing the mobility of the reagents and then increase the reaction rate, the difference between the two methods is that in the latter there are traces of additive salts to accelerate even more the reaction [19, 24]. Using these techniques, the synthesis for almost all families of metal-organic frameworks has been demonstrated [15].

Mechanochemistry is a versatile method that allows the synthesis of most of the common MOF structures but for many of the performed syntheses described there is a problem in up-scaling the process to an industrial scale, indeed all the processes have very low yield. For this reason, extrusion and batch mixing techniques have been explored for the up-scaling of MOF production under solvent-free or low-solvent conditions. Although batch mixing is still a discontinuous manufacturing technique, it was proved that allows to use the mechanochemical method and can be used as primary step before passing to continuous processes such as extrusion [20]. Indeed, extrusion is one of the most well-known continuous manufacturing processes, it has many applications in industry like metal, plastic, food and pharmaceuticals processing, and it was proved to be an effective

technique for the synthesis of MOFs in higher volume respect to all the other methods mentioned before.

It was demonstrated that mechanochemical synthesis can either be performed by batch mixing and extrusion. In 2018 Crawford, McNally et al. showed the possibility to perform mechano-chemical synthesis with batch mixer. With the use of batch mixer was possible to correlate the progress of the reaction with the temperature, specific mechanical energy and machine torque. This knowledge and the fact that the batch mixer used was designed to mimic a short segment of a twin-screw extruder enabled the possibility to optimize the mechanochemical reactions by extrusion tailoring the parameters of the extruder, such as temperature, screw speed and feed rate, for obtaining the best reaction conditions [20]. In 2015, Crawford, McNally and co-workers showed that the mechano-chemical synthesis of HKUST-1, ZIF-8 and aluminium fumarate metal-organic frameworks with both single-screw (SSE) and twin-screw extrusion (TSE) was possible [19]. The metal-organic frameworks were obtained feeding the extruder with the precursors and catalytic amounts of solvent, in the case of ZIF-8 the synthesis was solvent-free, let them passing through the barrel of the extruder at the temperature wanted and then collecting the extrudate at the exit die. The extrudate was then activated and XRD measurement confirmed the synthesis of the wanted metal-organic frameworks. Since extrusion is a continuous processing technique the space-time-yield (STY) of the reaction is very high compared to one of the solvothermal synthesis. Furthermore, the data on STY of extrusion process are very promising and the this type of process, with further studies on this method for the synthesis of the metal-organic frameworks and by using large-scale equipment, could lead to kilogram scale production and in some cases the process will be even solvent-free [19]. Furthermore, in 2018 Kardeniz et al. have showed that the liquid-assisted mechano-chemical synthesis of the metal-organic framework UiO-66-NH_2 with the twin screw extruder was possible. They obtained the metal organic framework wanted, the synthesis was confirmed by XRD analyses, with a yield of 1.4 $kg \cdot h^{-1}$ that was way higher than the one obtained with the planetary mills in the same work [25]. Extrusion can be an efficient way to produce metal-organic frameworks with solvent free reactions with high and very promising space-time-yield (STY). Kilogram scale production could be achieved by using a large-scale equipment paired with a more detailed knowledge and understanding of the MOF synthesis by this methodology.

1.1.4 Gas adsorption and separation in MOFs

Metal-organic frameworks have many interesting properties such as excellent surface area, tuneable pore surface properties and, thanks to mechano-chemical synthesis and the application of that synthesis on well-known processing techniques, have made them a potential candidate for scalability to industrial scale. For all these reasons, these materials became an attractive subject for further study and for finding suitable applications for exploiting all their properties. One of the most studied application of metal-organic frameworks is the applicability of these materials on the field of gas adsorption and separation.

As mentioned before, there are various synthesis techniques to produce the metal-organic frameworks and there are many differences on the conditions that lead to the formation of the desired products, but in most cases the void spaces within the pores of the resulting materials, that are fundamental for the gas adsorption and separation properties, are occupied by the solvent used during synthesis or for the activation or in some other cases by the by-products of the reaction [12]. Thus, for having good performances the solvents or the by-products that occupy the void spaces within the pores must be removed, this can be done by applying heat or vacuum. After freeing up the void spaces the pore volume and surface area are increased and the pores became accessible to guest molecules like gases [12]. The emptied pores can then be utilized to perform the gas separation or gas adsorption.

The gas that has received most attention on being adsorbed or separated is the CO_2, for obvious environmental reasons. Furthermore, even in the context of CO_2 capture, the possibility to modify the surface chemistry of metal-organic frameworks is a topic of interest, because ensure the ability to install the desired chemical features for installing the desired chemical features (i.e. amines or polarizing groups) for improving the properties of the material. As said above, the two ways of installing the wanted functionalities on the framework are the direct insertion in the structure choosing an already functionalized linker or a metal ion with an exposed cation site and the post-synthetic modification of the surface functional groups that follows the initial formation of the crystalline structure [10]. These functional groups can facilitate selectivity properties by enhancing the affinity to the desired gas and also enhance gas storage

properties since they permit to the guest molecule to approach closer to the pore surface [12].

A high selectivity for CO_2 among the other gases that compose the gas mixture for gas separation and adsorption is required, and this selectivity can be achieved by two main mechanisms. In size-based selectivity take place a kinetic separation, the small pore size of the selected metal-organic framework could allow to diffuse in the pores only the molecules until a certain kinetic diameter, so with this mechanism the gas molecules are basically separated depending on their size (Figure 1.7) [26].

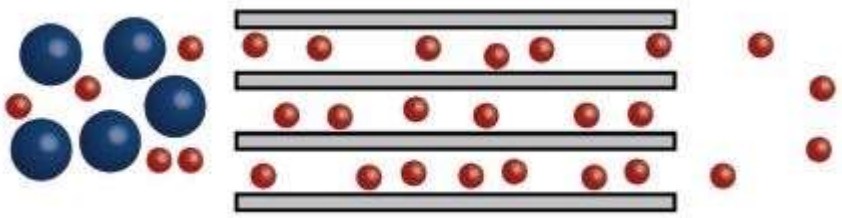

Figure 1.7 – Kinetic separation [4]

In kinetic separations the difficulty lies in the fact that these molecules have a similar kinetic diameter, for example in CO_2/N_2 the kinetic diameters are 3.64 Å for Nitrogen and 3.30 Å for carbon dioxide [27]. This similarity in the kinetic diameters of the molecules would require material with very small pore size for operating on a size-based mechanism, but this could lower the overall gas diffusion through the material [28]. There are metal-organic frameworks that have pore size in this range, but those that have high surface area and exhibit high adsorption capacities for CO_2 possess pore apertures that are way higher than the size of these molecules [12].

Indeed, the major part of the studies conducted for the separation of molecules on metal-organic frameworks is based on the mechanism of adsorption phenomena. The adsorptive selectivity, that can be termed even thermodynamic separation, relies on the fact that the components of the gas mixture have different affinities in being adsorbed on the pore surface of the metal-organic framework.

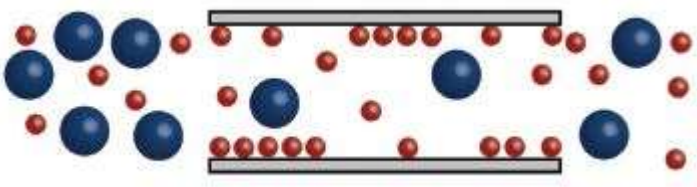

Figure 1.8 – Adsorptive separation [4]

For this type of mechanism a physisorptive interaction can be used for the separation. In this case the separation process is based on guest molecules having small differences in physical properties, like the dipole or quadrupole moment or the polarizability, that results in a higher enthalpy of adsorption of some gas molecules over other [10]. In CO_2/N_2 separation for example the two gas molecules have differences in both polarizability and quadrupole moment. Carbon dioxide has higher polarizability ($29.1x10^{-25}$ cm^{-3}) and quadrupole moment ($13.4x10^{-40}$ $C{\cdot}m^2$) that nitrogen (that has respectively $17.4x10^{-25}$ cm^{-3} and $4.7x10^{-40}$ $C{\cdot}m^2$). This paired with the insertion of structural components that have high charge densities, like exposed metal cation sites or polar organic substituents, on the framework surface can be used to enhance the selectivity on the gas mixture [1, 29].

As an alternative, the adsorptive selectivity can be achieved even by chemisorptive interactions. In this other case the separation process is based on the chemical interactions between the guest molecules and the surface functionalities installed on the structure. Respect to the purely physisorptive mechanism, the chemisorptive one can result in higher selectivity owing to defined molecules that can chemically interact and create bond with the functionalities on the framework surface [12]. Always in CO_2/N_2 separation, the high susceptibility of the C atom in carbon dioxide to attack by nucleophiles can be exploited with surface appended groups possessing strong Lewis bases, like amines [10]. The interaction between the carbon dioxide molecule and the amine can lead to the formation of C-N bond resulting in higher selectivity over N_2 [12].

However, these materials for being applied should work even in the real-world conditions, for example for post-combustion flue gas of coal, where the gas mixture is not only a binary mixture but contains many other gases in different percentages and his temperature and pressure can vary in a wide range. An ideal adsorbent for CO_2 from post-combustion flue gas would have high volumetric and gravimetric CO_2 adsorption capacities, high selectivity over the other gases, fast diffusion of the gas, stability under the operating conditions and low energy input for regeneration [12]. Nowadays metal-organic frameworks can't yet fulfil all these requirements, even though a lot of significant progresses has been made in these years and that are still on going because there is a lot of research in this field.

1.1.5 Mixed Matrix Membranes (MMMs)

Gas separation by membranes is a field that is constant and rapid growing and has attracted a lot of interest in the recent years [30, 31]. The concept behind the membrane-based gas separation process is to exploit the differences in permeation trough membranes of the single components that have to be separated from gas mixtures. There are several advantages in using membranes for separation such as low energy requirements, low operating and capital costs and generally ease of operation [30]. For these reasons membrane gas separation process has acquired strong interest in industry, since flue gas separation is a very actual problem in many industrial fields [31, 32]. Nowadays the applications of membrane-based gas separation include the removal of carbon dioxide and of volatile organic compounds from flue gases, oxygen and nitrogen enrichment, natural gas separation and hydrogen recovery. For totally exploiting all the opportunities given by membrane separation some requirements have to be respected. In general, those materials, besides having high permeability rate and selectivity that are the basic parameters, have to be durable, mechanically and thermally suitable for the operating conditions and have a considerable separation efficiency and productivity. A paired high permeability and high selectivity lead to more flexible operation parameters, lower driving force and smaller membrane area are needed to have the wanted separation [30]. Polymer membranes used for membrane application such as gas separation have been used mostly in already commercialized devices, this is because polymers have the advantages of economical and well-known processing capabilities and the desired mechanical properties. In non-porous polymers the mechanism of transport is the solution-diffusion model. The permeation of molecules through membranes is ruled by two material properties: the solubility (S) and the diffusivity (D). The solubility coefficient is the ratio of the concentration of the dissolved penetrant in the surface of the polymer to the partial pressure of the penetrant. The diffusivity measures the mobility of the single molecule passing through the spaces between the polymeric chains [30]. The permeability (P) represents the capacity of molecules to permeate through a membrane and is defined as:

$$P = D \cdot S \tag{1}$$

Then the differences in permeability of a membrane are given by the differences in diffusivity of the various gas species in the polymer and by the differences in physiochemical interactions of the gas species with the polymer. These parameters control the amount that can be accommodated per unit volume on the polymer matrix [30].

The capacity of a membrane to separate the molecule i by the molecule j, is the ratio of their own permeabilities in the membrane, this property is called selectivity (α):

$$\alpha_{ij} = \frac{P_i}{P_j} \tag{2}$$

And combining the Eq. 1 and Eq. 2 results:

$$\alpha_{ij} = \frac{D_i}{D_j} \cdot \frac{S_i}{S_j} \tag{3}$$

The balance between the selectivity given from the diffusivity and the selectivity given from the solubility controls the selective transport of the components in the gas mixture. As seen, the gas separation performances of non-porous polymeric membranes are determined by the intrinsic properties of the polymer material, such as diffusivity and solubility [33].

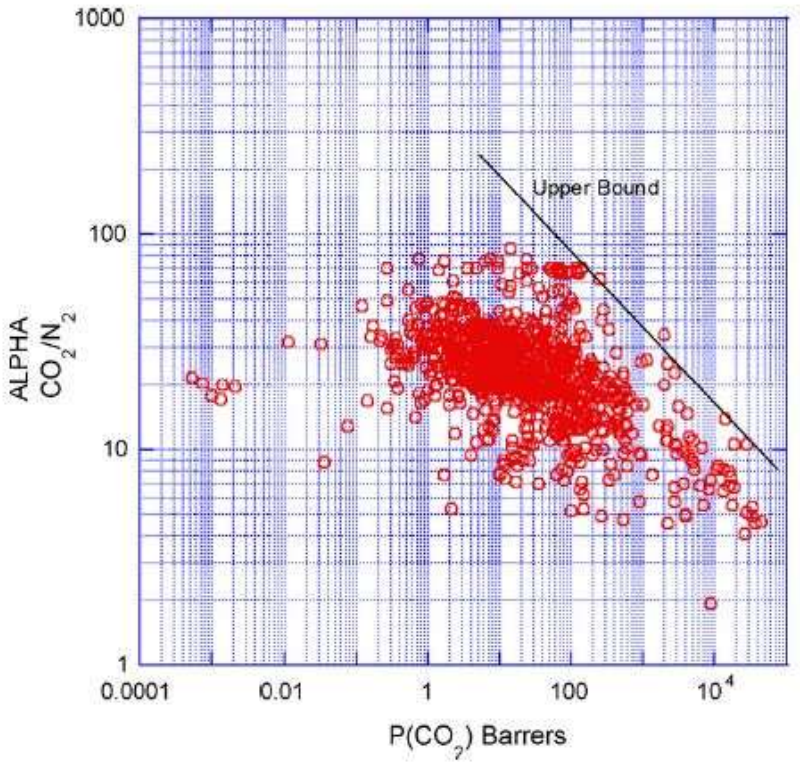

Figure 1.9 – Revised Robeson upper bound for CO_2/N_2 separation [34]

In the last years there was a strong interest in research on membranes to enhance the separation performances tailoring the polymer structures but, even though there was a lot of work on this topic, the gas separation performances of polymeric membranes mostly stays in the limits of trade-off between permeability and selectivity determined by Robeson plot that was firstly indicated in 1991 and then revised in 2008 (Figure 1.9) [35, 36, 34].

Contrarywise, the separation performances of some inorganic membrane materials, such as zeolites, metal-organic framework and structured carbons have been reported to be very good and, in some cases, well above the upper bound [35]. Besides their exceptional separation properties, these inorganic materials also have better thermal and chemical stabilities as opposed to polymer materials [3]. However, these materials have even drawbacks respect to the polymers, such as the lack of processability, because of their fragility, and the high cost, since the production yields are low. These things make the large-scale production difficult. For example, in low pressure and high-volume applications, like CO_2 capture from flue gases, the production of inorganic membrane modules with a high packing density membrane is an issue [35].

To resolve these problems, the research was addressed to combine the advantages of both inorganic and polymeric material to create a new class of membrane and nano-composite materials. This new class is called mixed-matrix membranes. A mixed-matrix membrane typically contains a main phase that consist of a polymeric material and a dispersed phase that consist of inorganic material particles. The idea to make a composite with a polymeric and an inorganic phase has the aim to pair the advantages, and then to overcome the drawbacks, of the two phases used singly. Hence, having the inorganic phase dispersed in a polymer matrix, the mixed-matrix membrane could enhance the gas separation performances thanks to the inorganic particle and keep even the advantages of the polymer, such as ease of processability, suitable flexibility for membrane application and low cost. Nowadays, metal-organic frameworks are playing a central role as fillers in mixed-matrix membranes respect to others inorganic particles, this is due to their exceptional properties in gas separation and adsorption mentioned above. The most used metal-organic framework at the moment in this field are HKUST-1, ZIF-8 and UiO-66 [37, 38, 39, 40].

For an ideal gas transport, the mixed-matrix membrane should have a morphology that allow the molecules to be transported preferentially through the inorganic phase rather than the polymer phase [35]. Hence, one of the most important issues to take into account for this topic is the choice of the morphology of mixed-matrix membranes. The two main morphologies for mixed-matrix membrane are symmetric or asymmetric morphologies (Fig. 1.10).

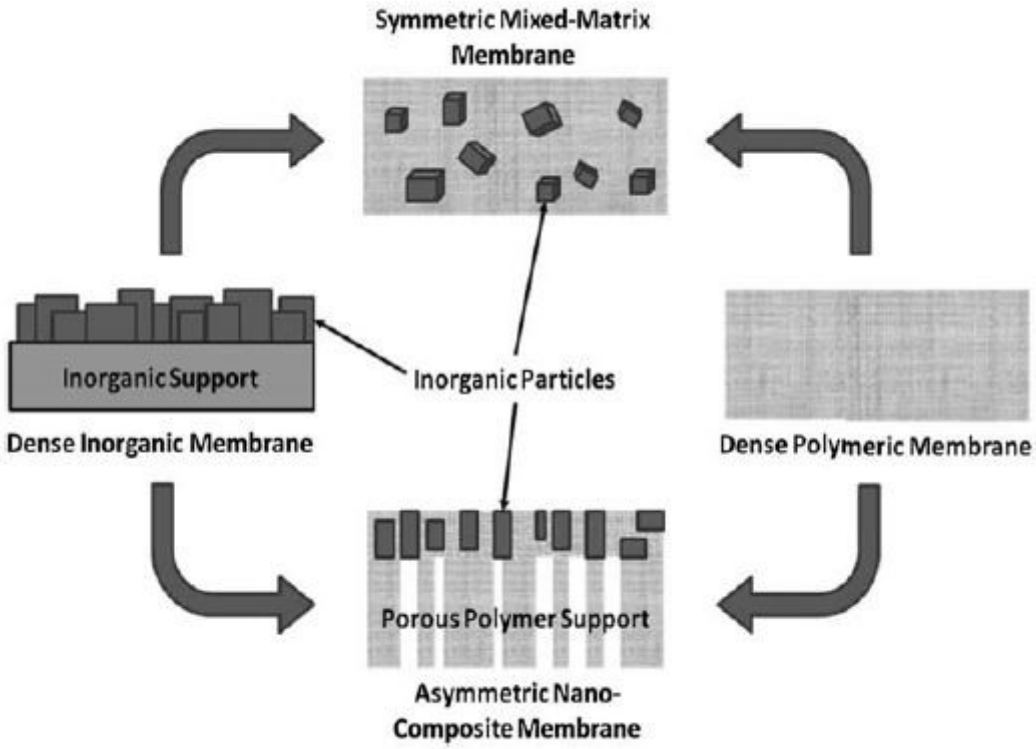

Figure 1.10 – Morphologies for mixed-matrix membranes [35]

The main aims on selecting a membrane morphology should be to maximise the rate of permeation of the molecules through the inorganic filler and to reduce the total path covered by the molecule trough the membrane [35].

Due to the ease of the fabrication process, the symmetric morphology is the most frequently studied one for the application on mixed-matrix membranes. A key parameter of this morphology is a good dispersion of the inorganic particles into the polymer matrix. However, a criticality with the mixed-matrix membranes is that the inorganic particle loading can't be above a certain limit, this is because at high loading the particle tends to agglomerate [41]. Hence, there is a difficulty to exceed percolation threshold and therefore the gas transport through the symmetric membranes is more likely still to be

dominated by the polymer phase rather than the inorganic one. [35]. Then the properties on gas separation of the inorganic cannot fully exploited and only a limited improvement on the separation properties can then be expected. Another defect to consider for symmetric mixed-matrix membrane is that the thickness of the membrane has to be suitable for real-world application. Due to the mechanical properties of the materials involved the result is that the thickness required is high and can generate resistance for the permeation of gas molecules and the lowering drastically the overall permeability of the system [35]. A further parameter to consider in mixed-matrix membranes is the interface between the polymer matrix and the inorganic filler. These interfaces can have five different morphologies [42, 43] (Figure 1.11).

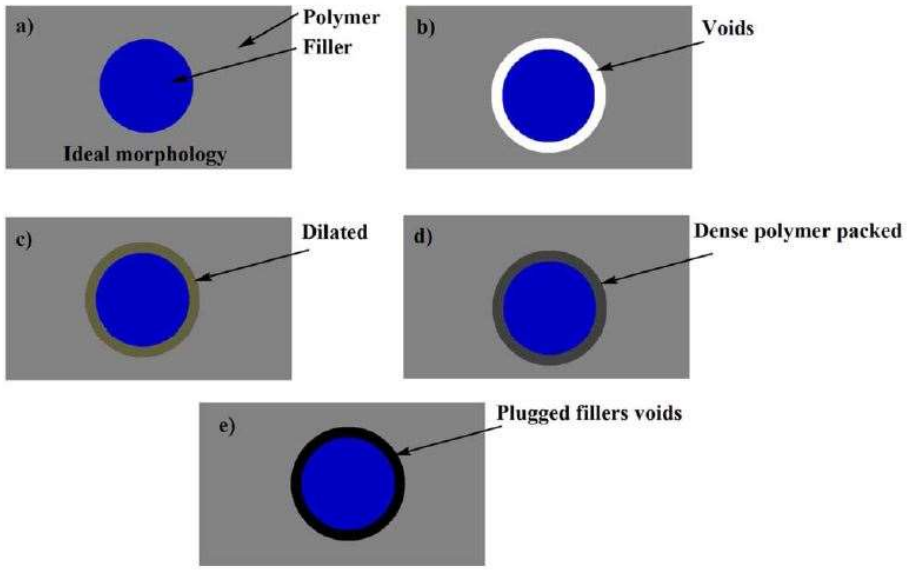

Figure 1.11 – The five different morphologies of interface between the polymer and the organic filler [43]

Figure 1.11(a) shows the ideal interface between the phases that is ideally free of defector distortions, which is generated when the two phases have good interfacial interactions. Figure 1.11(b) shows when the polymer and the filler are incompatible, the result of incompatibility is that void are present on the interface and this can dramatically affect the gas selection properties. Figure 1.11(c) shows a low density of the polymer chain near the filler, that results in a dilated interface. Figure 1.11(d) shows a dense interface that is the result of a densely packed polymer zone around the filler that is a sign of strong interaction between the two phases. Besides of the morphologies mentioned, it is

possible that the filler can be plugged, as shown in Figure1.11(e) and this can occur during the fabrication process of the mixed-matrix membranes [43].

On the other hand, nano-composite asymmetric membranes are typically composed by an ultra-thin top layer, which is made by a thin polymer matrix and filled with the wanted inorganic particles that have a size similar to the one of the polymer layer, and a porous substrate under the top layer to provide physical support (Figure 1.10).

With this morphology a lower resistance to permeability can be achieved compared to symmetric morphology, the reason of this is that the selective layer is thinner respect to symmetric one because it doesn't need to have mechanical resistance that is provided from the porous support [35]. Furthermore, another advantage of this morphology is that a potentially higher particle could be inserted on thin layer, thus the percolation threshold could be achieved and the gas transport could be led by the inorganic phase with the molecules passing preferentially trough the inorganic particles enhancing the selectivity properties [44].

However, the main drawbacks of this morphology are the difficulty of the fabrication process, its scalability to an industrial scale and the difficulty to obtain defect-free membranes [30]. Indeed, these problems are an hinderance for real applications because they can significantly affect the membrane separation performances.

1.2 Field of application

The continuous increase of the level of atmospheric CO_2 has been studied in detail in recent times due to its implication in global warming, developing environmental concerns about the use of fossil carbon-based fuels. Indeed, the data confirm that concerns because in modern time history the concentration CO_2 has never been as high as in the present time (409 ppm in 2018) [45] and the growth is on-going as can be seen in Figure 1.12.

Before to the sudden increase observed over the past century, the atmospheric CO_2 level has only increased or decreased gradually in larger time windows within the range 100-300 ppm. Thus, the motivation of this rapid increase is to be found the continuous and exponential increase of global economic and industrial development over the past century and coupled with this the growing of the global population. This massive industrialization

has contributed to increase the level of CO_2 concentration creating anthropogenic sources of CO_2 taking the concentration of carbon dioxide above those expected from natural fluctuation [12].

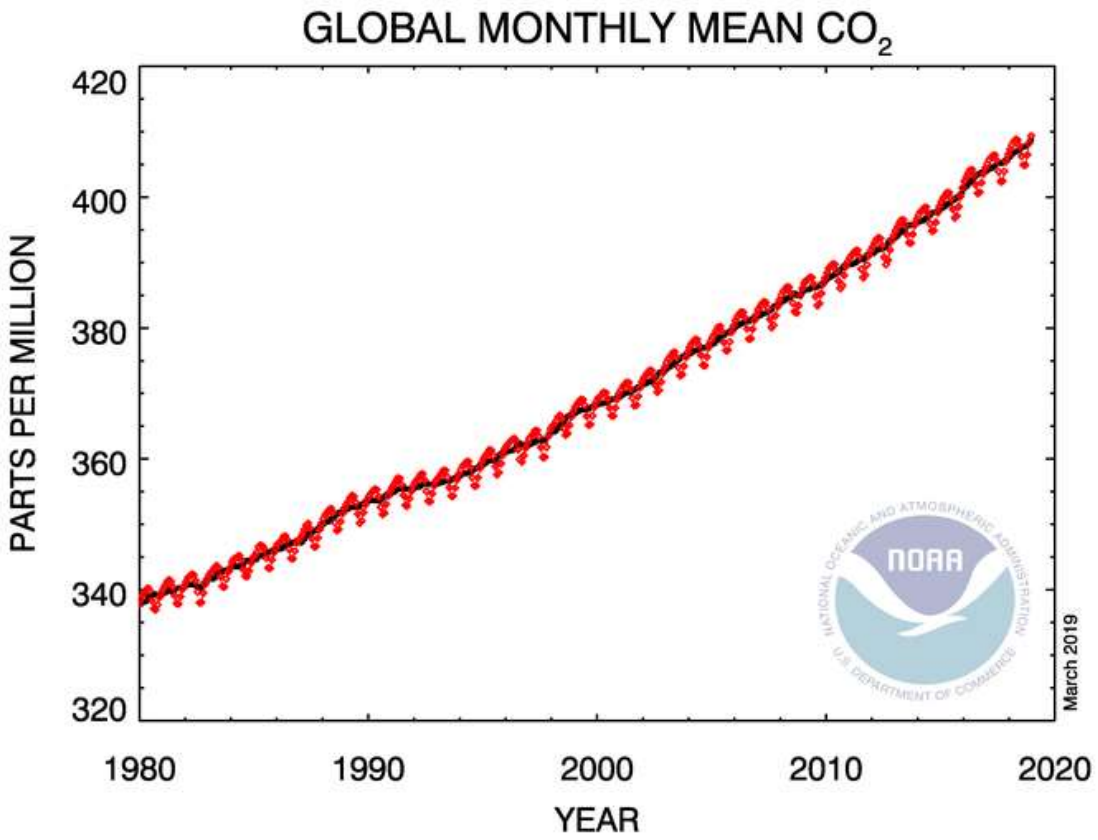

Figure 1.12 – Global monthly mean of CO_2 concentration since 1980 [45]

The fossil fuels combustion and the industrial processes are by far the major sources global greenhouse gas emissions [46]. These emissions, which arises mostly from the combustion of oil, natural gas and coal, will continue to increase in the future because of the economic, industrial and population growth, mostly in the developing countries [46, 47]. Even though the conversion of the current infrastructure from carbon-based sources to alternatives with lower environmental impact would be ideal, is a too drastic change to be applied immediately because it would need structural modifications to the actual energy framework and many technologies that have been proposed are not ready to be applied on large scale. Hence, carbon capture technologies, that are able to capture CO_2 from emission source will have a fundamental role in the near future on the field of carbon dioxide emission reduction, until cleaner sources of energy will be implemented on large scale [12].

Figure 1.13 – Carbon capture from flue gases [48]

One field in which CO2 capture technologies could be implemented at is stationary point sources of emissions, such as fossil fuels power plants, without altering the structure of the plants (Figure 1.13). On the total CO2 emissions, the 60% can be associate with electricity generation can be attributed to electricity generation, hence the installation of these capture systems on existing power plants could have a considerable effect on reduction in emissions [12, 46]. Then captured CO_2 have to be disposed with a permanent sequestration, where the CO2 is injected into underground geological formations, or reused as a reactant for other chemical reactions [12].

Due to their properties listed above that make them suitable for this applications, metal-organic frameworks and their implementation in mixed-matrix membranes, are two materials that have attracted a high interest in the research area regarding this topic. Indeed, there are many examples of mixed-matrix membranes filled with different metal-organic frameworks. In 2018 Marti et al proved that an in-situ synthesis of the metal-organic framework UiO-66 was possible during the production with, solution casting, of the composite, unifying the two processes of the synthesis of the UiO-66 and the composite production in only one step [38]. A drawback of these composites is the fact is that they are obtained mostly with solution casting method, that is a discontinuous

process with a very low yield, and only in few examples the composites are produced with continuous processes such as extrusion [49].

1.3 Project scope and objectives

The idea behind this project is to provide new functional solutions for the production of the composites containing metal-organic frameworks as filler. In particular, the recent progress in the mechanical-chemical synthesis of metal-organic frameworks, which has made possible to make the synthesis continuous and to have yields well above the yields given by the previous synthesis methods, allowed to have a try in coupling this method directly within the compounding process. Therefore, it is a matter of synthesizing the metal-organic framework continuously during the compounding process that takes place inside the extruder, and so having the composite already compounded with the polymer matrix at the exit of the extruder die. This would allow to reduce the number of steps necessary for the production of these composite materials, thus significantly increasing their rate of production and could render them suitable for industrial scalability.

2 MATERIALS AND METHODS

2.1 Materials

2.1.1 Poly(methylmetacrylate) (PMMA)

Plexiglass 6N Moulding Compound poly(methylmetacrylate) (PMMA) had a processing temperature range of 220–280 °C, a density of 1.19 g·cm^{-3} and a melt flow rate (MFR) of 14.28 g/10 min at 230 °C and 3.80 kg (ISO 1133) and was supplied by Evonik Corporation in pellet form.

2.1.2 2-Methylimidazole (2-MI)

2-Methylimidazole, with a melting point at 142-143 °C and a boiling point at 267-268 °C, a molecular weight of 82.10 g·mol^{-1} and a density of 1.09 g·cm^{-3}, was purchased from Sigma-Aldrich.

2.1.3 Basic Zinc Carbonate (BZC)

Basic Zinc Carbonate, with a molecular weight of 555.0 g·mol^{-1} and a density of 3.50 g·cm^{-3}, was purchased from Honeywell.

2.2 Equipment used

2.2.1 Twin screw extrusion

The Thermo Scientific Haake Mini-Lab II micro-compounder (Figure 2.1) was equipped with two conical corotating screws and it allows recirculation of compound within a chamber of volume 5 cm^3. The twin-screw extruder was employed with a barrel temperature set to 220 °C, a screw speed of 75 rpm and a recirculation time of 1, 2, 3 and 4 min. The polymer was dried at 80°C for 3 hours prior to mixing.

Figure 2.1 - Thermo Scientific Haake Mini-Lab II micro-compounder

2.2.2 Batch mixing

The Thermo Scientific Haake PolyLab Rehomix OS batch mixer (Figure 2.2) was equipped with two counter-rotating Roller rotors and had net chamber volume of 69 cm^3, considering also the volume occupied by the rotors. The batch mixer was employed at a temperature of 160 °C, a rotor speed of 75 rpm for an approximative residency time of 3 minutes and a filling volume of 60 %.

Figure 2.2 - Thermo Scientific Haake PolyLab Rehomix OS batch mixer

2.2.3 Hot press

The Collin hot press (Figure 2.3) was used for the compression moulding of both the neat polymer and the composites. The samples in pellet were placed in the mould and heated to 200 °C in the press for 30 second with no pressure applied, then a step of 50 bar pressure was applied alternatively to a no pressure step in a degassing stage, after this stage a continuous pressure of 50 bar was applied for 3 minutes and then the samples were cooled with the pressure applied until the temperature was lowered at 100 °C and finally extracted from the mould.

Figure 2.3 - Collin hot press

2.2.4 Thermo-Gravimetric Analysis (TGA)

Thermo-gravimetric analysis (TGA) was carried out using a Mettler Toledo TGA1-STARe system under the flow of air and nitrogen. The sample weights ranged from 5-10 mg and were loaded into 70 µl alumina pans. The samples were heated from room temperature to 1000 °C at a constant heating rate of 10 $K \cdot min^{-1}$. Decomposition temperatures of the materials analysed were determined from the onset of weight loss from the weight percent and first derivative curves.

Figure 2.4 - Mettler Toledo TGA1-STARe thermo gravimetric analyser

2.2.5 Fourier Transform Infra-Red Spectroscopy (FTIR)

FTIR measurements were taken using a Bruker Tensor 27 spectrometer equipped with an attenuated total reflectance (ATR) crystal and specac golden gate heating stage. Spectra were recoded the OPUS analysis software in the range of 500–4000 cm^{-1} at room temperature. The resolution was set to 4 cm^{-1} and averaged over 32 scans to acquire each spectrum.

Figure 2.5 - Bruker Tensor 27 spectrometer

2.2.6 X-Ray Diffraction (XRD)

X-ray diffraction (XRD) was used to characterise the crystalline structure of the composites. XRD spectra of the materials were collected using a PANalytical Empyrean X-ray diffractometer equipped with a Co (Kα1 (λ) = 1.789 Å) source and PIXcel3D detector and then converted to Cu (Kα1 (λ) = 1.541 Å) through the software PowDLL converter. A tube voltage of 40 kV and current of 40 amps was employed. The measurements were carried out under reflectance mode using a stage spinner. The patterns were collected in the 2θ range of 5° – 50°. The step size selected was a 2θ value of 0.1313° and the time needed for the acquisition of the spectra was 20 minutes.

2.2.7 Scanning Electron Microscope (SEM)

Scanning electron microscope images were obtained using a Zeiss sigma field emission SEM. The instrument is fitted with a Gemini column. For measurements using the InLens detector, a working distance of 2.5 mm was used and an acceleration voltage of 3.5 kV

and of 5 kV. Prior to imaging, the samples were cryo-fractured by placing them in a bath of liquid nitrogen for 30 minutes, then, when removed from the liquid bath, were immediately fractured using a hammer. The fractured surface was stuck on an aluminium SEM stub with carbon adhesive tape with the fractured surface in the vertical up direction. The sample was subsequently sputter coated using an Au/Pt metal target (Cressington 108 auto).

2.2.8 BET

The BET (Brunner-Emmet-Teller) analyses were carried out using a Micromeritics ASAP 2020. The samples were firstly degassed in tube sample holder, weighted before and after degassing keeping the vacuum for giving the correct mass input before the measurement. The resultant adsorption isotherm is calculated measuring the amount of N_2 adsorbed at different relative pressures at the constant temperature of 77 K since the experiment is performed using a bath of liquid nitrogen where the sample holders are immersed.

2.2.9 Nuclear Magnetic Resonance spectroscopy

All ^{13}C Solid State Nuclear Magnetic Resonance cross polarisation magic angle spinning (CPMAS) measurements were performed at 9.4 T using a Bruker Avance 400 MHz spectrometer operating at ^{13}C Larmor frequency (ν_o) of 100.59 MHz. These experiments were performed using a Bruker 4 mm HX probe which enabled a MAS frequency of 12 KHz to be implemented. Pulse length calibration was performed on alanine$_{(s)}$ from which a $\pi/2$ pulse time of 2.5 μs was measured. All measurements were undertaken with a $\pi/2$ nutation angle along with a delay between subsequent pulses of 5 s and a cross polarisation contact time of 1500 ms with a 70-100 % ramp.

All ^{1}H Solid State Nuclear Magnetic Resonance measurements were performed at 11.7 T using a Bruker Avance 500 MHz spectrometer operating at a ^{1}H Larmor frequency (ν_o) of 500 MHz. These experiments were performed using a Bruker 1.3 mm HXY probe which enabled a MAS frequency of 60 kHz. Pulse length calibration was performed on alanine$_{(s)}$ from which a $\pi/2$ pulse time of 2.5 μs was measured. All measurements were undertaken with a $\pi/2$ nutation angle along with a delay between subsequent pulses of 5 s.

All ^{13}C chemical shifts were externally referenced against the IUPAC recommended primary reference of Me_4Si (1 % in $CDCl_3$, δ_{iso} = 0.0 ppm), via the secondary solid alanine reference (δ_{iso} = 20.5 ppm). All ^{1}H chemical shifts were externally referenced against the IUPAC recommended primary reference of Me_4Si (1 % in $CDCl_3$, δ_{iso} = 0.0 ppm), via the secondary solid alanine reference (δ_{iso} = 1.1 ppm) [50].

2.3 Sample preparation procedures

2.3.1 Procedure for ZIF-8 synthesis

The reagents were prepared in a molar ratio of 1/5:3 Basic zinc carbonate:2-Methylimidazole.

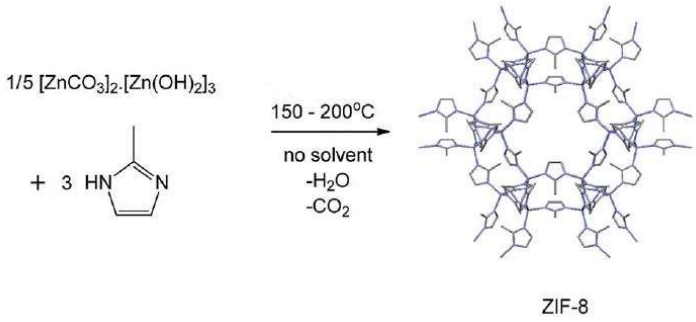

Figure 2.6 – Reaction schemes for the synthesis of ZIF-8 trough mechanochemical reaction [19]

The temperature of the batch mixer was set to 160 °C and the rotor speed was set to 75 rpm. Before feeding the reagents on the batch mixer, the mixture was stirred manually for 30 second to render it homogeneous. The result was a dry solid, with macroscopic agglomerated pieces, and was collected in a suitable container. To have a uniform particle size the solid was grinded with an automated mortar and pestle. Then the as synthetized ZIF-8 was activated stirring a 5g sample in 40mL HPLC grade Methanol for 2 hour and filtering. This procedure was carried out twice. The resulting solid was oven dried at a temperature of 150 °C for 2 hours.

2.3.2 Procedure for the composite production

- PMMA-ZIF-8 composite:

The PMMA was freeze milled to reduce the size of the pellet for being at least comparable with that of the filler for a better mixing. Then the PMMA was oven dried at a temperature of 80 °C for 3 hours. The milled polymer was mixed with ZIF-8, in weight percentage of 97% and 3% respectively, and stirred manually to homogenise the mixture before the feeding on the extruder. The extrusion of the composite was carried out at a temperature of 220 °C. The extrudate was collected and then pelletized.

- In-situ composite:

  The PMMA was freeze milled to reduce the size of the pellet for being at least comparable with that of the filler for a better mixing. Then the PMMA was oven dried at a temperature of 80 °C for 3 hours. The mixture of reagents was prepared in a molar ratio of 1/5:3 Basic zinc carbonate:2-Methylimidazole. The milled polymer was mixed with the mixture of reagents with two different weight percentages: the first with 97% of polymer an 3% of regents the second with 90% of polymer and 10% of reagents. The mixture was then stirred manually to homogenise the components before feeding them on the extruder. The extrusion of the composite was carried out at a temperature of 220 °C, the sample were then collected at different time of cycle in the extruder, namely at 1, 2 ,3 and 4 minutes of cycle time for the composite with 3% of filler version and 1 and 2 minutes of cycle time for the composite with 10% of filler. The extrudate collected was extruded another time for removing the bubbles that were developed during the first extrusion. The resultant material was then pelletized.

2.4 Characterization techniques

There are different characterization techniques that can be used to determine the different aspect of structure and properties of metal-organic frameworks and the relative composites, in particular for this work of ZIF-8 and the composites with PMMA. Usually the most used characterization technique for metal-organic frameworks is powder X-Ray Diffraction (XRD). XRD analysis is used to retrieve information about the crystal structure of the materials analysed. Since the wavelength of X-rays is comparable with the spacing of atoms in a crystal lattice gives rise to diffraction phenomena, which can be studied for

the determination of the structure of crystalline materials. The measurement of the scattered X-Ray and intensities gives an XRD pattern which can be compared to a known database of crystalline compounds and the compound can be then identified, if it has been synthesised previously and fully characterized. ZIF-8 has a characteristic XRD pattern, the pattern of synthetized material can be compared to a known pattern of ZIF-8 or to a simulated one and then the synthesis, as can be seen in Figure 2.7, or the presence of the metal-organic framework in the composite after the processing can be confirmed.

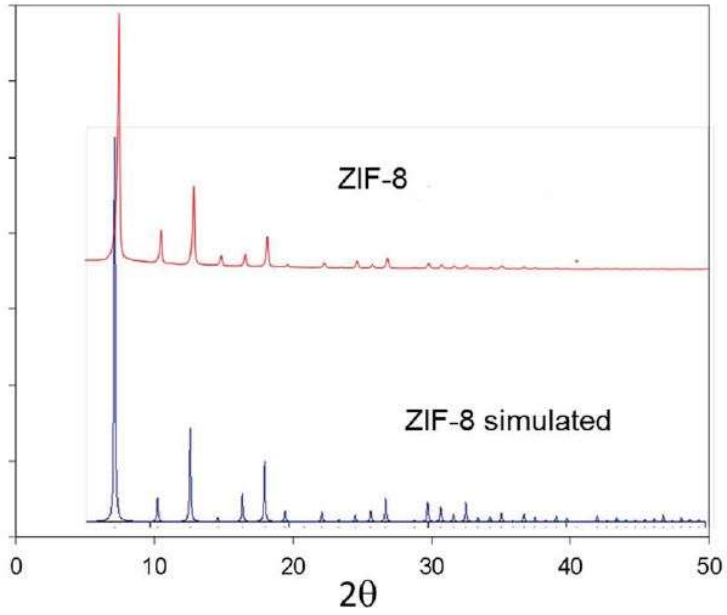

Figure 2.7 – Comparison of a simulated and as synthetized ZIF-8 XRD pattern [19]

Scanning electron microscopy (SEM) is another powerful tool for characterizing metal organic frameworks and composites. SEM is an electron microscope that directs a beam of electrons to the material and produces an image of the sample. For this reason, the sample must be conductive, hence it has to be coated with nanometric layer of a heavy metal, usually gold, for imaging to be effective. Electron microscopes have a higher definition respect to standard optical microscopes, SEM could go down to resolutions of nano- or micro-scale. Therefore, through SEM is possible to see and get images the shape and size of the particles synthetized and compare the images with a reference and to investigate the dispersion of the particles and the retaining of the crystal structure on the composite.

Another technique that could be used in characterization of metal-organic framework is Fourier Transform Infra-Red spectroscopy. The principle behind FTIR is that the infra-red radiation is passed through a sample and depending on the chemical structure of the sample the measurement could give adsorption or transmission, depending on how is carried out the analysis, at certain wavelengths. The resulting spectrum shows characteristic peaks depending on the chemical features, such as functional group for example, that are characteristic of the sample.

Thermo gravimetric analysis (TGA) is generally used for was retrieve information on thermal properties like the degradation temperature or the thermal stability of the materials measuring directly the weight losses of the sample while the temperature is increased or maintained at a certain level for the wanted period of time. TGA was used both in dynamic and isothermal mode in nitrogen and air atmospheres for investigate the thermal properties of ZIF-8 and the relative composite.

Another important parameter for the characterization of metal-organic frameworks, as a porous material, are the pore size, the surface area and the pore volume. These properties are generally measured by carrying out a Brunauer-Emmet-Teller (BET) analysis. BET measurements use an adsorption isotherm which is based on physisorption of gases on surface area of materials.

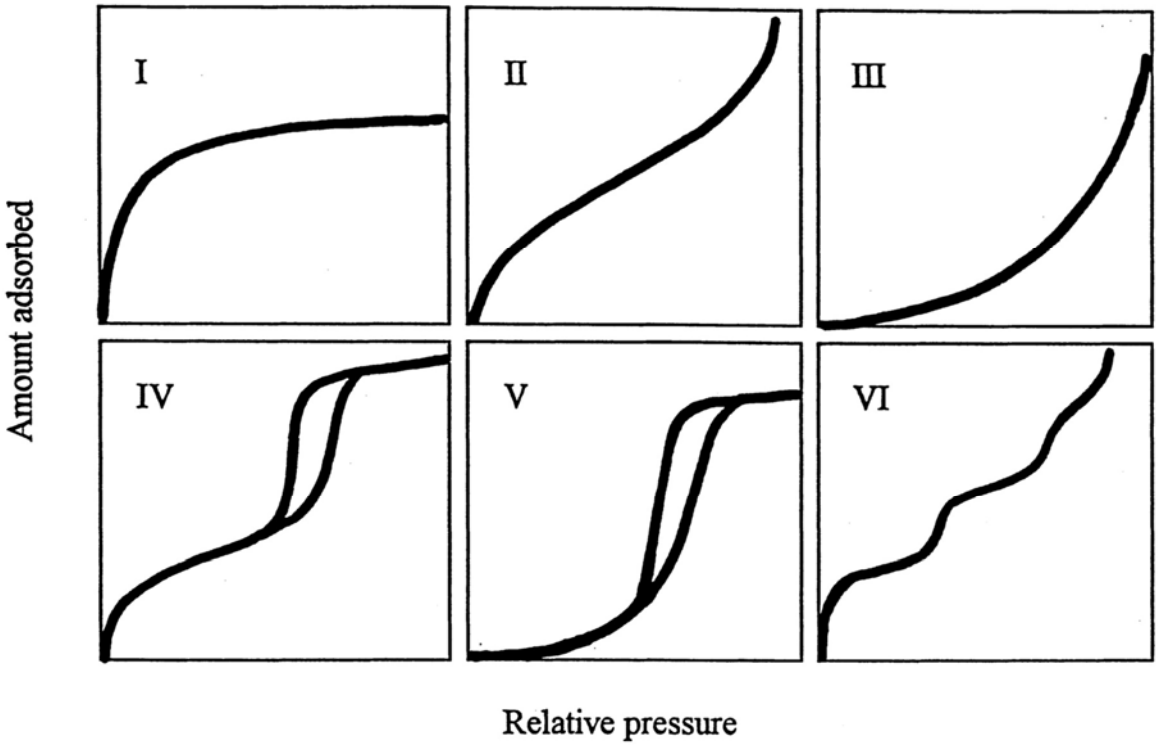

Figure 2.8 - The IUPAC Classification of gas adsorption isotherms [51]

The adsorption isotherm is calculated measuring the amount of gas adsorbed at a series of different pressures at the a temperature of 77 K, the experiment is performed using a bath of liquid nitrogen where the sample holders are inserted. The plot of the quantity of gas adsorbed against the relative pressures gives the graph of the adsorption isotherm. The shape of the curve on the graph gives insight int the type of pores the material has. Usually metal-organic frameworks have a curve of type I (Figure 2.8) that is characteristic of microporous materials.

Nuclear Magnetic Resonance (NMR) spectroscopy is technique used for finding out the content and purity of a sample and its own molecular structure. The chemical shift associate with this technique represent the resonant frequency of a nucleus relative to a standard in a magnetic field. The positions and the number of these resonances give information on the structure of the molecule. In this work was used for a confirmation of the synthesis of the ZIF-8 and of the presence of ZIF-8 inside the composite.

3 RESULTS AND DISCUSSION

3.1 ZIF-8 characterization

The ZIF-8 was synthetized in Haake PolyLab Rehomix OS batch mixer with a starting temperature of 160 °C, a rotor speed of 75 rpm and a filling volume 60%. At this temperature 2-methylimidazole is supposed to be melted, thus favouring the reaction. From Equation 3, a fill volume of 60% resulted in a mass of the mixture of the two reactants of 76.1263 g, of which 52.4739 g (0.639 moles) are of 2-methylimidazole and 23.6525 g (0.0426 moles) are of basic zinc carbonate.

$$m = \rho_{mixture} \cdot V_n \cdot V_{\%} \quad (3)$$

Where $\rho_{mixture}$ is the density of the mixture, V_n the net volume of the chamber of the batch mixer and $V_{\%}$ is the fill volume in percentage.

As can be seen in figure 3.1 the temperature and the torque during the synthesis were measured by the software of the batch mixer resulting in a rheogram.

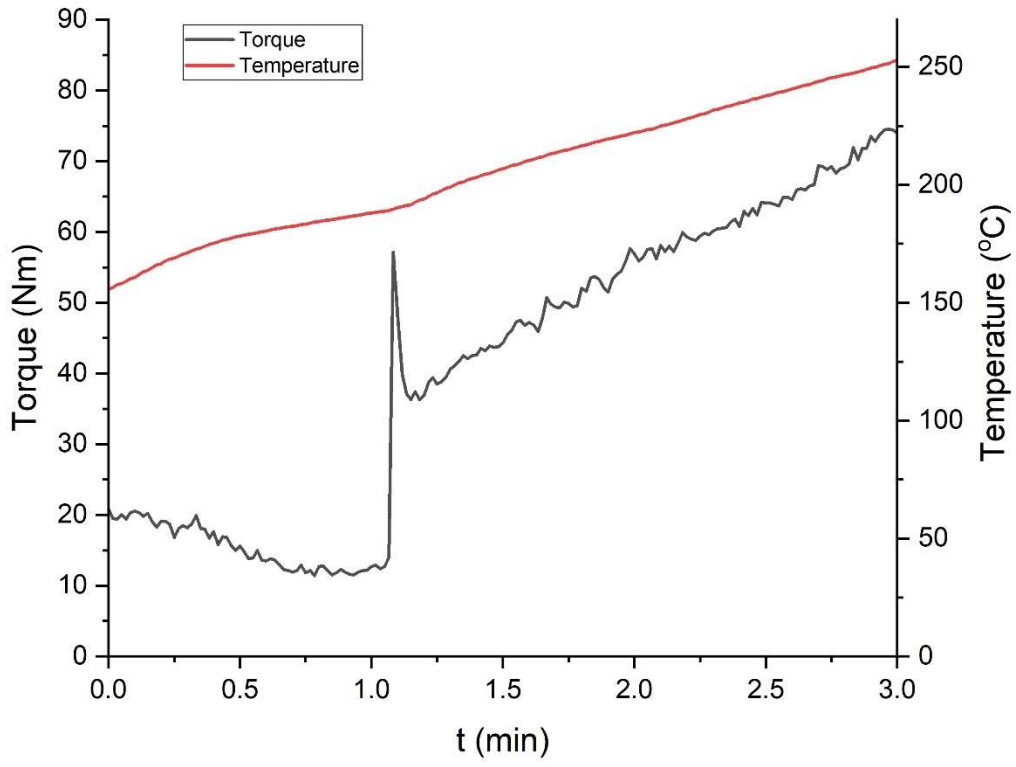

Figure 3.1 – Rheogram for the reaction of the synthesis of ZIF-8

The process of synthesis lasted 3 minutes, but even in that short period of time the increase of temperature due to the frictional heating was considerable arriving at a final temperature of 256 °C from a starting temperature of 160 °C, thus almost 100 °C indicating high shear stresses. The torque registered had a peak immediately after one minute of residency time, possibly indicating changes in rheology of the mixture within the batch mixer [20].

After the synthesis and the activation step, an FTIR analysis was performed to define the chemical structure of the synthetized ZIF-8 and the resulting peaks can be seen in Figure 3.2.

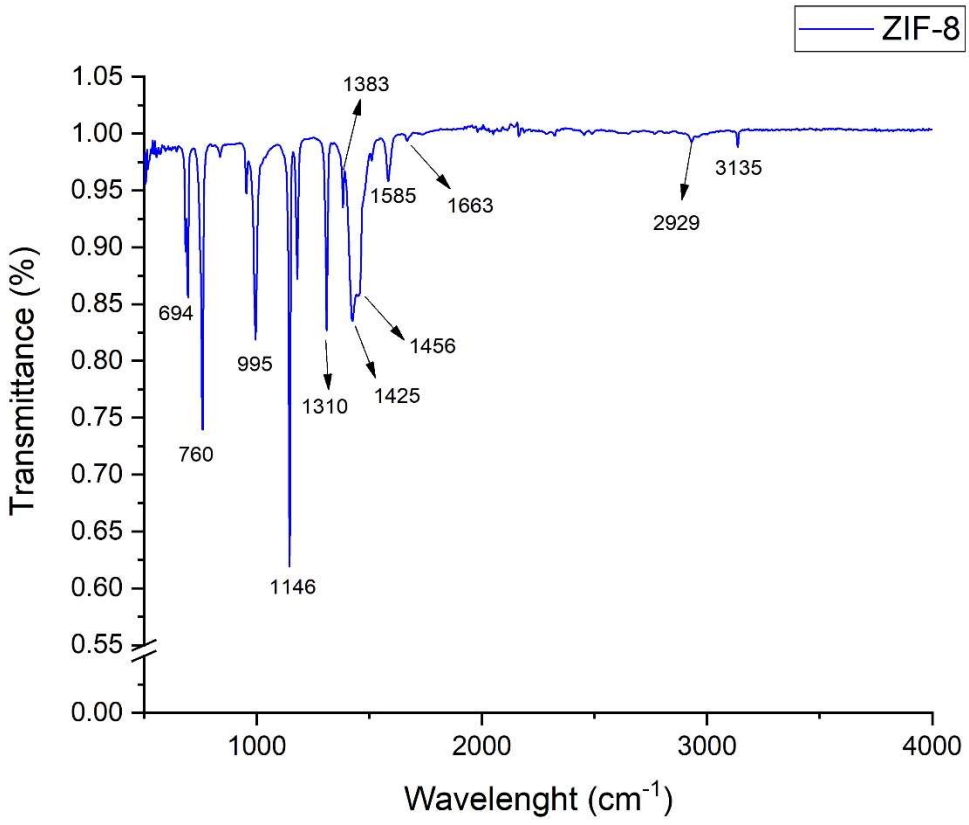

Figure 3.2 – ZIF-8 FTIR transmittance pattern with highlighted peaks

The FTIR pattern highlighted remarkable peaks 694, 760, 995, 1146, 1310, 1381, 1423, 1456, 1566, 1663, 2925 and 3132 cm^{-1}. This FTIR pattern was in accordance with those previously reported by Jomekian et al. and by Zhang et al. . The peak at 694 cm^{-1} could be assigned to the ring out-of-plane bending vibration of the linker. The peaks at 760 cm^{-1} and 995 cm^{-1} are due to the C–N bending vibration and C–H bending mode respectively. The peak at 1146 cm^{-1} could be assigned to the aromatic C–N stretching mode and the

peaks in the zone of 1300-1460 cm^{-1} are for the full ring stretching. The peak at 1566 cm^{-1} is due to the C=N stretch vibration and the signal at 1663 cm^{-1} corresponds to the C=C stretch mode. The last two peaks at 2925 and 3132 cm^{-1} are attributed to the aliphatic and aromatic C–H asymmetric stretching vibrations [52, 53]. The band at 3455 cm^{-1} reported in literature didn't show at all because it was due N–H stretching vibration relative to the residual 2-methylimidazole, thus indicating the effectiveness of the activation step.

Then was performed the most use characterization technique, regarding to metal-organic frameworks, that is powder XRD. The characterization is usually done comparing the peaks obtained with the references present in literature or with simulated XRD patterns. In this work the powder XRD pattern obtained can be seen in Figure 3.3.

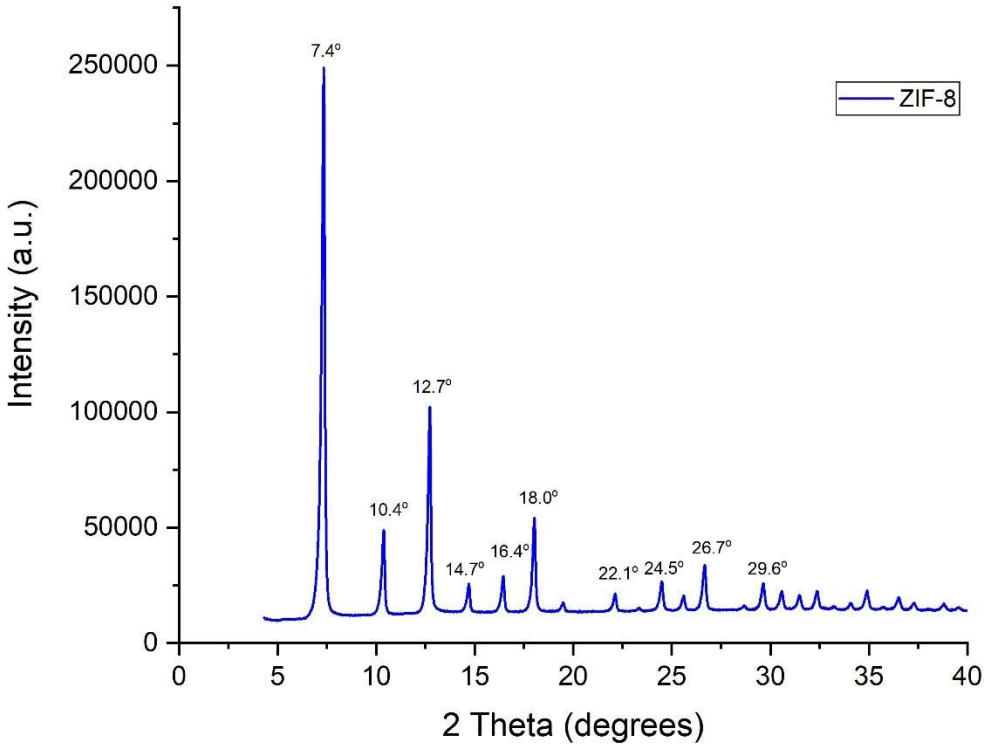

Figure 3.3 – ZIF-8 powder XRD pattern with highlighted peaks

The most remarkable are characteristic diffraction peaks, that can be found at values of 2θ of 7.4°, 10.4°, 12.7°, 14.7°, 16.4°, 18.0°, 22.1°, 24.5°, 26.7° and 29.6°, are clearly observed in the sample of ZIF-8 analysed [52]. These peaks can be respectively assigned to the planes (011), (002), (112), (022), (013), (222), (114), (233), (134) and (044). The

prominent reflections are in accordance with the literature, thus indicating the sodalite structure of ZIF-8 [52]. Therefore, the ZIF-8 synthesis is clearly confirmed by the XRD pattern.

Then was performed a TGA, both in dynamic and isothermal mode, for evaluating the thermal properties of ZIF-8. The dynamic TGA performed in air (Figure 3.4) showed a very limited weight loss around the temperature of 200 °C that could be due to the removal of a small amount residual impurities entrapped on the ZIF-8 pore structure. The most significant weight loss take place between 400 °C and 500 °C, where the organic linker is supposed to be fully degraded, even though the initial degradation temperature is around 350 °C. Hence, the ZIF-8 has to be considered thermally stable in air up to 320 °C. The residual weight fraction remained is the metal ion part of the metal-organic framework, namely zinc, that in air bonds with oxygen to form ZnO that doesn't degrade at all and is left as a residual.

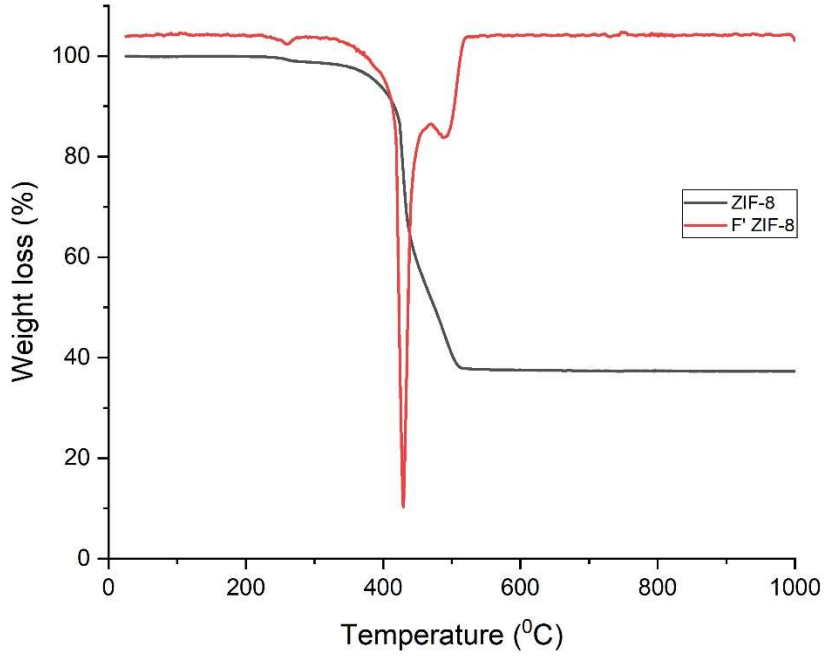

Figure 3.4 – ZIF-8 TGA performed in air and first derivative

In the TGA performed in Nitrogen atmosphere (Figure 3.5) ZIF-8 showed a higher thermal stability then the one performed in air. There is always the release of a little amount of impurities around 200 °C, but the onset of the degradation is around 450 °C. Therefore, the degradation rate of the organic linker part is lower than the one on air and lasts until the 800° C are passed. The residual weight fraction is the one that belongs to the metal

ion part of the metal-organic framework. Thus, the ZIF-8 is more thermally stable in an inert atmosphere.

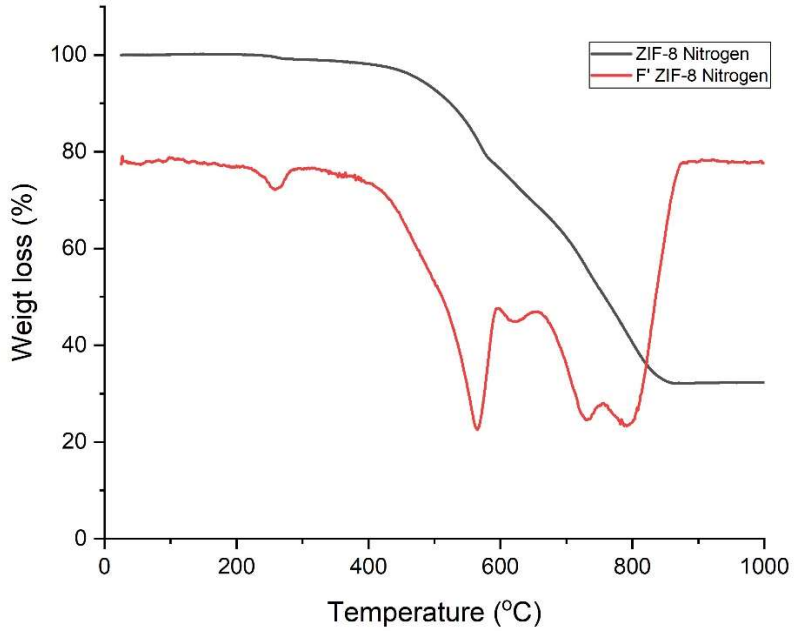

Figure 3.5 - ZIF-8 TGA performed in Nitrogen and first derivative

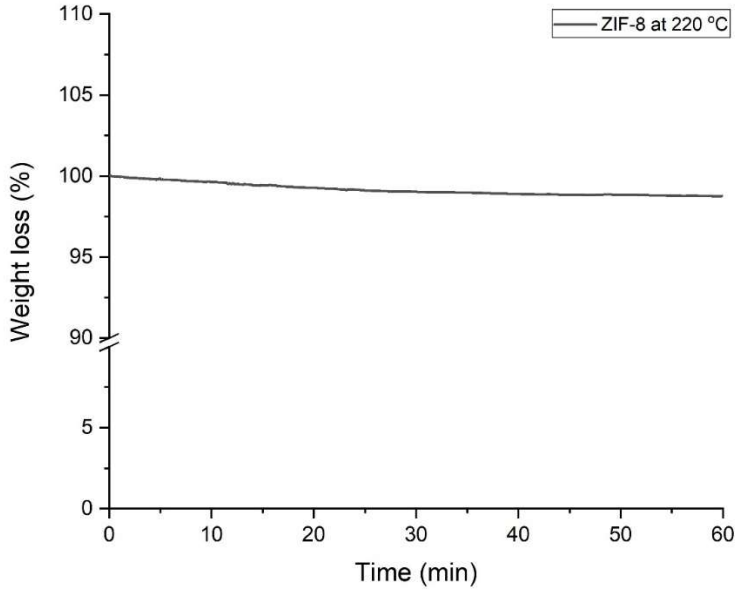

Figure 3.6 – ZIF-8 Isothermal TGA in air at 220 °C

Furthermore, it was performed an isothermal TGA in air at 220 °C for 60 minutes (Figure 3.6) to check if the ZIF-8 was suitable to the extrusion process temperatures. As a result, the weight losses at the end of the measurement amount to 1.2%, that are always due to

the residual impurities in the pore structure. Thus, ZIF-8 can be considered suitable for the extrusion process since it can withstand at the temperature of 220 °C without giving rise to any type of degradation.

All the data retrieved by TGA analyses found their confirmation in literature [54].

Subsequently it was performed a BET analysis for characterizing the pore structure and to define the textural properties of the synthetized ZIF-8. The textural properties of ZIF-8 are summarized in Table 1. The nitrogen adsorption-desorption isotherms (Figure 3.7) showed a Type I (Figure 2.8) isotherm curve, thus confirming the characteristic microporous structure of the synthetized ZIF-8. The sharp increase in the uptake of nitrogen at very low relative pressures corresponds to the presence of micropores, while the second increase in adsorption at high relative pressure suggest the existence of meso- or macroporosity formed by packing of nanoparticles [55]. The textural properties, calculated with BET and t-plot methods, of the mechanochemically synthetized ZIF-8 in this work were in line with the values founded in literature for other mechanochemical or solvothermal synthetized ZIF-8 [55, 56].

METAL-ORGANIC FRAMEWORK	BET SURFACE AREA	LANGMUIR SUFACE AREA	MICROPORE VOLUME	AVERAGE PORE WIDHT	EXTERNAL SURFACE AREA
ZIF-8	1072 $cm^2 \cdot g^{-1}$	1494 $cm^2 \cdot g^{-1}$	0.51 $cm^3 \cdot g^{-1}$	23.4 Å	34.1 $cm^2 \cdot g^{-1}$

Table 1 – Textural properties of the synthetized ZIF-8

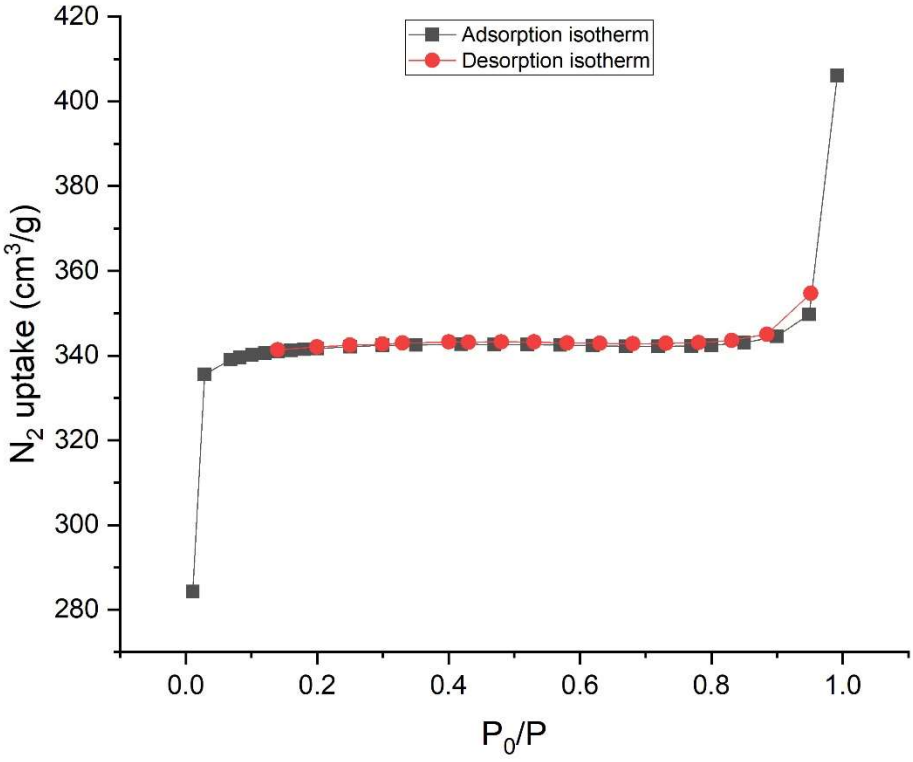

Figure 3.7 – Adsorption/desorption isotherm of ZIF-8

A further analysis on the crystal structure of ZIF-8 has been done with SEM images. Like mentioned before, ZIF-8 has a sodalite-type structure and forms a truncated octahedron (Figure 3.8). The images given by the SEM confirmed the crystal structure of the mechanochemically synthetized ZIF-8 showing a characteristic sodalite structure as can be seen in figures 3.9, 3.10, 3.11, 3.12 3.13 and 3.14, thus confirming another time the synthesis of wanted metal-organic framework. Another consideration that can be done with SEM images is that the particle size given by mechanochemical synthesis is quite broad, ranging from 100 nm to more than 1 µm sizes.

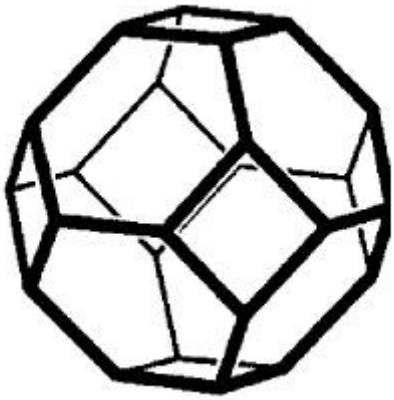

Figure 3.8– Sodalite unit cell [57]

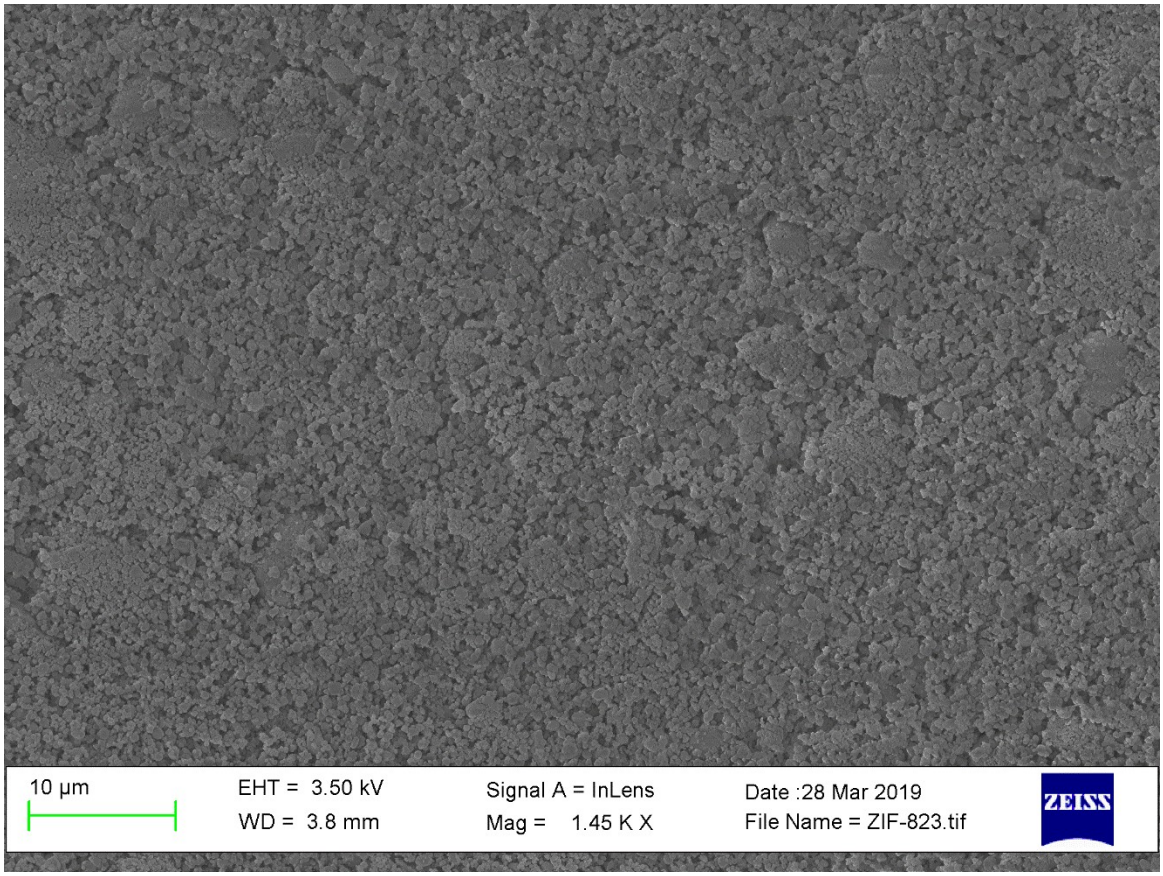

Figure 3.9 – SEM image of ZIF-8

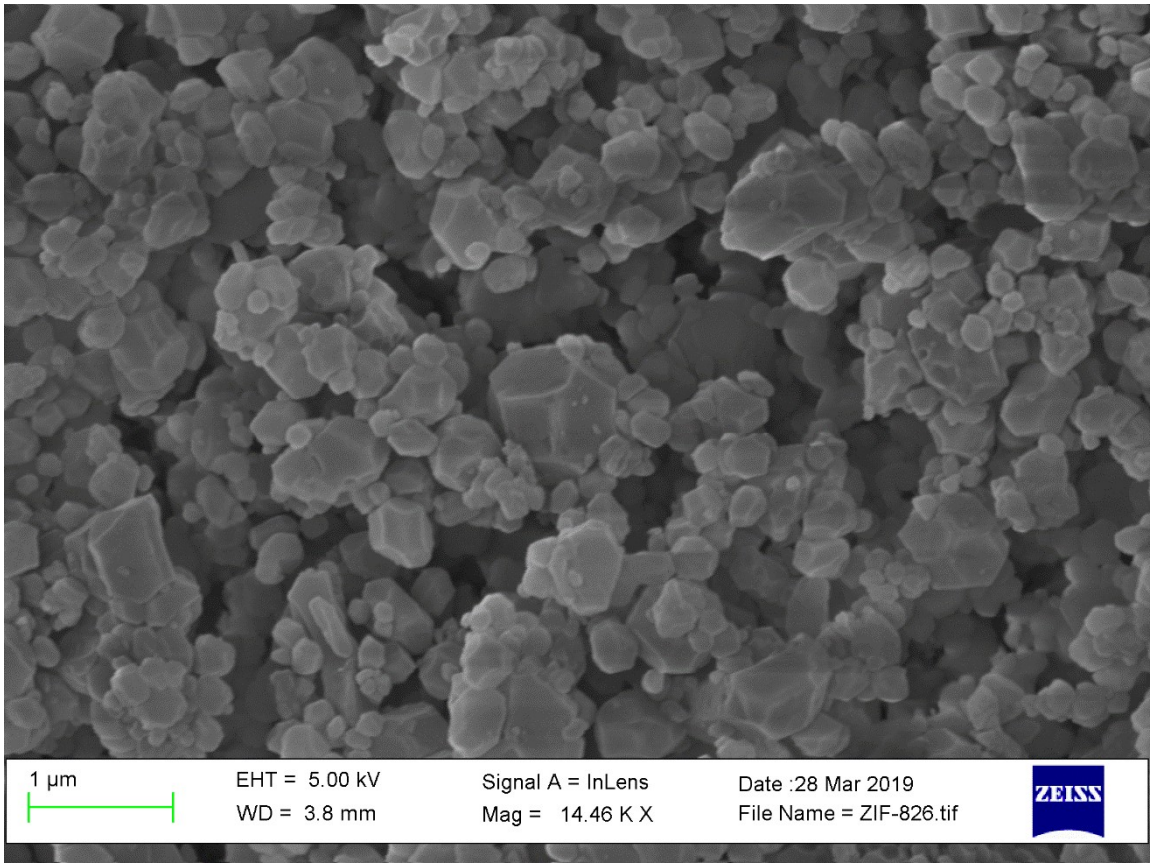

Figure 3.10 – SEM image of ZIF-8

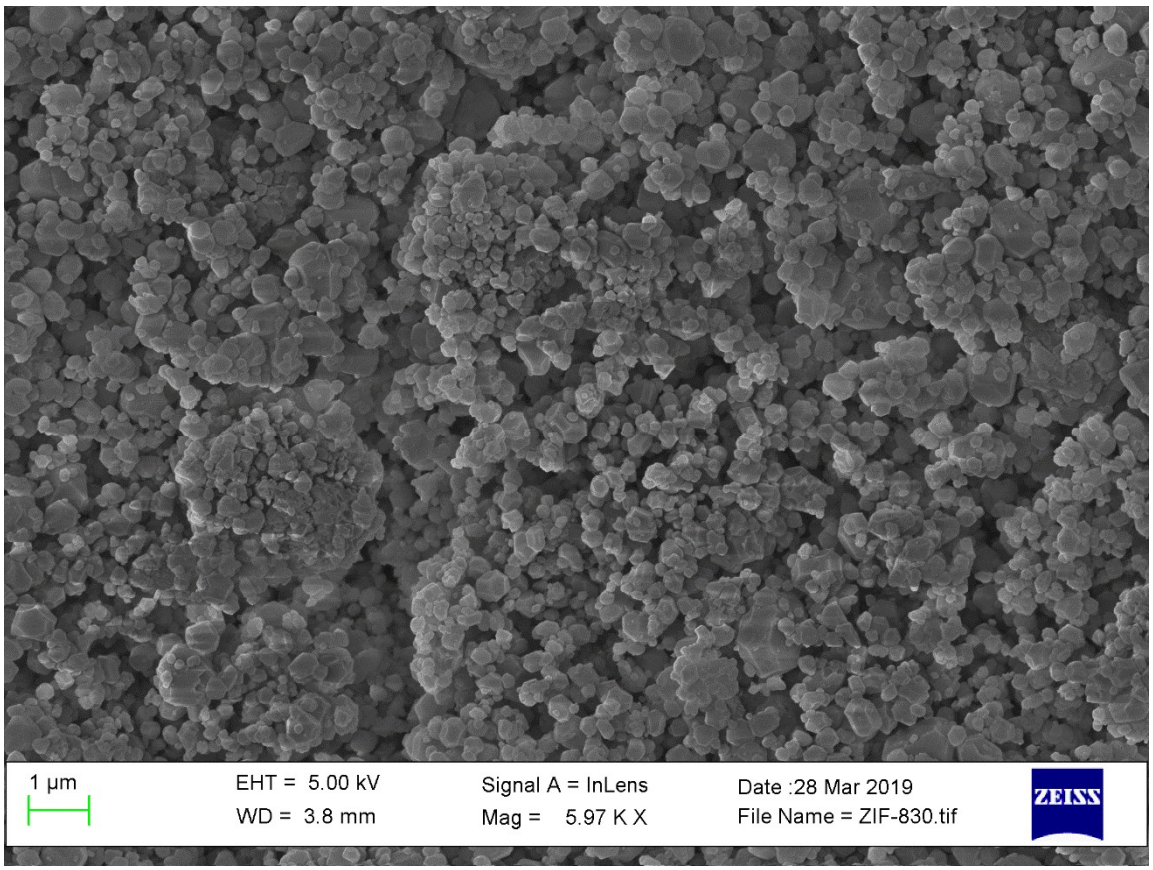

Figure 3.11 – SEM image of ZIF-8

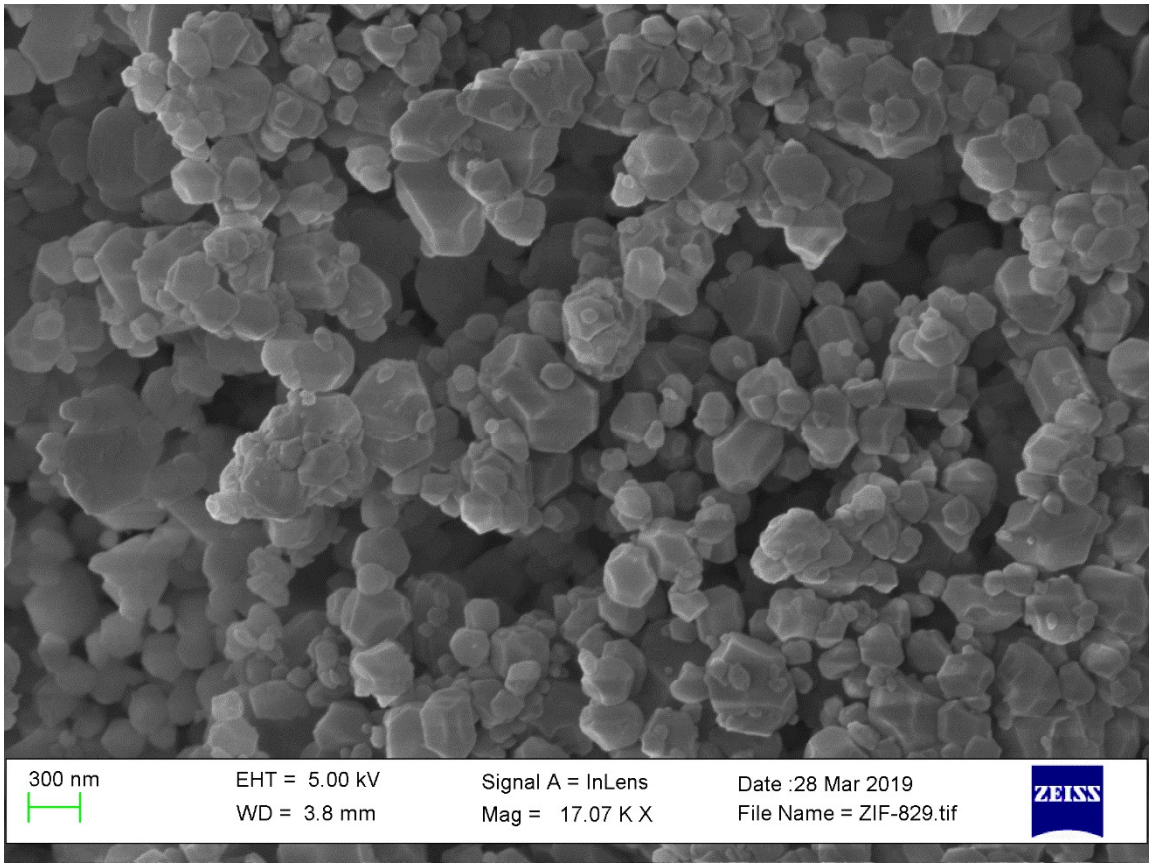

Figure 3.12 – SEM image of ZIF-8

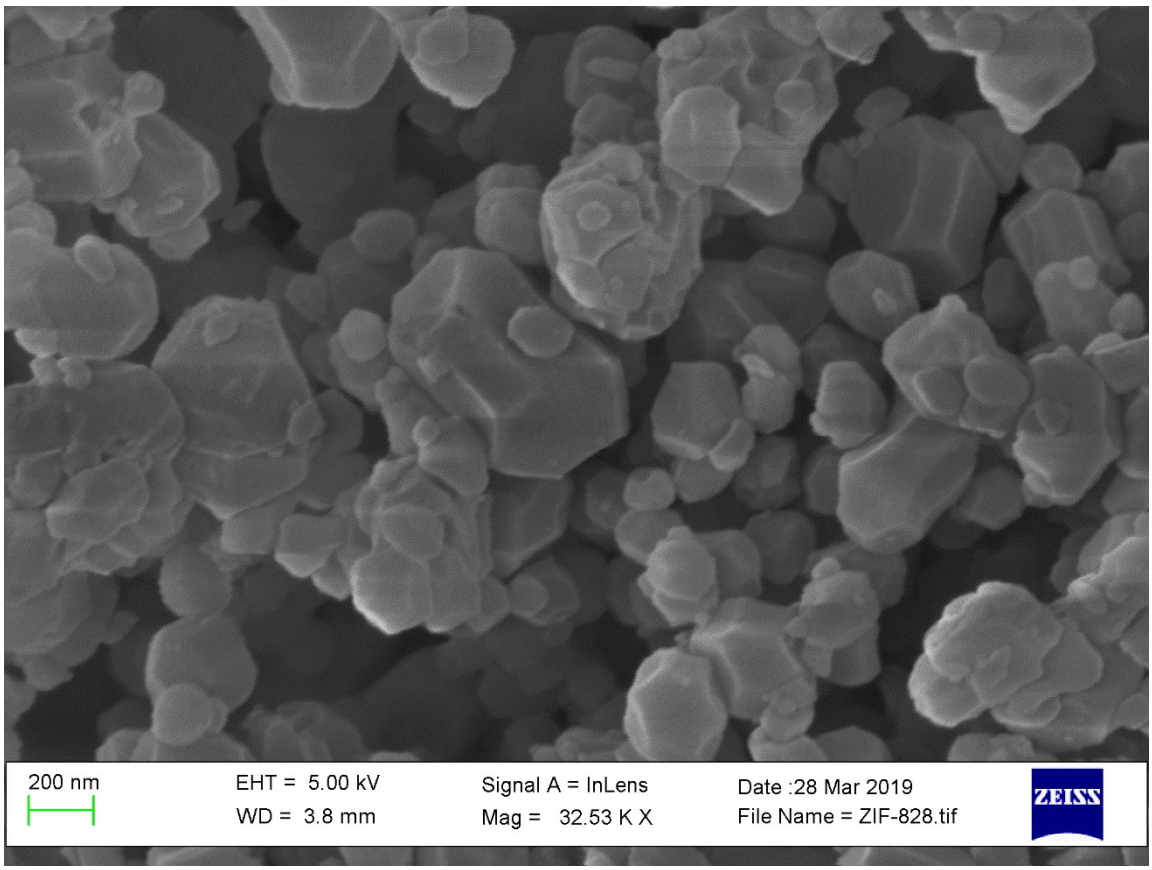

Figure 3.13 – SEM image of ZIF-8

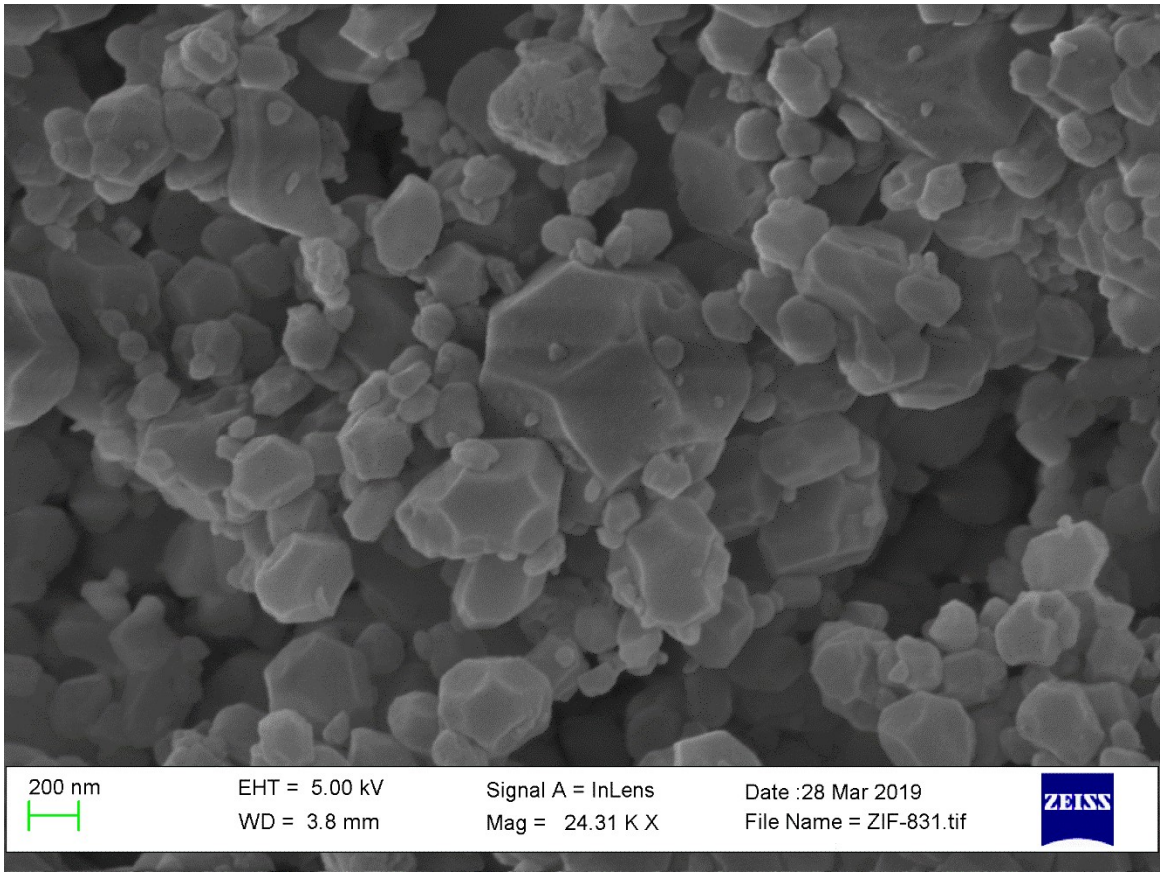

Figure 3.14 – SEM image of ZIF-8

3.2 Composite characterization

3.2.1 PMMA-ZIF-8 3% composite

The grinded neat polymer was manually mixed with ZIF-8 in weight proportion of 97% and 3% respectively. The mixture was compounded in Thermo Scientific Haake Mini-Lab II micro-compounder with a barrel temperature of 220 °C and a screw speed of 75 rpm and then pressed in Collin hot press for obtaining discoid samples.

Firstly, the composite was characterized with an XRD analysis. As it possible to see in Figure 3.15 the XRD pattern of the composite showed an amorphous base, due to the PMMA fraction, and crystalline peaks, due the ZIF-8 fraction. In Figure 3.16 is shown a comparison between the neat polymer (PMMA), the filler (ZIF-8) and the composite of the two phases compounded. As is clearly observable the peaks showed in the pattern of the composite, and that emerge by the amorphous pattern given by PMMA, belonged to the ZIF-8 phase. Thus, this is a confirmation that the metal-organic framework can withstand at the temperature of the processing without its properties being affected.

Furthermore, the XRD give a confirmation that not only on the thermal stability but even on the ability on retaining the crystal structure at high temperatures of ZIF-8.

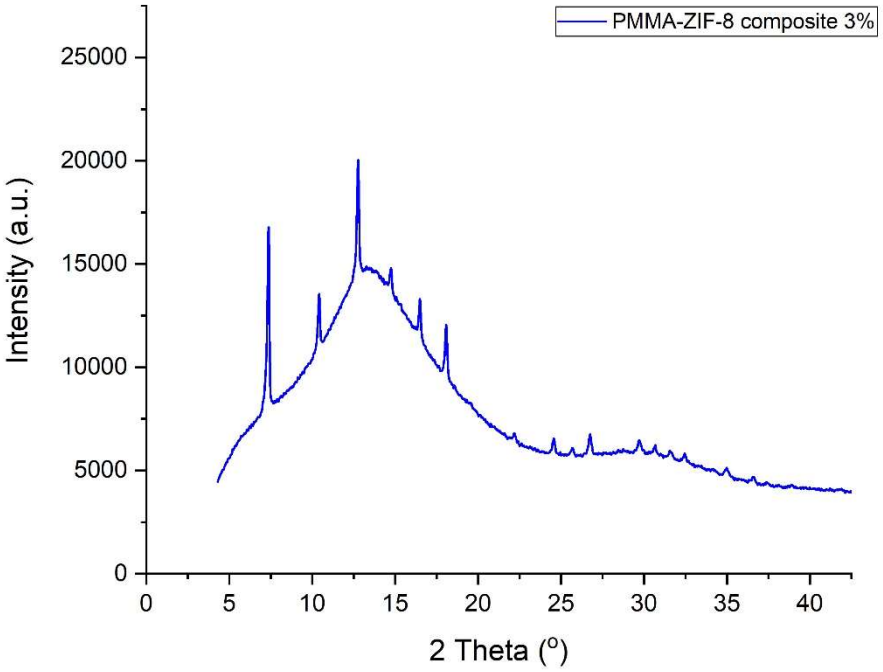

Figure 3.15 – XRD pattern of PMMA-ZIF-8 composite

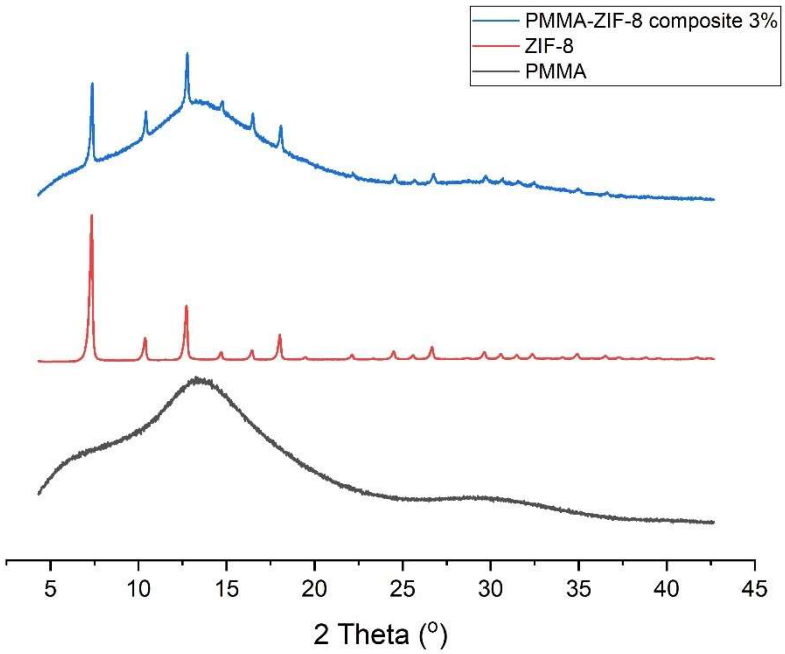

Figure 3.16 – Comparison of the XRD patterns of PMMA, ZIF-8 and the composite

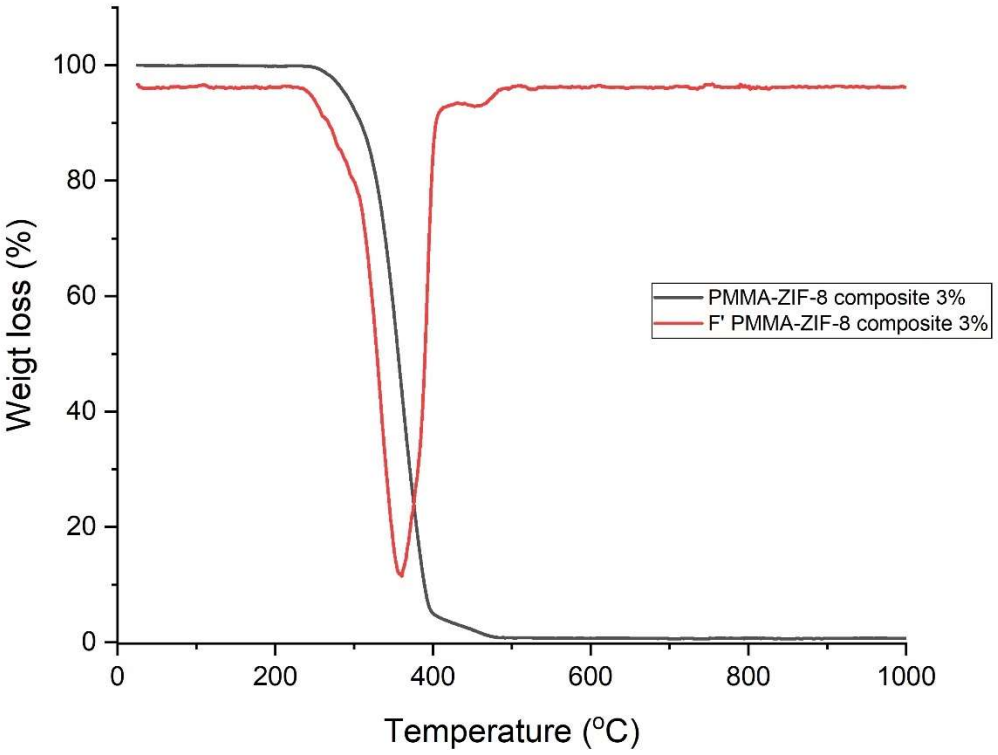

Figure 3.17 – PMMA-ZIF-8 TGA

The TGA of the composite (Figure 3.17) highlights the presence of the two phases, in fact the PMMA degrades before than the ZIF-8, that is more thermally stable and starts to degrade at a higher temperature. Respect to neat polymer, that showed a sudden degradation around 300 °C, the composite started to degrade before, around 260 °C, but the slope of degradation was not that sharp as the neat polymer one. The ZIF-8 phase degrades in the range of that goes from 400 °C to 500 °C, as expected.

Another confirmation of the retained crystallinity was given by the SEM images (Figures 3.18, 3.19 3.20, 3.21 and 3.22) as the sodalite structure of the ZIF-8 is clearly visible. These images highlighted even quite good dispersion obtained by the compounding and could give some information on the interface between the two phases. In fact, the interface didn't have significative voids between the two phases and seemed to be quite strong, as can be seen by the packed polymer areas around the metal-organic framework, suggesting some interaction between the two phases.

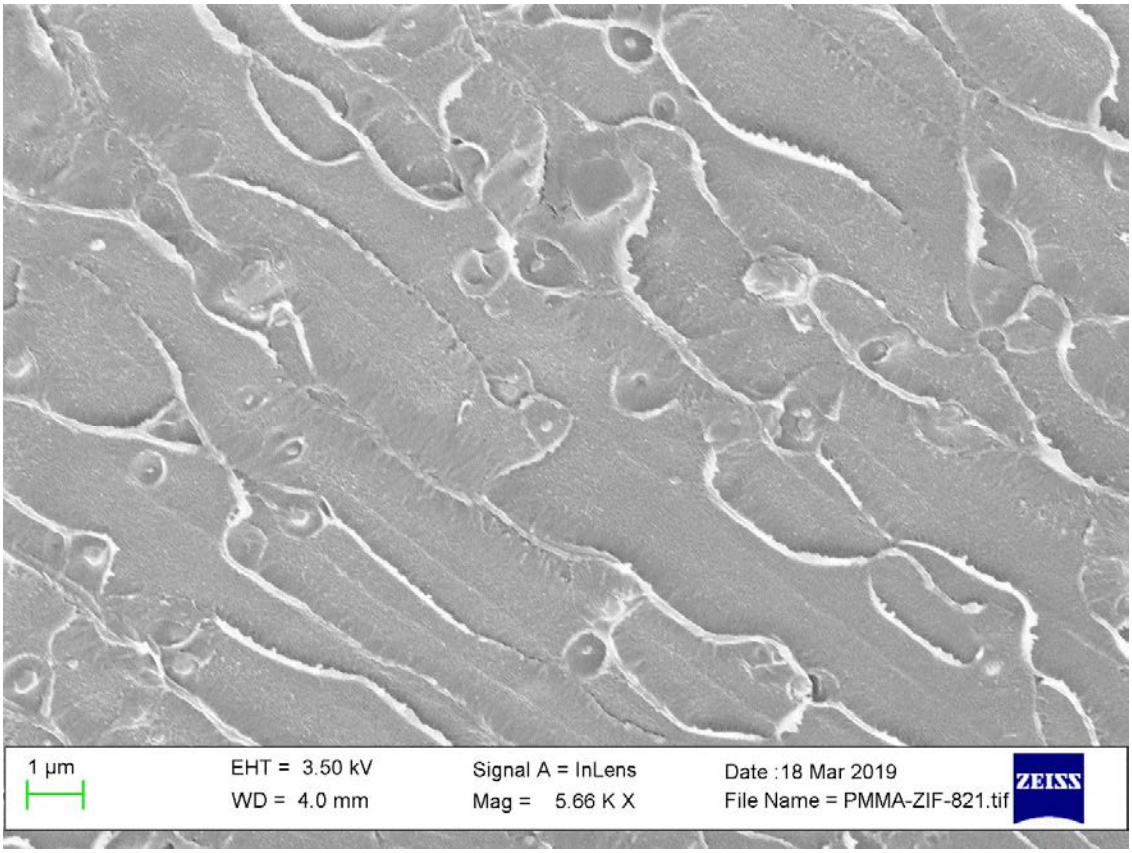

Figure 3.18 – SEM image of PMMA-ZIF-8 composite

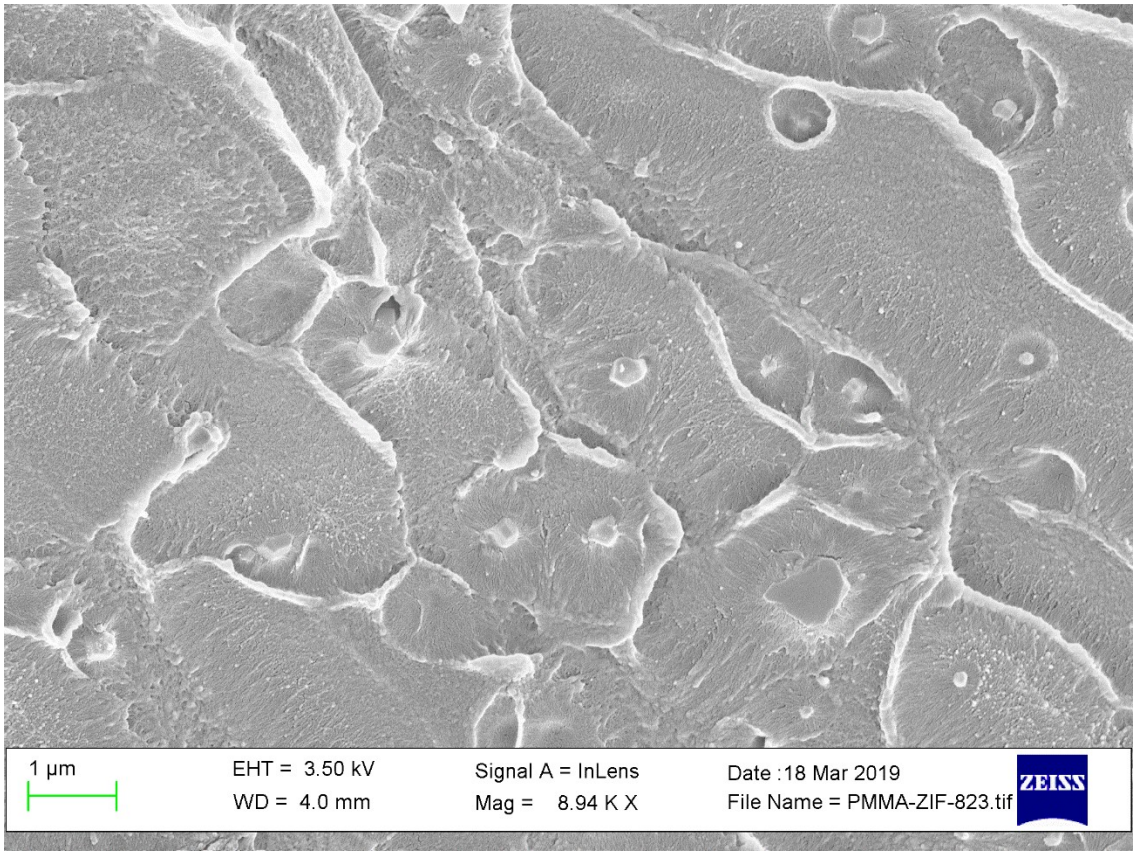

Figure 3.19 – SEM image of PMMA-ZIF-8 composite

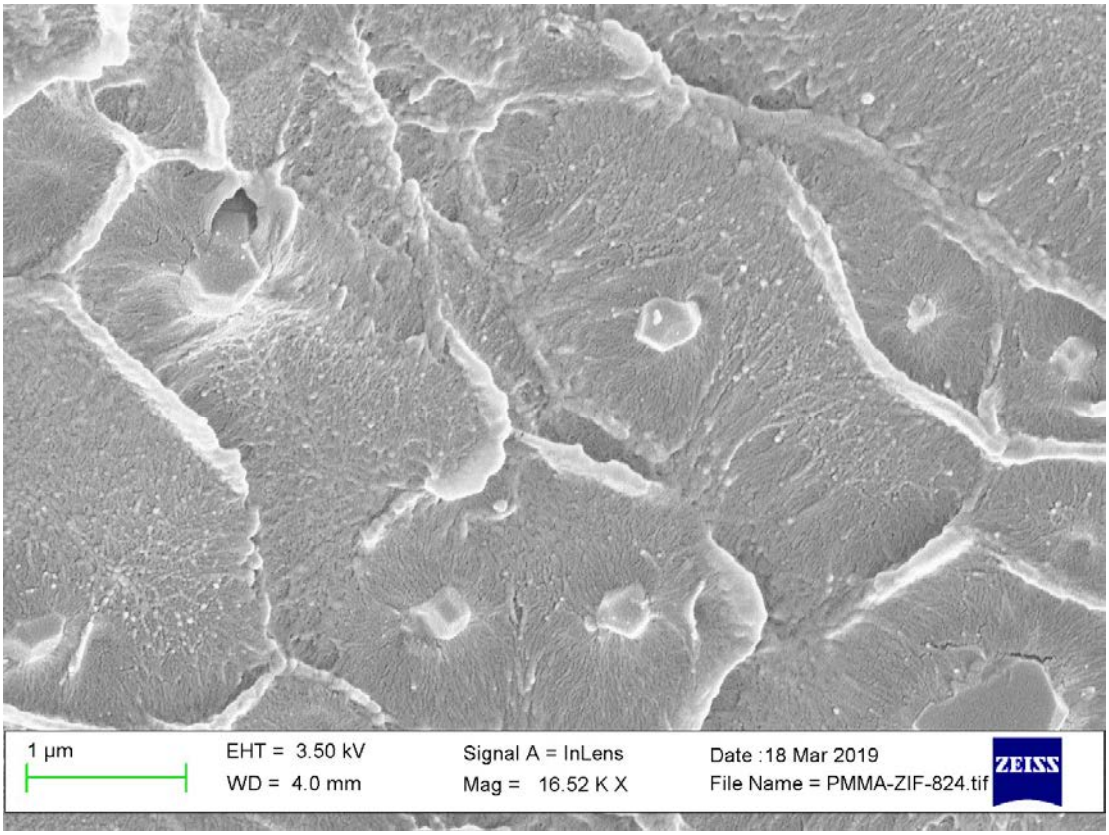

Figure 3.20 – SEM image of PMMA-ZIF-8 composite

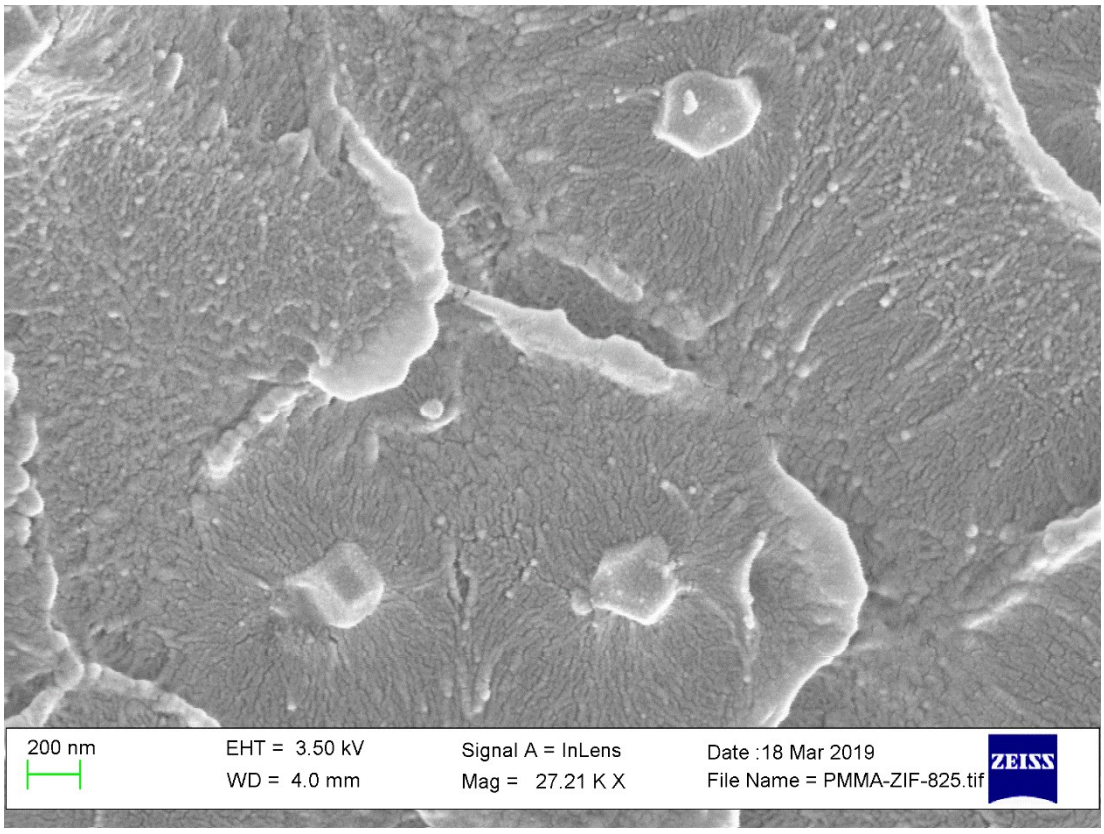

Figure 3.21 – SEM image of PMMA-ZIF-8 composite

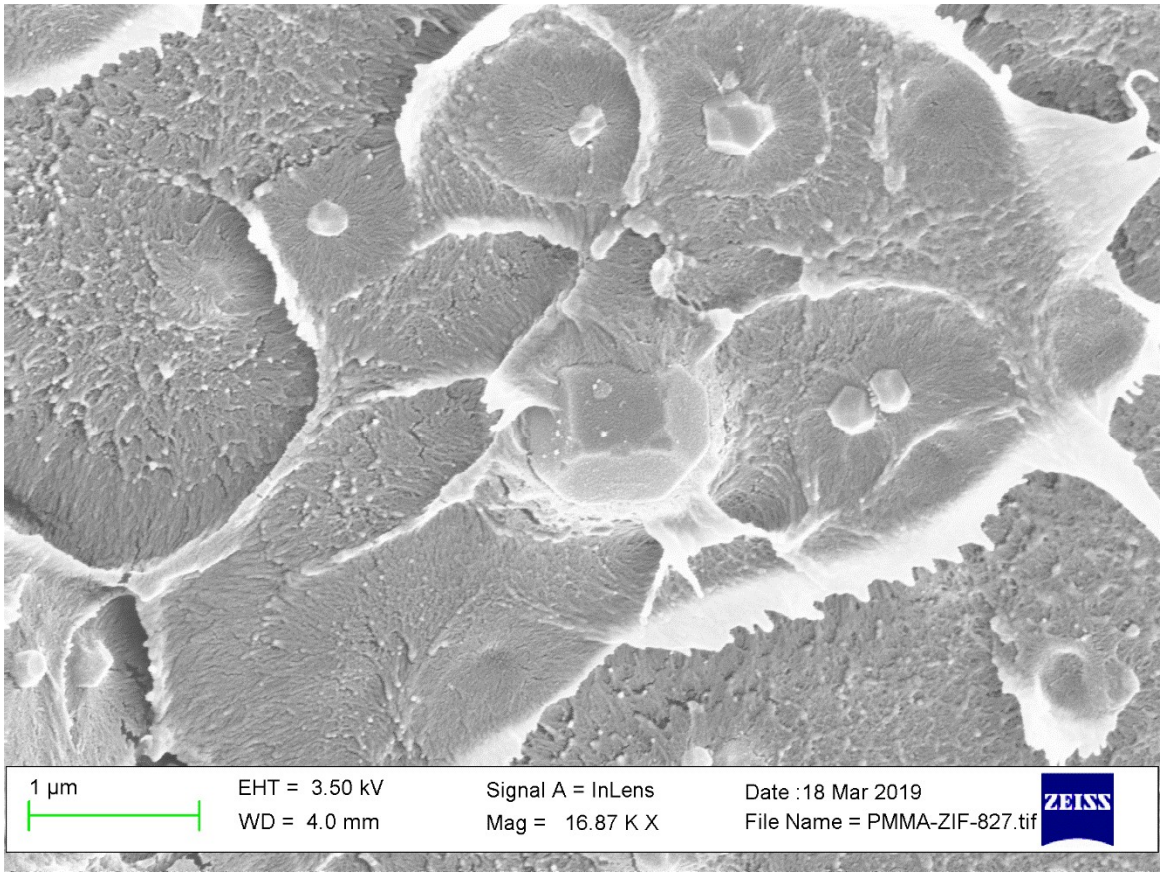

Figure 3.22 – SEM image of PMMA-ZIF-8 composite

3.2.2 In-situ composite 3%

The grinded neat polymer was manually mixed with the two reagents used for the synthesis of ZIF-8 (i.e. molar ratio 1/5:3 Basic zinc carbonate:2-Methylimidazole) in weight ratio of 97% and 3% respectively. The mixture was compounded in Thermo Scientific Haake Mini-Lab II micro-compounder with a barrel temperature of 220 °C and a screw speed of 75 rpm and recirculation times of 1, 2, 3 and 4 min. The extrudate collected had developed bubbles during the extrusion, that could be a suggestion that the reaction was taking place since the side products of the ZIF-8 synthesis are H_2O and CO_2. For removing the bubbles from the composite, the extrudate was passed a second time on time on the micro-compounder and then pressed in Collin hot press for obtaining discoid samples.
The samples were firstly characterized with an XRD analysis. The XRD pattern collected were then compared with the one of the PMMA-ZIF-8 3%, as is possible to see in the Figure 3.23 for the in-situ composite obtained with 1 and 2 minutes of recirculation and in Figure 3.24 for the in-situ composite obtained with 3 and 4 minutes of recirculation.

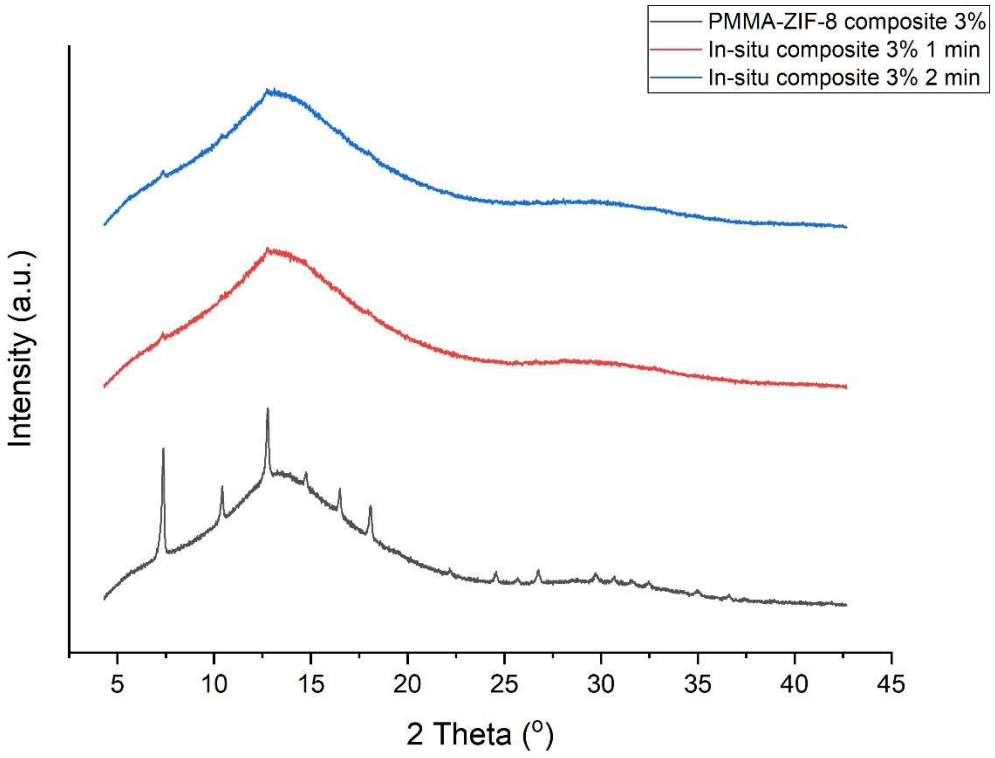

Figure 3.23 – Comparison between XRD patterns of PMMA-ZIF-8 3% composite and in-situ 3% composite 1 and 2 minutes cycle time

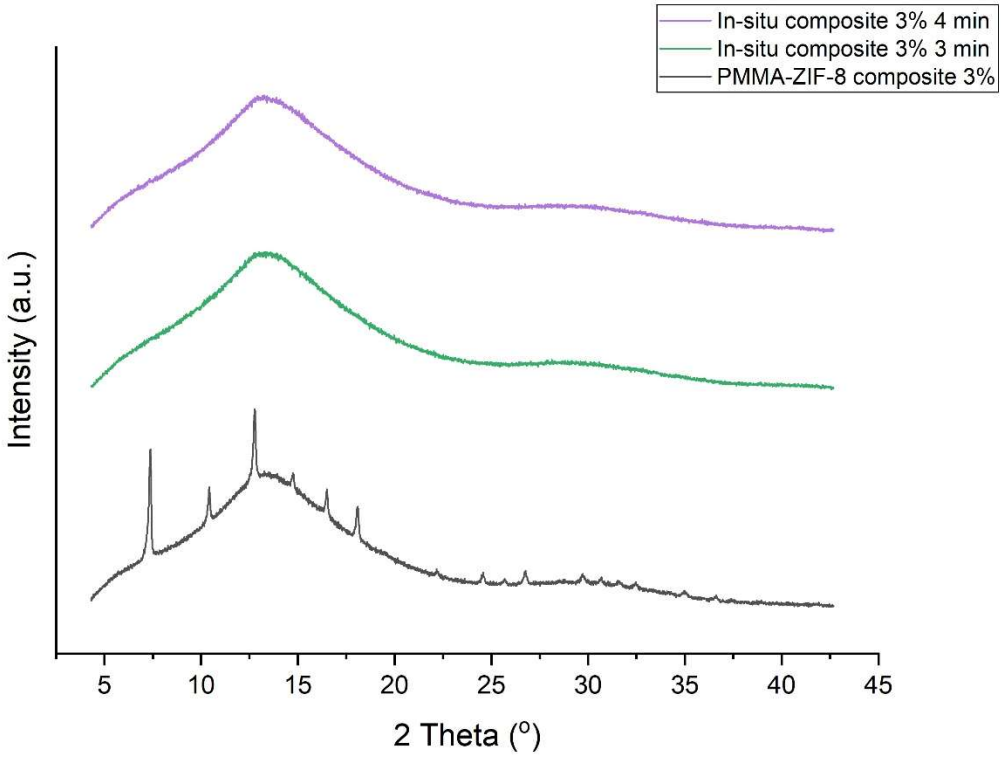

Figure 3.24 – Comparison between XRD patterns of PMMA-ZIF-8 3% composite and in-situ 3% composite 3 and 4 minutes cycle time

The XRD pattern of the in-situ composites with 1 and 2 minutes showed the more intense peaks showed by ZIF-8 at the same values of 2θ, such as 7.4°, 10.4°, 12.7°, 16.4°, 18.0° (Figure 3.25), indicating the formation of the ZIF-8 crystal structure, but with a much lower intensity suggesting a low yield in the conversion of the reactants. While for the version with 3 and 4 minutes of recirculation the peaks weren't showed at all, suggesting that higher residency times could have negative effects on the crystal structure.

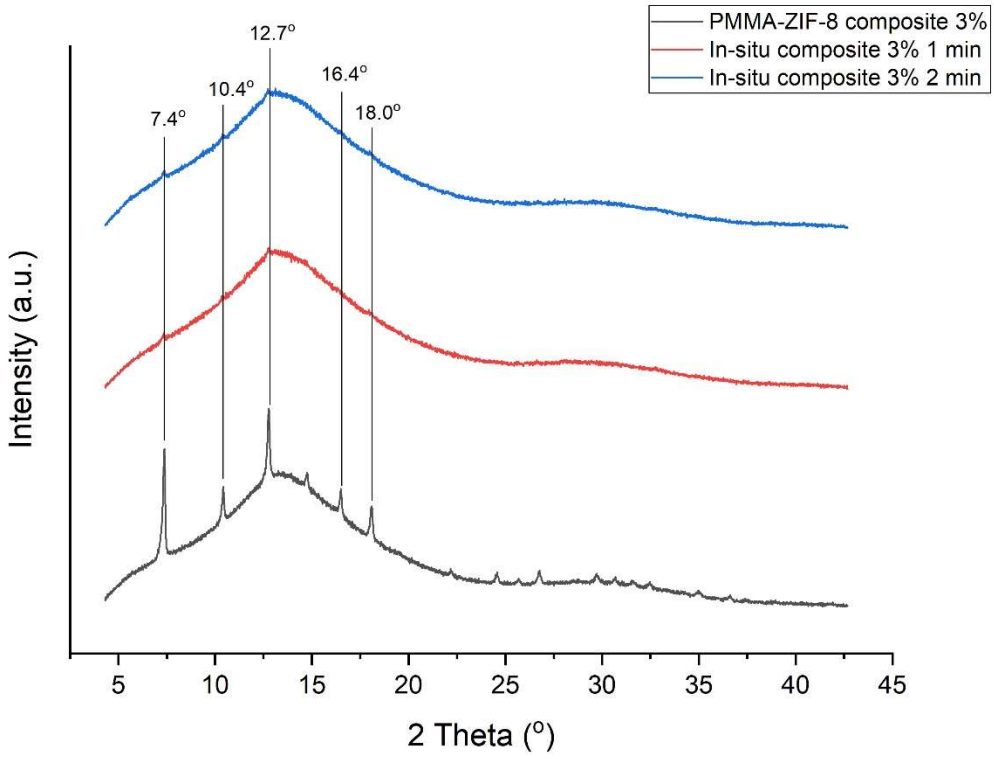

Figure 3.25 – XRD peak comparison between PMMA-ZIF-8 3% composite and in-situ composites 3% 1 and 2 minutes of cycle time

Another characterization technique used was NMR spectroscopy. The analysis was performed on PMMA, on ZIF-8 itself and on the composites and the relative spectra can be seen in Figure 3.26. The ^{13}C CPMAS NMR spectrum of ZIF-8 shows that three characteristic C resonances at 14 ppm, 125 ppm and 152 ppm, belonging respectively to the groups —CH_3, N—CH=CH—N and N—C(CH_3)—N, their presence between resonances of 100 ppm and 160 ppm (a part from the methyl group) indicates the aromatic nature of the linker and the presence of diamagnetic Zn metal centre [58]. The corresponding ^{1}H spectrum shows two H resonances at 1.5 ppm and 6.4 ppm. There are two clear ZIF-8 resonances present in the ZIF-8 PMMA 3 % composite C spectrum at 125 ppm and 152 ppm. There is one clear H peak at 6.4 ppm in the ZIF-8 PMMA 3 % composite attributable

to ZIF-8. In the in-situ composites the ZIF-8 resonances are present however require x10 magnification to be able to fully visualise the peaks. The ZIF-8 resonance in the ^{1}H spectra is more prevalent in the 3 % composite than the in-situ blends. The intensity of the ^{13}C ZIF-8 peaks decreases with increasing time of cycle, confirming the data from XRD analyses, the intensity of the ^{1}H ZIF-8 peak does not decrease. Interestingly the ZIF-8 peak at 152 ppm is shifted in the in-situ composites.

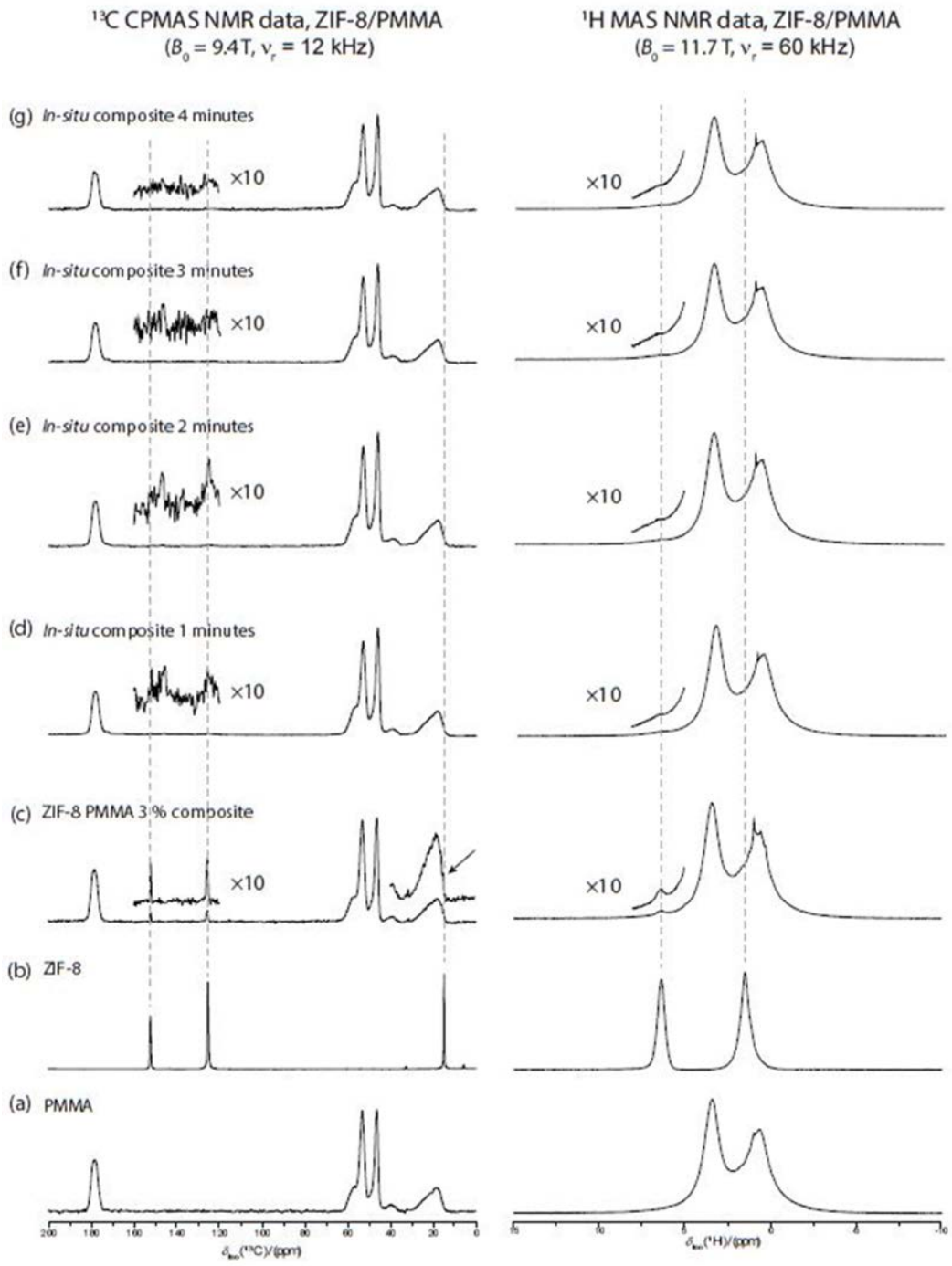

Figure 3.26 - ^{13}C and ^{1}H NMR spectra of neat polymer, filler and composites

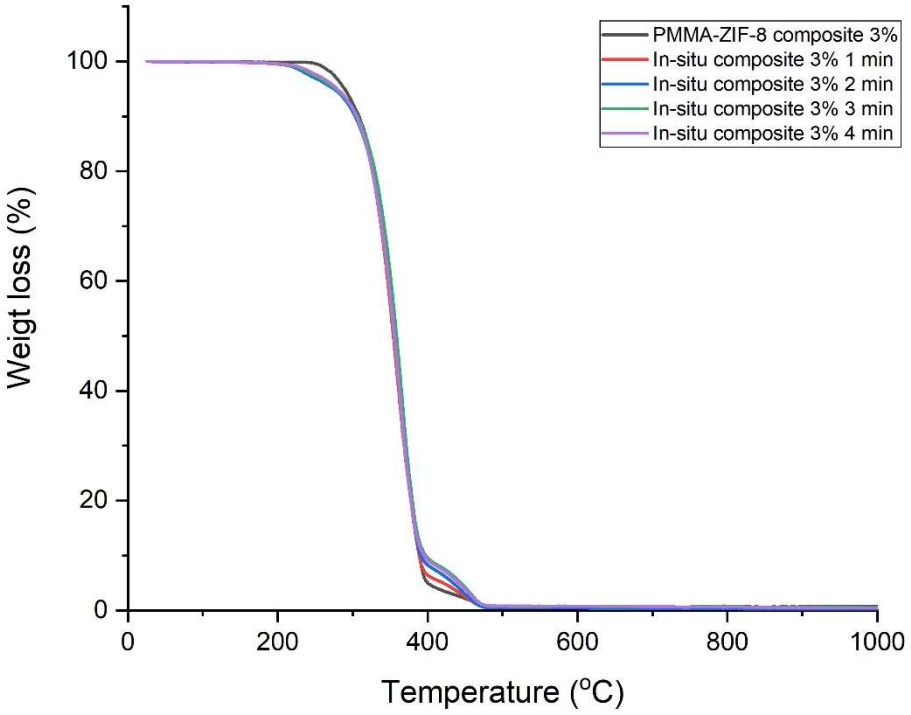

Figure 3.27 – Comparison between TGAs of PMMA-ZIF-8 3% composite and in-situ 3% composite

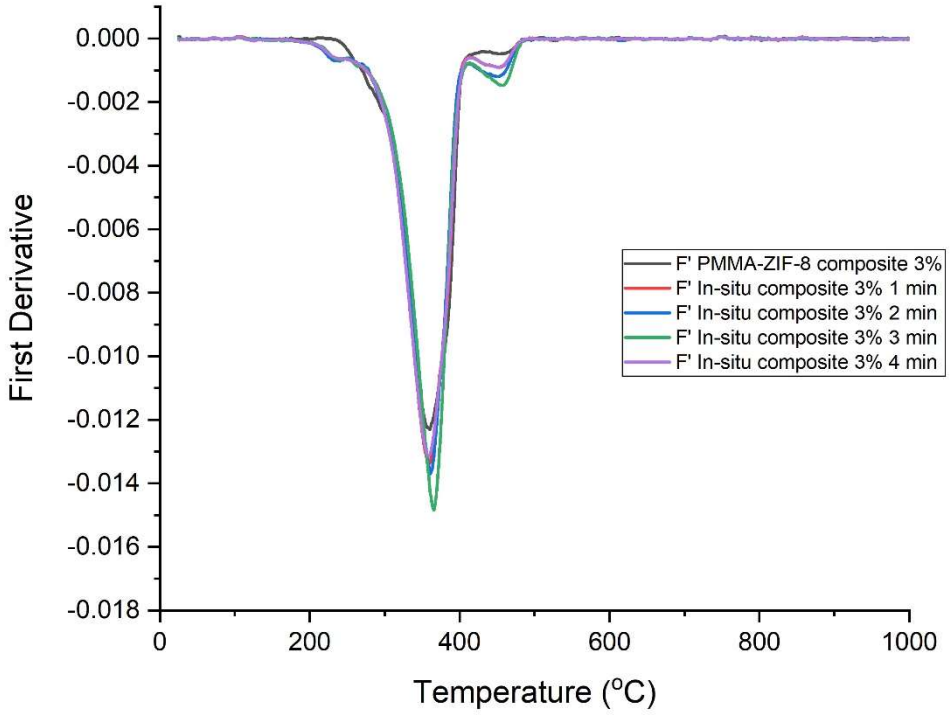

Figure 3.28 – Comparison between XRD patterns of PMMA-ZIF-8 composite and in-situ 3% composites

Then was performed a TGA for comparing the results with the PMMA-ZIF-8 composite, as shown in Figure 3.27 and 3.28. The TGA of the in-situ composites showed a loss in weight before the onset degradation showed by the PMMA-ZIF-8 composite due the unreacted reagent that are still in the composite, indeed basic zin carbonate has the onset of its degradation around 200 °C and 2-methylimidazole has the fusion point at 142-3 °C and is supposed to evaporate at this temperatures. The weight loss after the degradation of the polymer took place between 400° C and 500° C, that could be an indication of the formation of new phases thermally stable up to these temperatures.

Subsequently, the more meaningful samples (i.e. cycle times of 1 and 2 min) were characterized by SEM, as can be seen in Figures 3.29, 3.30, 3.31 and 3.32. The images showed lower concentration of dispersed particles that had a structure which in many cases seemed to be not close to the sodalite structure wanted. This fact could explain the low values of crystallinity detected by XRD analysis and hence only a low conversion of the reactants in the wanted structure.

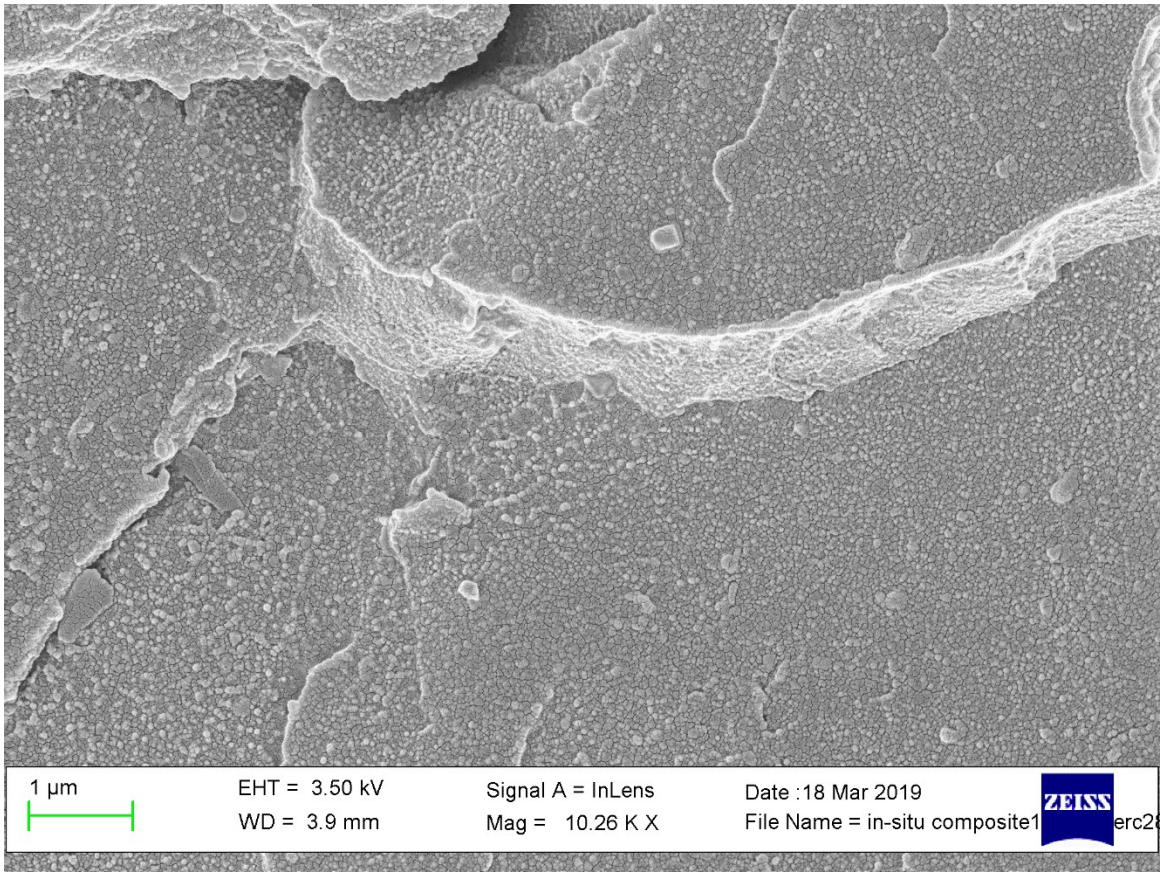

Figure 3.29 – SEM images of in-situ composite 3% 1 min

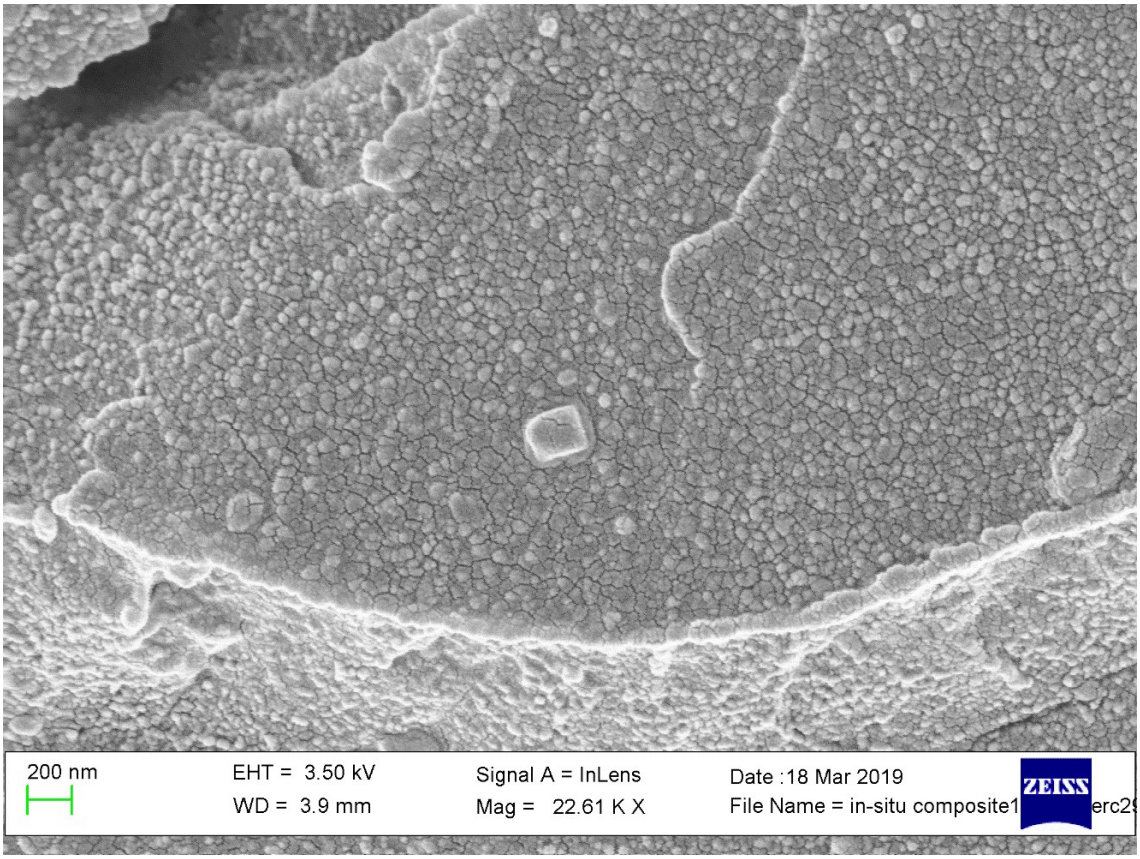

Figure 3.30 – SEM images of in-situ composite 3% 1 min

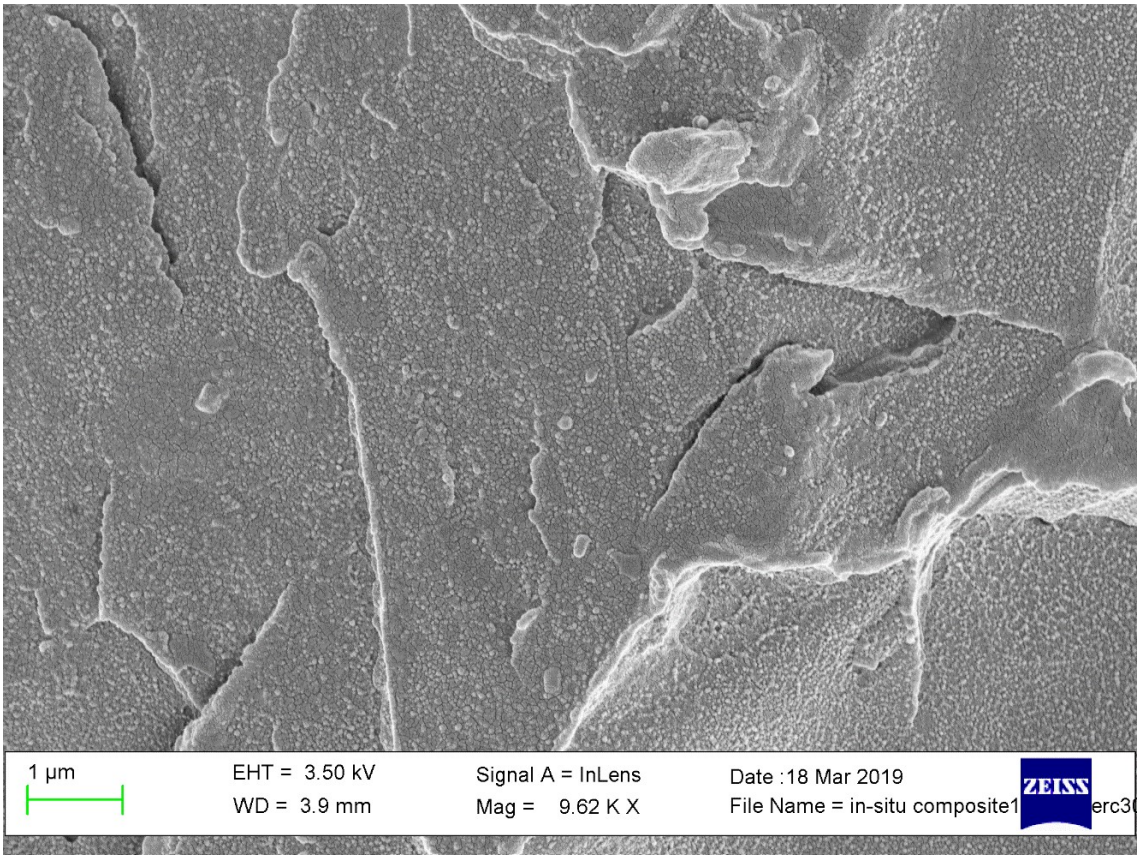

Figure 3.31 – SEM images of in-situ composite 3% 2 min

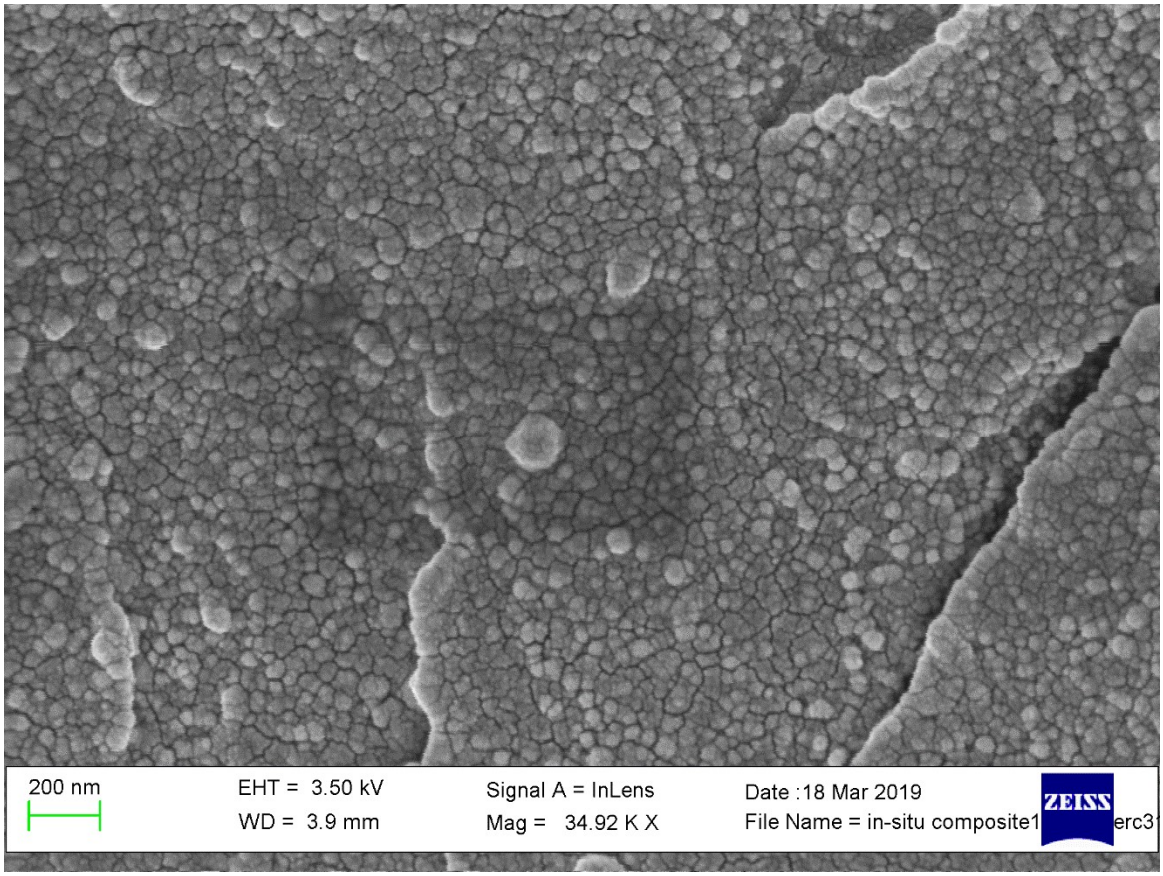

Figure 3.32 – SEM images of in-situ composite 3% 2 min

3.2.3 In-situ composite 10%

The grinded neat polymer was manually mixed with the two reagents used for the synthesis of ZIF-8 (i.e. basic zinc carbonate and 2-methylimidazole with molar ratio of 1/5:3) in weight ratio of 90% and 10% respectively. The mixture was compounded in Thermo Scientific Haake Mini-Lab II micro-compounder with a barrel temperature of 220 °C and a screw speed of 75 rpm and recirculation times of 1 and 2 min since were the cycle times that had the better results in the previous composition. The extrudate collected had again developed bubbles during the extrusion, that were removed with another passage within the extruder. Then the composite was pressed in Collin hot press for obtaining discoid samples.

The samples were analysed with XRD and the patterns obtained were compared with the PMMA-ZIF-8 composite for the identification of the crystalline peaks belonging to ZIF-8. In this case the in-situ composites showed more intense peaks respect to in-situ composite with 3% of loading of the reagents mixture, as is possible to see in Figure 3.33.

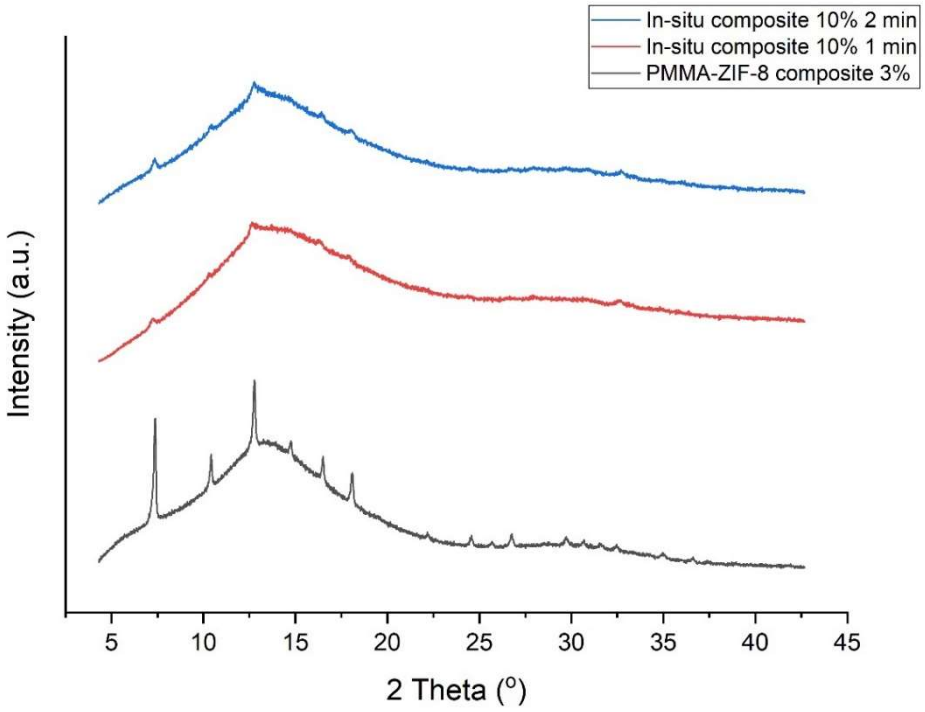

Figure 3.33 - Comparison between XRD patterns of PMMA-ZIF-8 3% composite and in-situ 10% composite 1 and 2 minutes cycle time

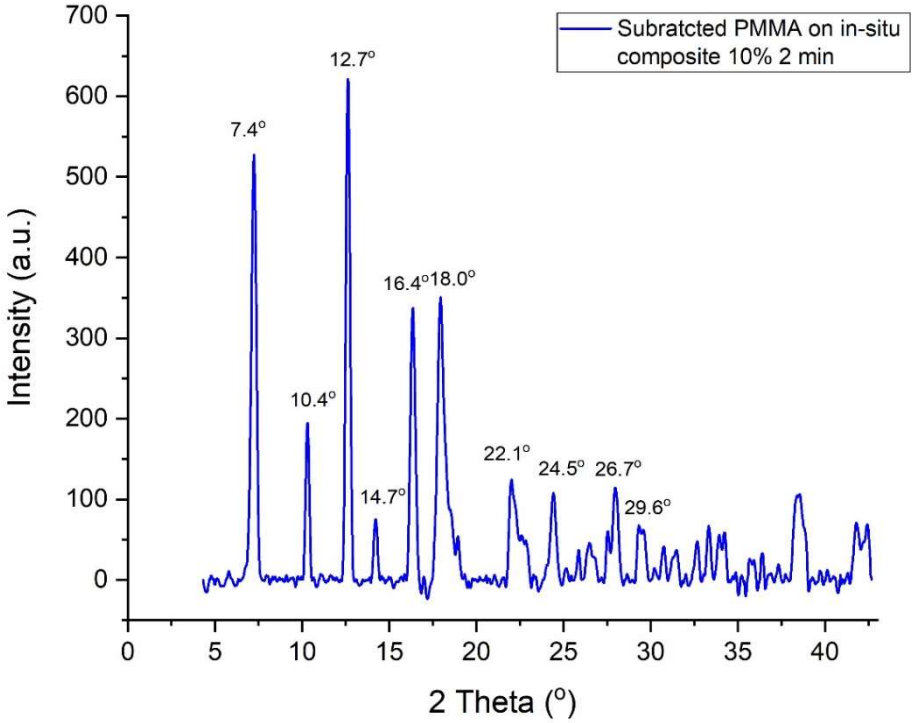

Figure 3.34 – Graph obtained from the subtraction of the pattern of PMMA on the pattern of in-situ composite 10% 2 min

To have a clearer view and a closer look on the position of the peaks, the pattern of PMMA was subtracted from the one of the in-situ composite 10% 2 minutes of cycle time, that was the one showing the most intense peaks regarding the version at 10% loading. As is possible to see in Figure 3.34, the subtracted pattern showed all the peaks belonging to ZIF-8 at values of 2θ of 7.4°, 10.4°, 12.7°, 14.7°, 16.4°, 18.0°, 22.1°, 24.5°, 26.7° and 29.6° suggesting the formation of a ZIF-8 crystalline structure on the composite. However, the intensities of these peaks are always lower respect to ones belonging to the PMMA-ZIF-8 composite 3%, indicating a low yield in the conversion of the reactants in the product wanted.

The TGA analyses of the two in-situ composites at 10% loading (Figures 3.35 and 3.36) showed a higher weight loss in the zone around 200 °C respect to the ones at 3% loading of reactants, as expected since this weight loss was due to the unreacted precursors. Even in this case after the degradation of the polymer phase remains a more thermally stable phase that degrades at a higher temperatures respect to the reactants indicating the formation of a new phase in the composite.

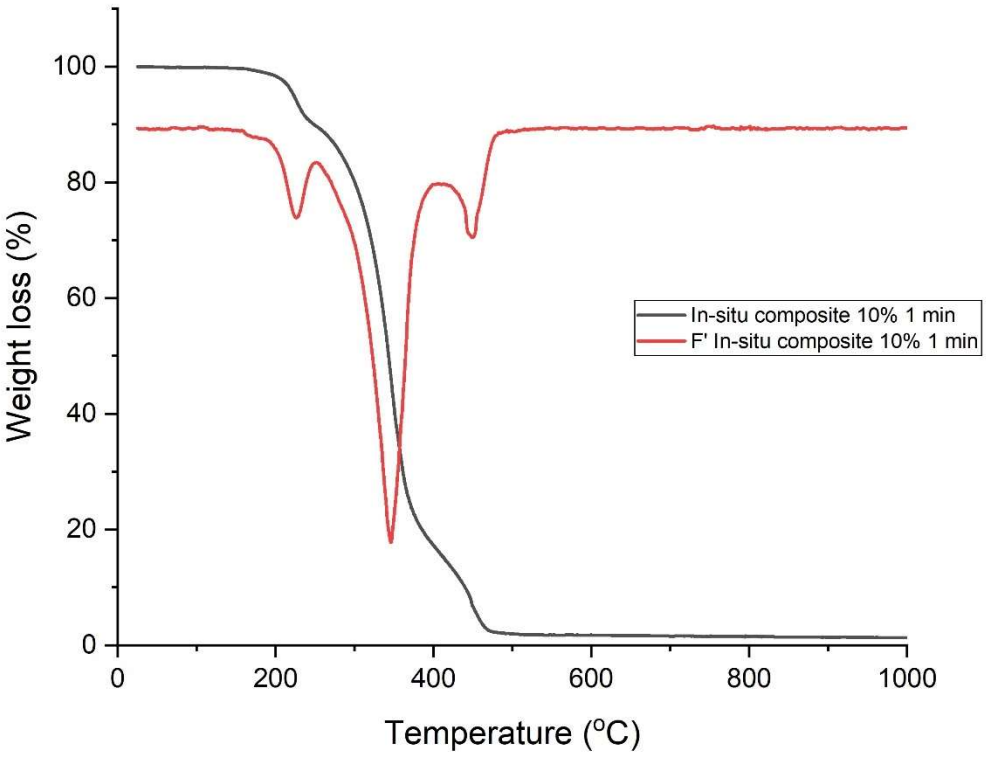

Figure 3.35 – In-situ composite 10% 1 min of cycle time TGA

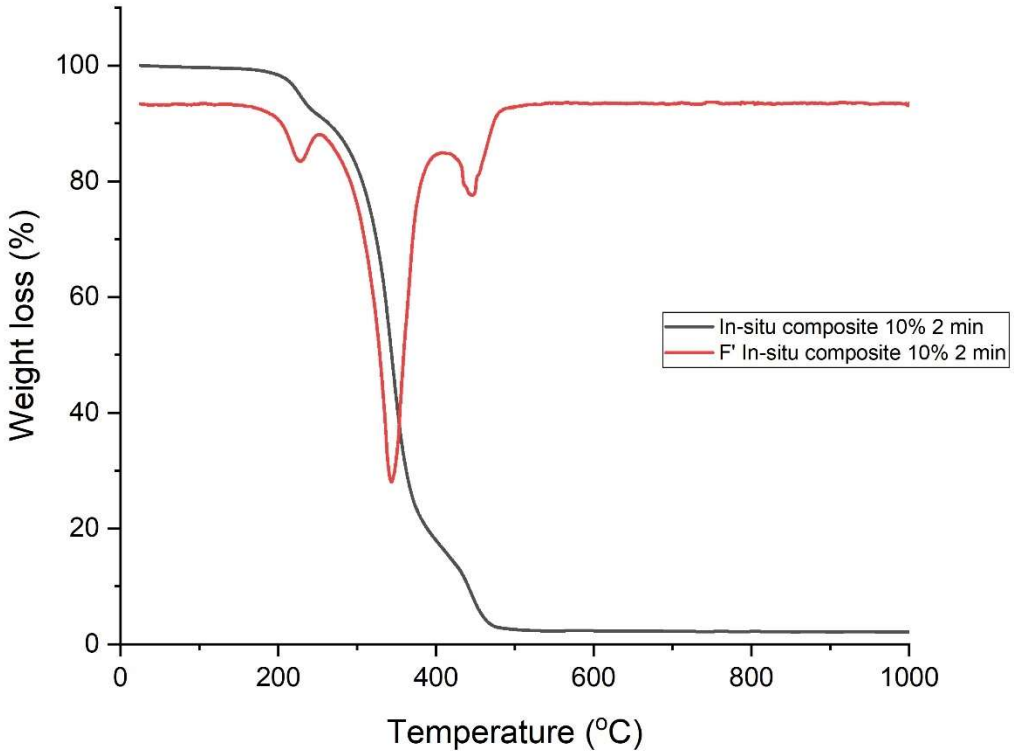

Figure 3.36 – In-situ composite 10% 2 min of cycle time TGA

The in-situ composites with 10% loading of reagents were then characterized with SEM (Figures 3.37, 3.38, 3.39, 3.40 and 3.41). The images of both cycle time indicate the presence of dispersed particles in higher concentration respect to the in-situ composites with 3% loading of reagents. Moreover, these particles seemed to have a better interaction with the polymer matrix and to have a more regular shape always respect to the 3% version of the in-situ composite, thus showing a greater congruence with the PMMA-ZIF-8 composite regarding the interface between the particle and the polymer, and with the crystal structure of the metal-organic framework regarding the particles shape and dimensions. These facts are in line with the higher values of crystallinity detected by the XRD analyses respect to the in-situ composites at the 3% of loading.

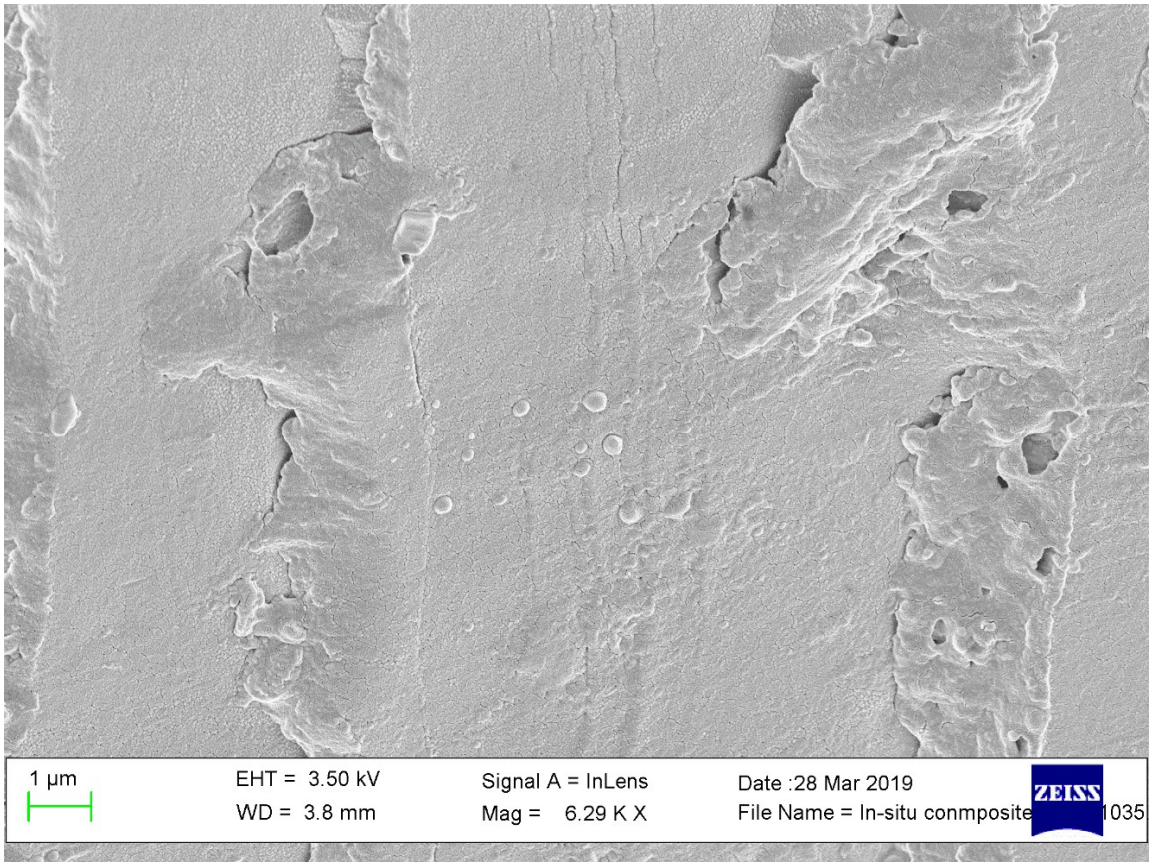

Figure 3.37 – SEM images of in-situ composite 10% 1 min

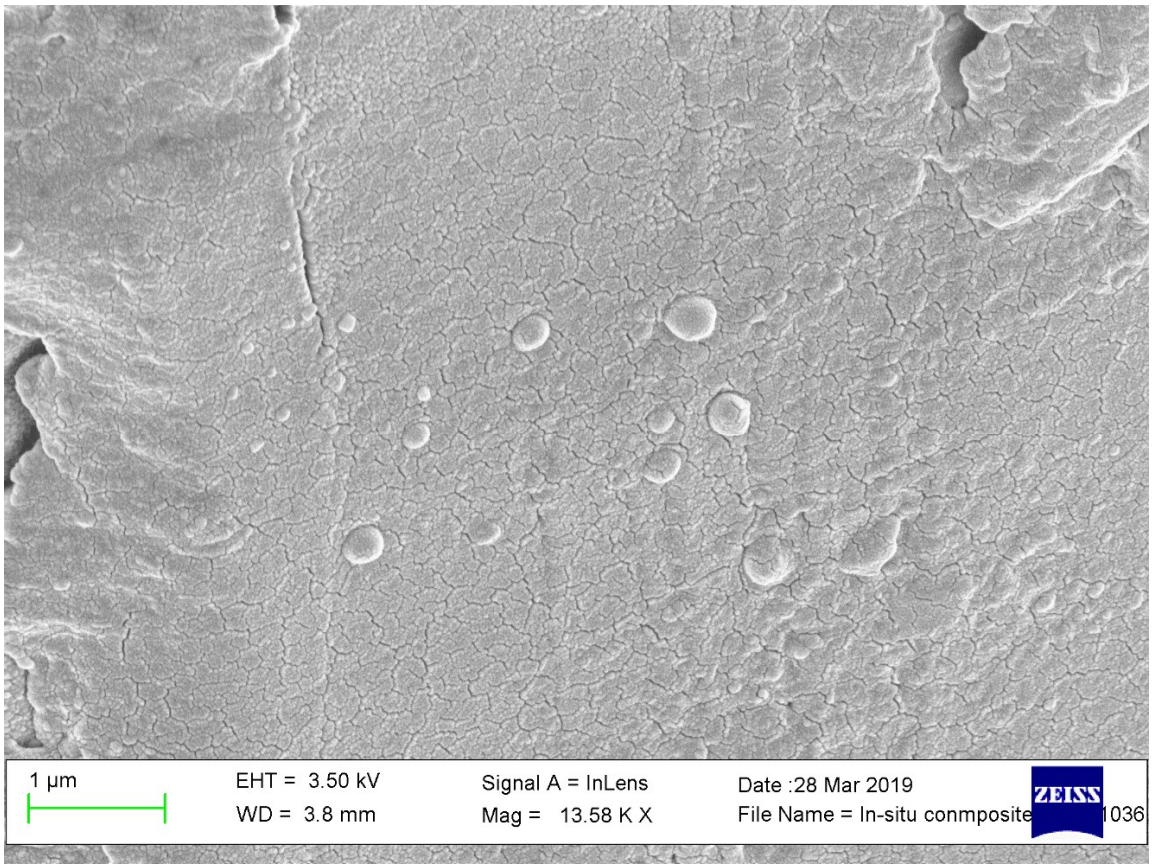

Figure 3.38 – SEM images of in-situ composite 10% 1 min

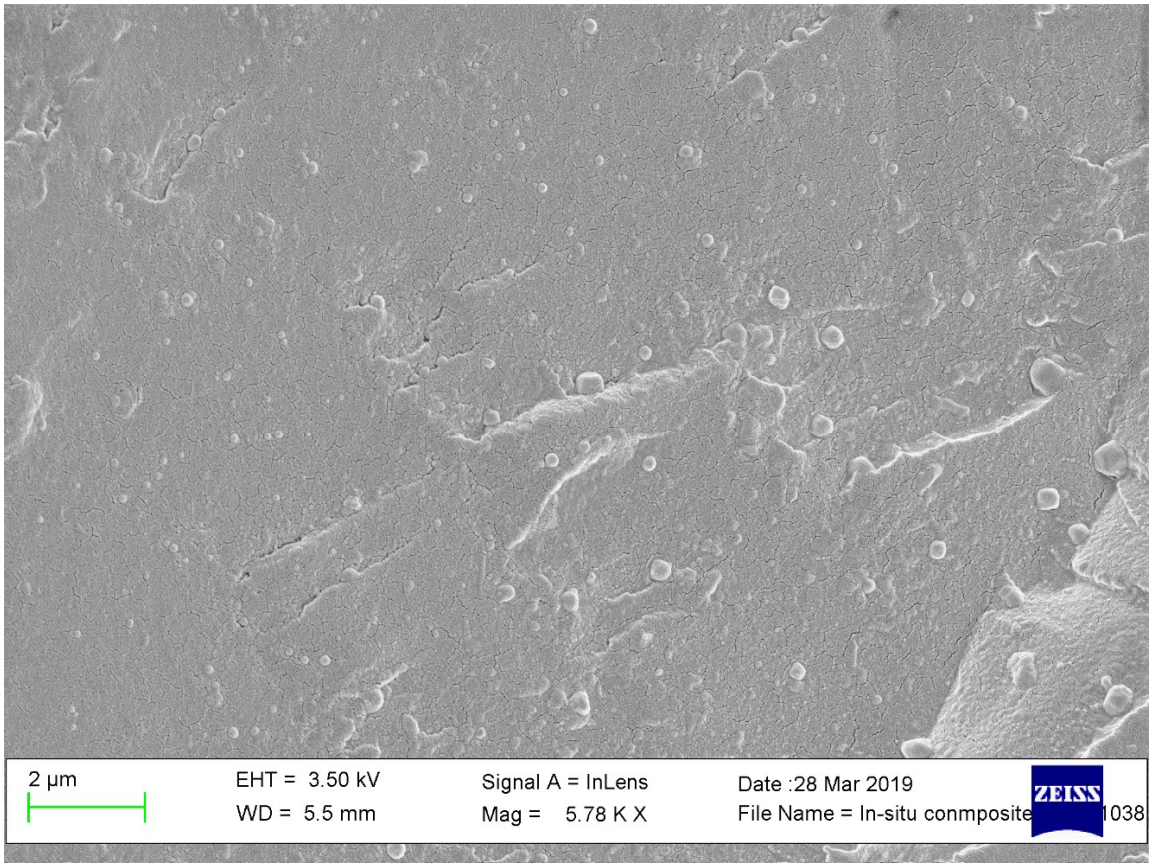

Figure 3.39 – SEM images of in-situ composite 10% 2 min

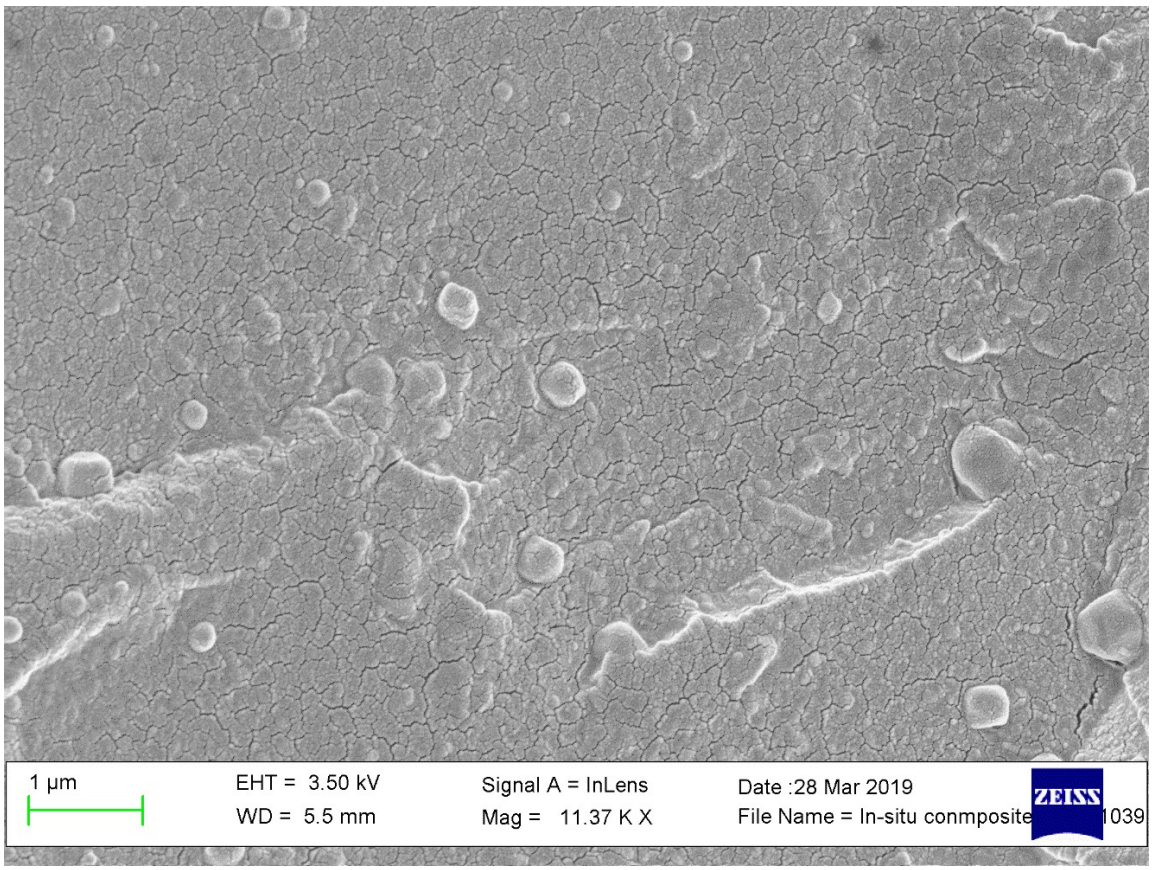

Figure 3.40 – SEM images of in-situ composite 10% 2 min

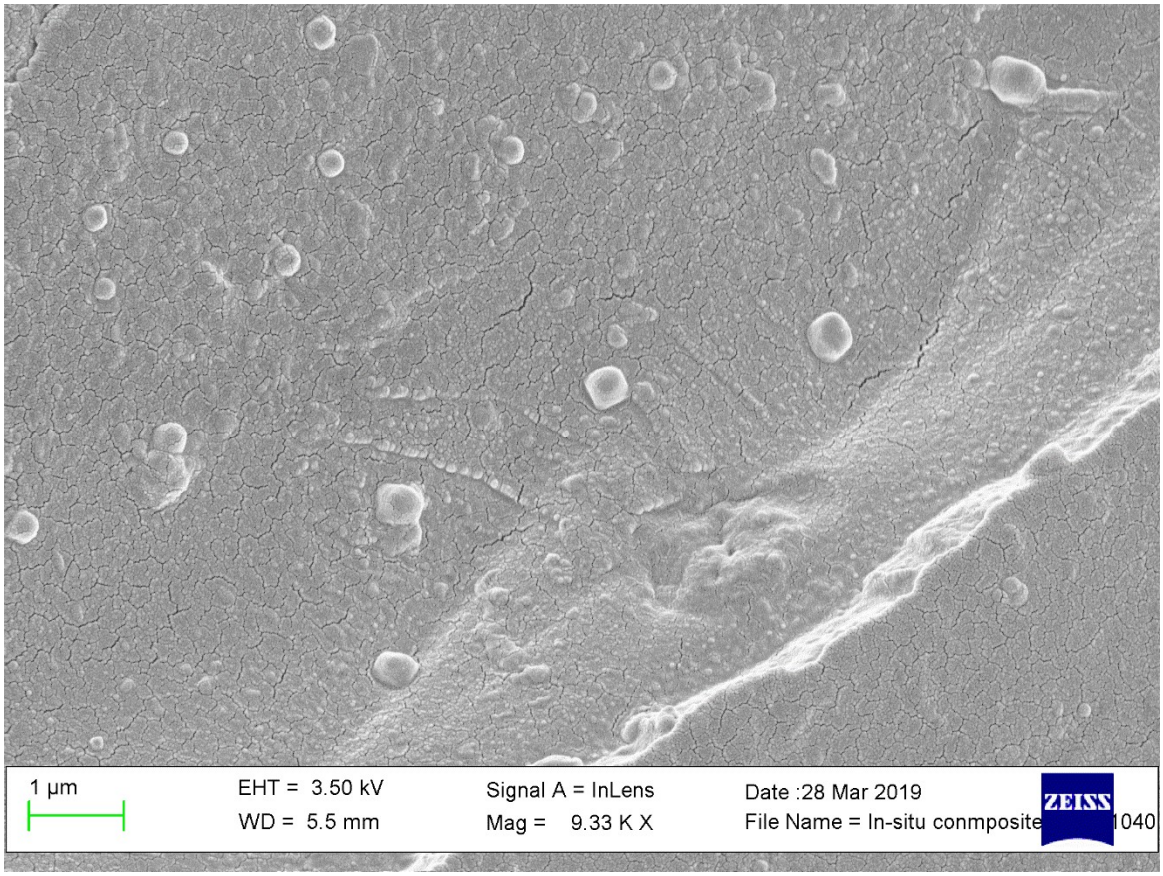

Figure 3.41 – SEM images of in-situ composite 10% 2 min

4 CONCLUSIONS

The aim of this work to provide new functional solutions for the production of the composites containing metal-organic frameworks as fillers. In this particular case the idea was to couple the compounding of the filler with polymeric matrix with the mechano-chemical synthesis of the metal-organic framework in a single processing step within the extrusion process.

Initially the metal-organic framework ZIF-8 was synthesized with a totally solvent-free mechanochemical synthesis. The metal-organic framework was then fully characterized to verify its synthesis and the properties obtained. ZIF-8 resulted to be synthetized and to have properties, such as surface areas, pore volume, thermal stability, etc., in line with the ones founded in literature. After that the synthetized metal-organic framework was compounded with a polymeric matrix. The composite was subsequently characterized to create a benchmark with which to compare the in-situ composites. Then it was tried to synthesize in-situ the metal-organic framework within the polymer matrix by feeding the micro-compounder with a mixture of polymer and precursors of the metal-organic framework in two different formulations, one at 3% and the other at 10% by weight of precursors. The characterization of in-situ composites, in particular with XRD and NMR analyses, has shown that a part of reagents has been converted, although the conversion showed a low yield, into the desired crystalline structure and thus confirming that the in-situ synthesis of the metal-organic framework was possible. Furthermore, it was noted that the increase of the residency time was harmful for the retaining of the crystalline structure desired.

Therefore, there are still some aspects to be studied regarding this new way of producing composites with metal-organic frameworks as a filler, since it was the first time that the in-situ synthesis was investigated in an extrusion process. Hence, it would be worth it to conduct further studies to enhance the yield of the conversion of precursors and to tailor the conditions of the process for obtaining the desired large-scale production.

AKCNOWLEDGMENTS

I would like to thank Prof. Tony McNally who gave me the opportunity to do my thesis project at the University of Warwick.

Thanks also to the IINM research group that welcomed me with affection.

My gratitude goes also to Prof. Lorenzetti, who allowed me to have this experience in England.

The final and the most important thanks goes to my family and my friends that always supported me.

Bibliography

[1] J.-R. Li, J. Kuppler and H.-C. Zhou, "Selective gas adsorption and separation in metal-organic frameworks," *Chemical Society reviews,* vol. 38, pp. 1477-1504, 2009.

[2] IUPAC, "Manual of symbols and terminology for physiochemical quantities and units-Appendix II," *Pure & Appl Chem.,* vol. 46, pp. 71-90, 1997.

[3] M. P. Attfield, "Microporous material," *Science Progress,* vol. 85, p. 319–345, 2002.

[4] C. Li, S. M. Meckler, Z. P. Smith, J. E. Bachman, L. Maserati, J. R. Long and a. B. A. Helms, "Engineered Transport in Microporous Materials and Membranes for Clean Energy Technologies," *Adv. Mater.,* p. 1704953, 2018.

[5] O. M. Yaghi and a. H. Li, "Hydrothermal Synthesis of a Metal-Organic Framework Containing Large Rectangular Channels," *J. Am. Chem. Soc.,* vol. 117, pp. 10401-10402, 1995.

[6] P. Z. Moghadam, A. Li, S. B. Wiggin, A. Tao, A. G. P. Maloney, P. A. Wood, S. C. Ward and a. D. Fairen-Jimenez, "Development of a Cambridge Structural Database Subset: A Collection of Metal–Organic Frameworks for Past, Present, and Future," *Chemistry of Materials,* vol. 29, pp. 2618-2625, 2017.

[7] B. Rungtaweevoranit, C. S. Diercks and M. J. K. a. O. M. Yaghi, "Spiers Memorial Lecture: Progress and prospects of reticular chemistry," *Faraday Discuss.,* vol. 201, pp. 9-45, 2017.

[8] I. M. Hoenicke, I. Senkovska, V. Bon, I. A. Baburin, N. Boenisch, S. Raschke, J. D. Evans and a. S. Kaskel, "Balancing Mechanical Stability and Ultrahigh Porosity in Crystalline Framework Materials," *Angew. Chem. Int. Ed.,* vol. 57, p. 13780–13783, 2018.

[9] H. Furukawa, K. E. Cordova, M. O'Keeffe and O. M. Yaghi, "The Chemistry and Applications of Metal-Organic Frameworks," *Science ,* vol. 341, p. 1230444, 2013.

[10] K. C. Stylianou and a. W. L. Queen, "Recent Advances in Carbon Capture with Metal–Organic Frameworks," *Chimia,* vol. 69, pp. 274-283, 2015.

[11] S. M. Cohen, “Postsynthetic Methods for the Functionalization of Metal-Organic Frameworks,” *Chem. Rev.,* vol. 112, p. 970–1000, 2012.

[12] K. Sumida, D. L. Rogow, J. A. Mason, T. M. McDonald, E. D. Bloch, Z. R. Herm, T.-H. Bae and a. J. R. Long, “Carbon Dioxide Capture in Metal-Organic Frameworks,” *Chem. Rev.,* vol. 112, pp. 724-781, 2012.

[13] K. W. Chapman, G. J. Halder and a. P. J. Chupas, “Guest-Dependent High Pressure Phenomena in a Nanoporous Metal-Organic Framework Material,” *J. AM. CHEM. SOC. 2008, 130, 10524–10526,* vol. 130, p. 10524–10526, 2008.

[14] H. Wang, Q.-L. Zhu, R. Zou and a. Q. Xu, “Metal-Organic Frameworks for Energy Applications,” *Chem,* vol. 2, p. 52–80, 2017.

[15] M. Rubio-Martinez, C. Avci-Camur, A. W. Thornton, I. Imaz, D. Maspoch and a. M. R. Hill, “New synthetic routes towards MOF production at scale,” *Chem. Soc. Rev.,* vol. 46, p. 3453, 2017.

[16] J. Klinowski, F. A. A. Paz, P. Silva and a. J. Rocha, “Microwave-Assisted Synthesis of Metal–Organic Frameworks,” *Dalton Trans.,* vol. 40, pp. 321-330, 2011.

[17] D.-W. Jung, D.-A. Yang, J. Kim, J. Kim and a. W.-S. Ahn, “Facile synthesis of MOF-177 by a sonochemical method using 1-methyl-2-pyrrolidinone as a solvent,” *Dalton Trans.,* vol. 39, pp. 2883-2887, 2010.

[18] H. Al-Kutubi, J. Gascon, E. J. R. Sudhçlter and a. L. Rassaei, “Electrosynthesis of Metal–Organic Frameworks: Challenges and Opportunities,” *ChemElectroChem,* vol. 2, pp. 462-474, 2015.

[19] D. E. Crawford, J. Casaban, R. Haydon, N. Giri, T. McNally and S. L. James, “Synthesis by extrusion: continuous, large-scale preparation of MOFs using little or no solvent,” *Chem. Sci.,* vol. 6, pp. 1645-1649, 2015.

[20] D. E. Crawford, S. L. James and a. T. McNally, “Use of Batch Mixing To Investigate the Continuous Solvent-Free Mechanical Synthesis of OLED Materials by Twin-Screw Extrusion (TSE).,” *ACS Sustainable Chem. Eng.,* vol. 6, pp. 193-201, 2018.

[21] N. Stock and a. S. Biswas, “Synthesis of Metal-Organic Frameworks (MOFs): Routes to Various MOF Topologies, Morphologies, and Composites,” *Chem. Rev. 2012,* vol. 112, pp. 933-969, 2012.

[22] D. E. Crawford and a. J. Casaban, “Recent Developments in Mechanochemical Materials Synthesis by Extrusion,” *Adv. Mater.,* vol. 28, p. 5747–5754, 2016.

[23] S. L. James, C. J. Adams, C. Bolm, D. Braga, P. Collier and e. al., “Mechanochemistry: opportunities for new and cleaner synthesis,” *Chem. Soc. Rev.,* vol. 41, pp. 413-447, 2012.

[24] T. Friscic, D. G. Reid, I. Halasz, R. S. Stein, R. E. Dinnebier and a. M. J. Duer, “Ion- and Liquid-Assisted Grinding: Improved Mechanochemical Synthesis of Metal–Organic Frameworks Reveals Salt Inclusion and Anion Templating,” *Angew. Chem. Int. Ed.,* vol. 49, pp. 712-715, 2010.

[25] B. Karadeniz, A. J. Howarth, T. Stolar, T. Islamoglu, I. Dejanović, M. Tireli, M. C. Wasson, S.-Y. Moon, O. K. Farha, T. Friščić and a. K. Užarević, “Benign by Design: Green and Scalable Synthesis of Zirconium UiO-Metal-Organic Frameworks by Water-Assisted Mechanochemistry,” *ACS Sustainable Chem. Eng.,* vol. 6, pp. 15841-15849, 2018.

[26] A. t. Bosch, “Kinetic theory of gas separation in a nanopore and comparison to molecular dynamics simulation,” *THE JOURNAL OF CHEMICAL PHYSICS,* vol. 122, p. 084711, 2005.

[27] N. Mehio, S. Dai and a. D.-e. Jiang, “Quantum Mechanical Basis for Kinetic Diameters of Small Gaseous Molecules,” *J. Phys. Chem.,* vol. 118, p. 1150−1154, 2014.

[28] Y. Wang and a. D. Zhao, “Beyond Equilibrium: Metal−Organic Frameworks for Molecular Sieving and Kinetic Gas Separation,” *Cryst. Growth Des.,* vol. 17, pp. 2291-2308, 2017.

[29] Z. Zhang, Y. Zhao, Q. Gong, Z. Li and a. J. Li, “MOFs for CO2 capture and separation from flue gas mixtures: the effect of multifunctional sites on their adsorption capacity and selectivity,” *Chem. Commun.,* vol. 49, p. 653, 2013.

[30] T.-S. Chung, L. Y. Jiang, Y. Li and S. Kulprathipanja, “Mixed matrix membranes (MMMs) comprising organic polymers with dispersed inorganic fillers for gas separation,” *Prog. Polym. Sci.,* vol. 32, p. 483–507, 2007.

[31] D. F. Sanders, Z. P. Smith, R. Guo, L. M. Robeson, J. E. McGrath, D. R. Paul and B. D. Freeman, “Energy-efficient polymeric gas separation membranes for a sustainable future: A review,” *Polymer,* vol. 54, pp. 4729-4761, 2013.

[32] P. Pandley and R. Chauhan, “Membranes for gas separation,” *Prog. Polym. Sci.,* vol. 26, pp. 853-893, 2001.

[33] S. Wang, X. Li, H. Wu, Z. Tian, Q. Xin, G. He, D. Peng, S. Chen, Y. Yin, Z. Jiang and a. M. D. Guiver, “The mixed-matrix membrane could be either symmetric or asymmetric membrane materials for CO2 separations,” *Energy Environ. Sci.,* vol. 1863, p. 9, 2016.

[34] L. M. Robeson, “The upper bound revisited,” *Journal of Membrane Science,* vol. 320, pp. 390-400, 2008.

[35] G. Dong, H. Li and a. V. Chen, “Challenges and opportunities for mixed-matrix membranes for gas separation,” *J. Mater. Chem.,* vol. 1, p. 4610, 2013.

[36] L. M. Robeson, “Correlation of separation factor versus permeability for polymeric membranes,” *Journal of Membrane Science,* vol. 62, pp. 165-185, 1991.

[37] E. Mahdi and Jin-ChongTan, “Mixed-matrix membranes of zeolitic imidazolate framework (ZIF-8)/Matrimid nanocomposite:Thermo-mechanicalstability and viscoelasticity under pinning membrane separation performance,” *Journal of Membrane Science,* vol. 498, pp. 276-290, 2016.

[38] A. M. Marti, S. R. Venna, E. A. Roth, J. T. Culp and a. D. P. Hopkinson, “Simple Fabrication Method for Mixed Matrix Membranes with in Situ MOF Growth for Gas Separation,” *ACS Appl. Mater. Interfaces,* vol. 10, p. 24784−24790, 2018.

[39] B. Ge, Y. Xu, H. Zhao, H. Sun, Y. Guo and a. W. Wang, “High Performance Gas Separation Mixed Matrix Membrane Fabricated by Incorporation of Functionalized Submicrometer-Sized Metal-Organic Framework,” *Materials,* vol. 11, p. 1421, 2018.

[40] N. Jusoh, Y. F. Yeong, K. K. Lau and A. M. Shariff, “Mixed Matrix Membranes Comprising of ZIF-8 Nanofillers for Enhanced Gas Transport Properties,” *Procedia Engineering,* vol. 148, pp. 1259-1265, 2016.

[41] M. L. Lind, A. K. Ghosh, A. Jawor, X. Huang, W. Hou, Y. Yang and a. E. M. V. Hoek, “Influence of Zeolite Crystal Size on Zeolite-Polyamide Thin Film Nanocomposite Membranes,” *Langmuir ,* vol. 25, p. 10139–10145, 2009.

[42] H. Vinh-Thang and a. S. Kaliaguine, “Predictive Models for Mixed-Matrix Membrane Performance: A Review,” *Chem. Rev.,* vol. 113, p. 4980−5028, 2013.

[43] A. Kathuria, S. Al-Ghamdi, M. G. Abiad and a. R. Auras, “The Influence of Cu3(BTC)2 metal organic framework on the permeability and perm-selectivity of PLLA-MOF mixed matrix membranes,” *J. Appl. Polym. Sci.,* vol. 132, p. 42764, 2015.

[44] B.-H. Jeong, E. M. Hoeka, Y. Yan, A. Subramani, X. Huanga, G. Hurwitz, A. K. Ghosh and A. Jawor, “Interfacial polymerization of thin film nanocomposites: A new concept for reverse osmosis membranes,” *Journal of Membrane Science,* vol. 294, pp. 1-7, 2007.

[45] “Earth System Research Laboratory,” [Online]. Available: https://www.esrl.noaa.gov/gmd/ccgg/trends/global.html. [Accessed 2019].

[46] R. K. Pachauri and L. Meyer, “Climate Change 2014 Synthesis Report,” IPCC, 2014.

[47] R. Quadrelli and S. Peterson, “The energy–climate challenge: Recent trends in CO2 emissions from fuel combustion,” *Energy Policy,* vol. 35, pp. 5938-5952, 2007.

[48] U. Patil, A. Fihri, A.-H. Emwas and a. V. Polshettiwar, “Silicon oxynitrides of KCC-1, SBA-15 and MCM-41 for CO2capture with excellent stability and regenerability,” *Chem. Sci.,* vol. 3, p. 2224, 2012.

[49] A. Kathuria, S. Al-Ghamdi, M. G. Abiad and a. R. Auras, “The Influence of Cu3(BTC)2 metal organic framework on the permeability and perm-selectivity of PLLA-MOF mixed matrix membranes,” *J. APPL. POLYM. SCI.,* vol. 132, p. 42764, 2015.

[50] R. K. Harris, E. D. Becker, S. M. C. d. M. Menezes, R. Goodfellow and P. Granger, “Nomenclature: Nuclear Spin Properties and Conventions for Chemical Shifts: IUPAC Recommendations 2001,” *Solid State Nuclear Magnetic Resonance,* vol. 22, pp. 458-483, 2002.

[51] M. Donohue and G. Aranovich, “Classification of Gibbs adsorption isotherms,” *Advances in Colloid and Interface Science,* Vols. 76-77, pp. 137-152, 1998.

[52] Y. Zhang, Y. Jia and a. L. Hou, “Synthesis of zeolitic imidazolate framework-8 on polyester fiber for PM2.5 removal,” *RSC Adv.,* vol. 8, p. 31471, 2018.

[53] A. Jomekian, R. Behbahani, T. Mohammadi and A. Kargari, “Innovative layer by layer and continuous growth methods for synthesis of ZIF-8 membrane on porous polymeric support using poly(ether-block-amide) as structure directing agent for gas separation,” *Microporous and Mesoporous Materials,* vol. 234, pp. 43-54, 2016.

[54] H. Yin, H. Kim, J. Choi and A. C. Yip, “Thermal stability of ZIF-8 under oxidative and inert environments: Thermal stability of ZIF-8 under oxidative and inert environments:,” *Chemical Engineering Journal,* vol. 278, pp. 293-300, 2015.

[55] Y. Pan, Y. Liu, G. Zeng, L. Zhao and a. Z. Lai, “Rapid synthesis of zeolitic imidazolate framework-8 (ZIF-8) nanocrystals in an aqueous system,” *Chem. Commun.,* vol. 47, pp. 2071-2073, 2011.

[56] Y.-R. Lee, M.-S. Jang, H.-Y. Cho, H.-J. Kwon, S. Kim and W.-S. Ahn, “ZIF-8: A comparison of synthesis methods,” *Chemical Engineering Journal,* vol. 271, p. 276–280, 2015.

[57] S. Khajavi, F. Kapteijn and J. C. Jansen, “Synthesis of thin defect-free hydroxy sodalite membranes: New candidate for activated water permeation,” *Journal of Membrane Science 299 (2007) 63–72,* vol. 299, pp. 63-72, 2007.

[58] S. Sneddon, J. Kahr, A. F. Orsi, D. J. Price, D. M. Dawson, P. A. Wright and S. E. Ashbrook, “Investigation of zeolitic imidazolate frameworks using 13C and 15N solid-state NMR spectroscopy,” *Solid State Nuclear Magnetic Resonance,* vol. 87, p. 54–64, 2017.